The role of *farnesyltransferase β-subunit* in neuronal polarity in *Caenorhabditis elegans*

David Carr

This thesis is submitted as a partial fulfillment of the M.Sc. program in Neuroscience

Faculty of Medicine

Department of Neuroscience, Faculty of Medicine

University of Ottawa

Ottawa, Ontario, Canada

2013

ABSTRACT

Little is known about the molecular components and interactions of the planar cell polarity pathway that regulate neuronal polarity. This study uses a *prkl-1* induced backwards locomotion defect as an array to perform a *prkl-1* suppressor screen in *C. elegans* looking for new components of the planar cell polarity pathway involved in the neuronal polarization of VC4 and VC5. The screen discovered twelve new alleles of *vang-1*, one new allele of *fntb-1* and five new mutations in unknown polarity genes. *fntb-1* encodes for the worm ortholog of Farnesyltransferase β-subunit and is important for neuronal polarization. Acting cell and non-cell autonomously, *fntb-1* regulates the function and localization of *prkl-1* through the recognition of a CAAX motif. Therefore, *fntb-1* modifies *prkl-1* to regulate the neuronal polarity of VC4 and VC5.

TABLE OF CONTENTS

LIST OF TABLES

LIST OF FIGURES

LIST OF ABBREVIATIONS

ACP	Adenomatous polyposis coli
AKT/PKB	Serine/threonine-specific protein kinase
AP	Anterior-posterior
APC	Adenomatous polyposis coil
aPKC	Atypical protein kinase C
BL	Backwards locomotion
cat	Abnormal catecholamine distribution
CDC	Cell division control
CE	Convergence extension
C. elegans	*Caenorhabditis elegans*
cfz	*Caenorhabditis* Frizzled homolog
CK	Casein kinase
CRD	Cysteine-rich domain
CRMP	Collaspin response mediator protein
C-terminal	Carboxyl terminal
cwn	*C. elegans* WNT family
DA	Dorsal cord neuron type A
DAAM	Dishevelled-associated activator of morphogenesis
DGO	Diego
DNA	Deoxyribonucleic acid
dNTP	Dinucleotide triphosphate
DSH/DVL	Dishevelled
DV	Dorso-ventral
E	Endoderm
E3	ubiquitin-protein isopeptide ligase
E. coli	*Escherichia coli*
egl	Egg laying defective
Ex	Extra-chromosomal
FJ	Four-jointed
FMBN	Facial branchiomotor neuron

FMI/CELSR	Flamingo
FNTA	Farnesyltransferase α-subunit
FNTB	Farnesyltransferase β-subunit
FT	Farnesyltransferase
FTI	Farnesyltransferase inhibitor
FZ	Frizzled
GDP	Guanosine diphosphate
GEF	Guanine nucleotide exchange factor
GFP	Green fluorescent protein
GGT	Geranylgeranyltransferase
GSK-3β	Glycogen synthase kinase 3β
GTP	Guanosine-5'-triphosphate
GTPase	guanosine-5'-triphosphate hydrolase enzyme
HCC	Hepatocelluar carcinoma
HSN	Hermaphrodite-specific neuron
KIF3	Kinesin-2 motor protein
L	Larval
LB	Luria-Bertani
lef	Lymphoid enhancer factor
let	Lethal
LG	Linkage group
lin	Abnormal cell lineage
LRP	Lipoprotein receptor-related protein
MAP	Microtubule associated protein
mig	Abnormal cell migration
ML	Medio-lateral
mom	More of mesoderm
MS	Mesoderm
MT	Microtubule
NGM	Nematode growth medium
NIH3T3	Mouse embryonic fibroblast cell line

NTD	Neural tube closure defect
N-terminal	Amino terminal
odr	Odorant response abnormal
PAR	Partitioning-defective
PCP	Planar cell polarity
PCR	Polymerase chain reaction
PDK	Phosphoinositide-dependent kinase
PH	Pleckstrin homology
PI3-K	Phosphoinositide 3-kinase
PIP_3	Phosphatidylinositol (3,4,5)-triphosphate
PKD	Polycystic kidney disease
pop	Posterior pharynx defect
PRKL	Prickle
RAC	Ras-related C3 botulinum toxin substrate
RFP	Red fluorescent protein
RNA	Ribonucleic acid
RHO	Ras homologue
ROCK	RHO kinase
RT	Room temperature
SCRIB	Scribble
STAN	Starry night
STEF	T-cell lymphoma invasion and metastasis-inducing protein 2
STMB	Strabismus
TAU	Tau protein
tcf	T-cell factor
TIAM	T-cell lymphoma invasion and metastasis-inducing protein
unc	Uncoordinated
UTR	Un-translated region
VANG	Vang gogh
VC	Ventral cord type C
WNT	Wingless glycoprotein

wrm	Worm Armadillo
WT	Wild type
XWNT	*Xenopus larvae* wingless homolog
ZPRKL	Zebrafish prickle

ACKNOWLEDGEMENTS

I would like to express my gratitude to my thesis advisor, Dr. Antonio Colavita, for the opportunity to learn in his lab. His consistent support, guidance, encouragement and patience throughout my studies have inspired me greatly.

I would also like to thank my thesis advisory committee, Dr. Chris Kennedy and Dr. Johnny Ngsee, for their guidance, inspiration, and focus in science and career.

I would like to thank all of the members of the Colavita lab: Carlos Carvalho, Nasrin Habibi-Babadi, Andrea McEwan, Leticia Sanchez-Alvarez, Cristina Slatculescu, Anna Su, Raymond 'Matt' Tanner, and Jiravat Visanuvimol. Their continued support and encouragement have greatly helped me and truly made the lab an enjoyable place to work. I have learned so much from each of them. I would also like to thank the past summer students for assisting in lab work.

Above all, I would like to thank my parents and family. My deepest gratitude goes to all my siblings, especially Janine and Charlie Gorman, for their support and love throughout my life. Mom and Dad, your unconditional support, encouragement and love is the backbone of my success.

CHAPTER 1

INTRODUCTION

1.1 Planar Cell Polarity

Establishment of polarity is crucial for the proper development of an organism. Organisms undergo symmetry breaking events at a global and sub-cellular level that lead to the development of different body axes: anterior-posterior (AP), dorso-ventral (DV) and apical-basal (Gray et al., 2011; Hashimoto and Hamada, 2010). Another important plane is that of the epithelium. Cells in a flat epithelium tend to be polarized at both cellular and sub-cellular levels to acquire an orientation or polarity along the plane of the epithelium (Figure 1A) (Bayly and Axelrod, 2011; Goodrich and Strutt, 2011; Vladar et al. 2011). This planar polarity is largely controlled by the planar cell polarity pathway. Planar cell polarity (PCP) refers to the organized orientation of cells, and sub-cellular structures within a sheet of cells or within the plane of the epithelium (Bayly and Axelrod, 2011; Goodrich and Strutt, 2011; Vladar et al. 2009). That is to say that the PCP pathway is primarily responsible for orienting sub-cellular structures, cells or organs in an axis other than apical-basal.

In addition to cell polarization within a plane of the epithelium, the PCP pathway may also act in non-epithelial cells. Parts of the pathway have been linked to cell fate determination such as the cell fate of R3 and R4 ommatidial cells in the *Drosophila* eye and the EMS blastomere cell fate in *C. elegans* (Figure 1E and 1F) (Axelrod, 2009; Cooper

and Bray, 1999; Walston and Hardin, 2004; Zheng et al., 1995). Components of the PCP pathway are also important in dynamic processes such as cell motility as demonstrated by cells undergoing convergent extension (CE) and migrating neurons, or through the development of metastatic cancers (Goodrich and Strutt, 2011; Mapp et al., 2011; Tissir and Goffinet, 2010; Vladar et al., 2009; Wang, 2009). While the mechanisms for the newly discovered roles of PCP-like pathways are not well defined, the classical pathway is well characterized and has been studied extensively in *Drosophila.* Many components of the PCP pathway are well conserved throughout invertebrates and vertebrates; however, studying the PCP pathway in vertebrates provides an additional challenge as many components have multiple homologues that appear to function redundantly (Goodrich and Strutt, 2011; Lapebie et al., 2011; Vladar et al., 2009). Mutations or defects in one or multiple components of the PCP pathway in vertebrates can be severe and have been known to result in neural tube closure defects (NTDs), polycystic kidney disease (PKD), deafness and even seizures (Benzing et al. 2007; Bosoi et al., 2011; Curtin et al. 2003; Robinson et al., 2012; Tao et al., 2011).

The PCP pathway can be categorized into three separate modules: symmetry breaking or global cues, the core PCP components, and downstream effectors (Bayly and Axelrod, 2011; Goodrich and Strutt, 2011; Lapebie et al., 2011; Vladar et al., 2009). The downstream effectors of the PCP pathway are specific to different cells and tissues (Vladar et al. 2009). While little information is known about global cues that cause the symmetry breaking event, the core PCP pathway mechanisms remain relatively unchanged and independent of cell or tissue type.

1.1.1 The Core Planar Cell Polarity Pathway

The planar cell polarity pathway was first discovered by Gubb and Garcia-Bellido in 1982 through studies involving cells in the wing and abdomen of the model organism *Drosophila melanogaster*. The fly wing is composed of numerous epithelial cells that are oriented in a way such that hairs or chaetae grow uniformly from the distal end and in the distal direction (Figure 1A) (Goodrich and Strutt, 2011; Gubb and Garcia-Bellido, 1982; Vladar et al., 2009; Wang, 2007). Similarly, the fly abdomen is also composed of a sheet of cells containing hairs growing from the distal tip of the cell and also in the in the distal direction (Goodrich and Strutt, 2011; Gubb and Garcia-Bellido, 1982; Vladar et al., 2009). By studying the subcellular placement and growth direction of trichomes and chaetae in wild type flies and flies with various genetic mutations, Grubb and Garcia-Bellido were able to observe changes of the trichomes and chaetae located on the fly wing and abdomen. Mutations in several genes resulted in a displayed change of location for the hairs on the fly wing and abdomen from a distal location to a central location as well as a random growth direction (Figure 1B) (Gubb and Garcia-Bellido, 1982). These discovered genes are now part of six genes considered to be the core of the planar cell polarity pathway: *frizzled (fz), dishevelled (dsh/dvl), strabismus/vang gogh (stmb/vang), spiny-legs/prickle (prkl), starry night/flamingo (stan/fmi),* and *diego (dgo)*.

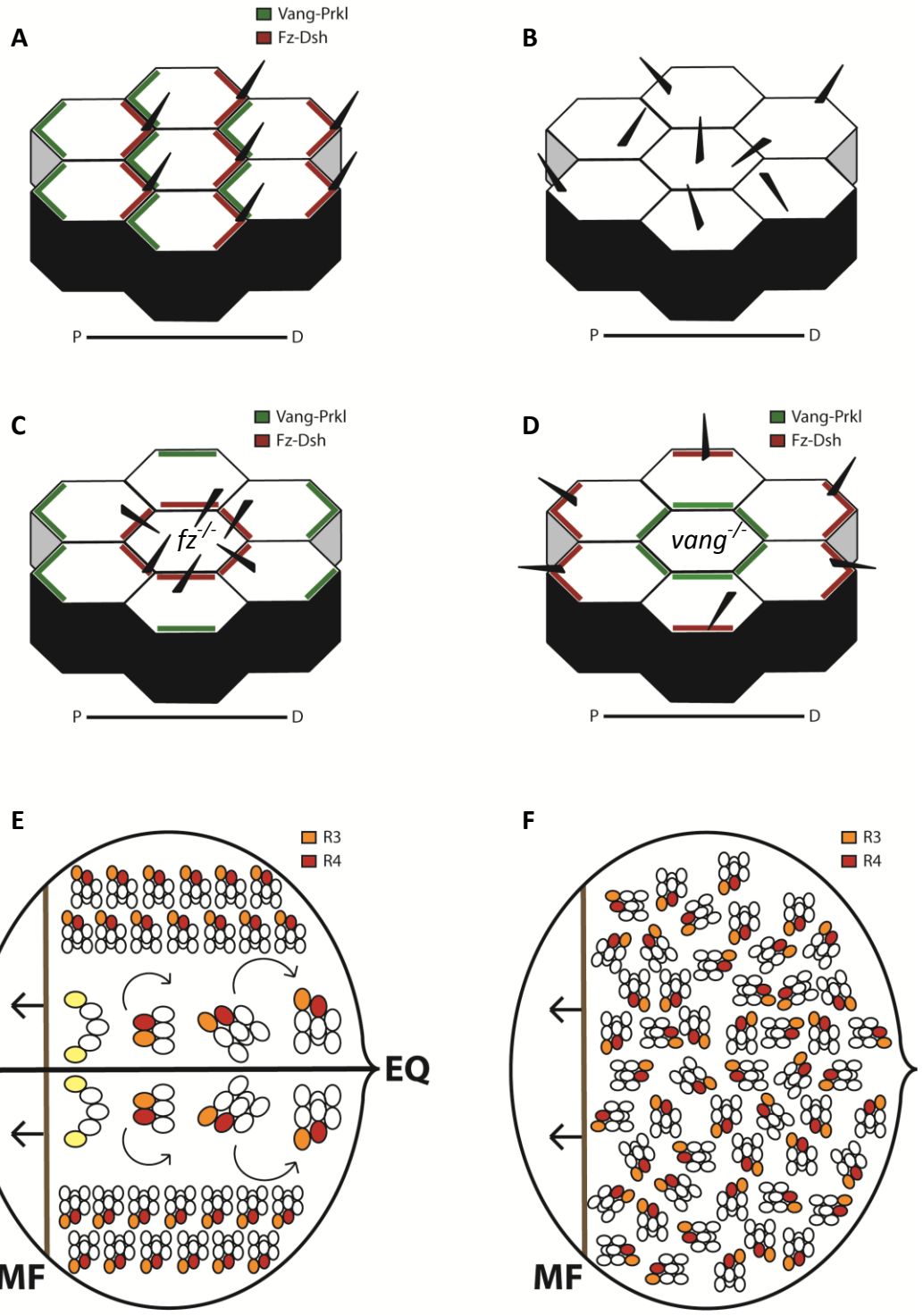

Figure 1. PCP protein localizations and defects in *Drosophila* wing and eye cells. (A) The localization of Fz-Dsh and Vang-Prkl complexes in the polarization of hairs in the fly wing. **(B)** A mutation in any PCP gene presents random hair growth. **(C-D)** A *fz* or *vang* mutant cell cloned into the fly wing has a domineering non-autonomous effect of directing hair either towards or away from the clone respectively. **(E)** The interactions between PCP components between R3 and R4 cell types determine cell fate and polarity of ommitidia in the fly compound eye. **(F)** A mutation in PCP components causes a loss of polarity and chirality of ommatidia. MF = morphogenetic furrow, EQ = equator, P = proximal, D = distal.

1.1.1.1 Core Planar Cell Polarity Mechanisms

It is thought that the core PCP components act to amplify asymmetric polarity cues in the local environment in order to regulate cell morphogenesis (Bayly and Axelrod, 2011; Goodrich and Strutt, 2011). The mechanisms of interaction between the core planar cell polarity proteins is complex and as the pathway becomes further defined in different organisms, disparities among protein interactions appear. In the classical example of the PCP pathway, the fly wing, the core proteins are initially recruited uniformly to the apical cell membrane and then assume an asymmetric localization pattern upon activation from a global cue (Figure 2) (Gray et al., 2011). This polarity is then further refined by cell-cell interactions (Gray et al., 2011). FZ, DSH, and DGO localize to the distal apical membrane where they form a complex, while VANG and PRKL are localized to the proximal apical membrane (Figure 1A and 2) (Bayly and Axelrod, 2011; Goodrich and Strutt, 2011; Gray et al., 2011; Strutt and Strutt, 2007; Vladar et al., 2009). Once located on opposite sides of the cell, the core proteins participate in a feedback mechanism to maintain polarity and signal to downstream effectors regulating cell morphogenesis and tissue polarity (Figure 2) (Bayly and Axelrod, 2011; Goodrich and Strutt, 2011; Gray et al., 2011; Strutt and Strutt, 2002; Vladar et al., 2009). FMI is located at both the proximal and distal membranes and is therefore thought to play a role in promoting the core protein asymmetries in a FZ dependent manner (Chen et al., 2008; Gray et al., 2011; Usui et al., 1999).

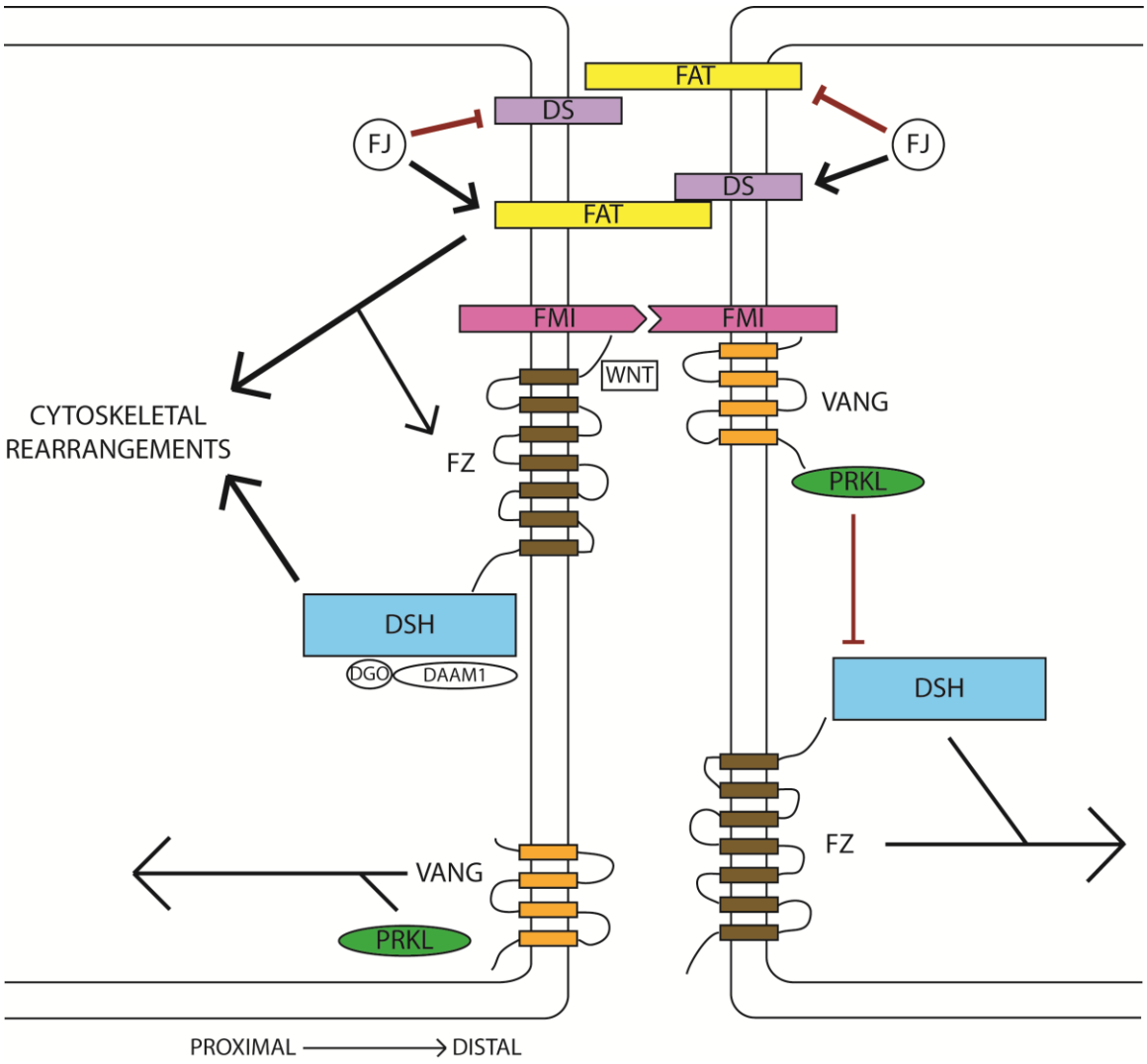

Figure 2. Schematic of PCP pathway. Four-jointed (FJ), Dachous (DS), Fat and WNT polarize the core PCP module. Frizzled (FZ) and Dishevelled (DSH) form a complex located at the distal membrane while Van Gogh (VANG) and Prickle (PRKL) form a complex located at the proximal membrane. The antagonizing effects of PRKL on DSH serve as a feedback loop further polarizing the core PCP module. The Fat/DS pathway also has the ability to modify the cytoskeleton. Flamingo (FMI) is located on both membranes.

Frizzled is a seven-pass transmembrane protein that functions upstream of DSH in multiple diverging and possibly converging pathways (Lapebie et al., 2011). FZ is composed of an extracellular cysteine-rich domain (CRD), seven transmembrane segments with three extra- and intra-cellular loops as well as a carboxyl terminal (C-terminal) cytoplasmic domain containing an important KTXXXW motif (Bhanot et al., 1996; Umbhauer et al., 2000; Vinson et al., 1989; Wong et al., 2003). The KTXXXW motif in FZ is important as it functions in both the canonical Wnt pathway and the PCP pathway to localize DSH to the membrane where it binds and leads to the phosphorylation of DSH (Rothbacher et al., 2000; Singh et al., 2010; Wong et al., 2003). The presence of a low density lipoprotein receptor-related protein 5/6 (LRP5/6) and FZ-WNT binding affinity apparently control the activation of the non-canonical Wnt pathway as opposed to the PCP pathway (Pinson et al., 2000; Tamai et al., 2000; Wu and Herman, 2007).

Initially, FZ is uniformly distributed along the apical membrane (Gray et al., 2011). After a symmetry breaking event occurs, FZ is the first of the core PCP proteins to localize asymmetrically to the apical junctions along the distal membrane (Axelrod, 2009; Bayly and Axelrod, 2011; Ma et al., 2003). Although the symmetry breaking signal is responsible for the activation and asymmetric localization of FZ, there exists an important feedback signal from the downstream signal transduction protein DSH (Shafer et al., 2011; Wu and Herman, 2007). DSH is also important for the asymmetrical localization of FZ, as deletion of DSH in *C. elegans* B cells during gastrulation and in mouse commissural axons leads to disruption of FZ asymmetry and function in the PCP

pathway (Shafer et al., 2011; Wu and Herman 2007). Once distally located, FZ has the ability to recruit and activate the cytoplasmic protein DSH.

DSH is a cytoplasmic protein that is often referred to as the hub of the Wnt-Fz pathway because of its shared role in the canonical and the non-canonical Wnt-Fz pathways. DSH is a signal transduction molecule consisting of three highly conserved domains: an amino terminal DIX domain, a central PDZ domain and a carboxyl-terminal DEP domain (Gao and Chen 2010). The DIX domain plays an important role in the canonical Wnt signalling pathway where it is necessary to interact with Axin. DSH and Axin form a complex with adenomatous polyposis coli (APC), glycogen synthase kinase 3β (GSK3β) and casein kinase 1 (CK1) leading to the nuclear accumulation of β-Catenin and subsequent activation of *tcf/lef* factors (Gao and Chen 2010). The PDZ domain has the ability to bind to the KTXXXW site of FZ as well as to the ESAV site of VANG, which is required for PCP pathway signaling (Hoffmann et al., 2010; Torban et al., 2004). Although there appears to be many phosphorylation sites that are important pathway determining factors for DSH involvement, the PDZ contains key sites that are necessary for signal transduction in the PCP pathway (Gao and Chen, 2010). The DEP domain is required for membrane localization and for transduction of the PCP pathway signaling (Gao and Chen, 2010). Membrane localization of DSH to the distal membrane is dependent on several factors including FZ. Deletion mutations for FZ disrupt the distal localization of DSH in vertebrates and *C. elegans* during embryogenesis (Gao and Chen, 2010; Hoffmann et al., 2007; Torban et al., 2004).

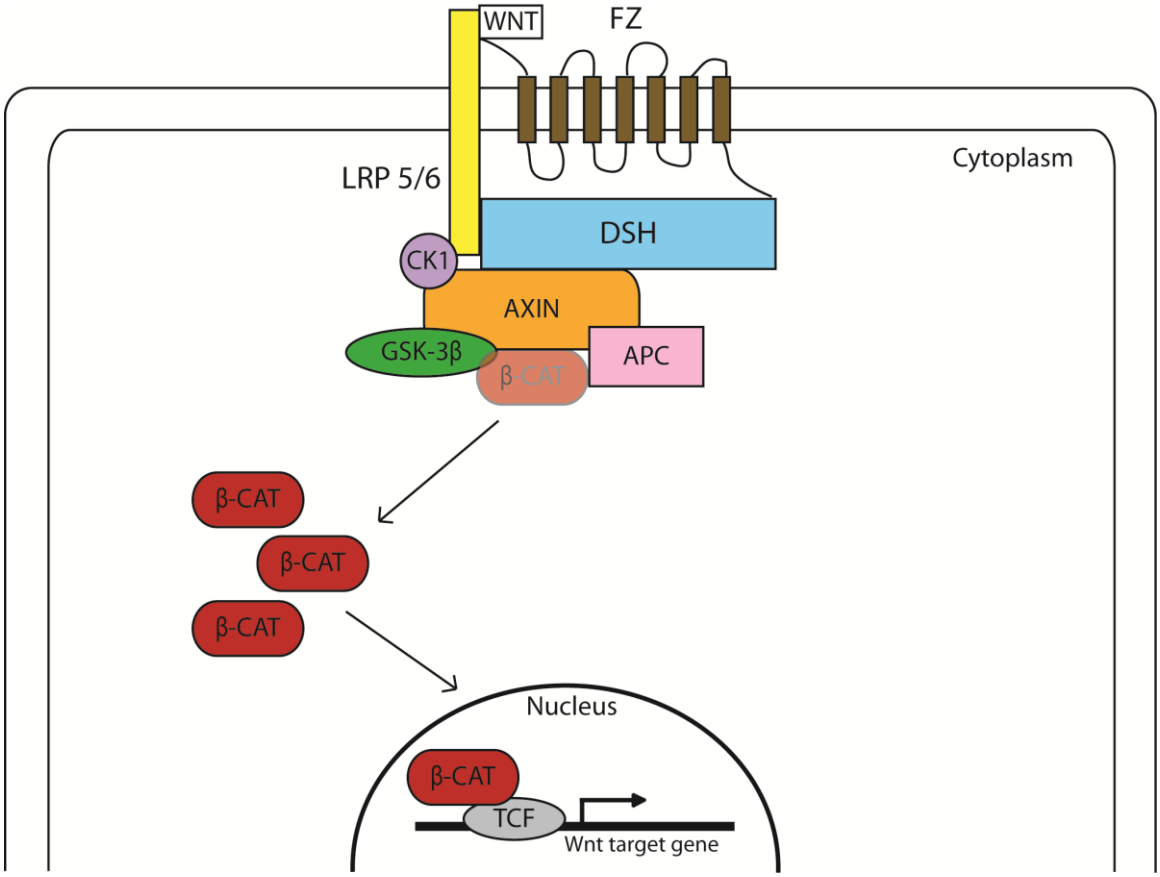

Figure 3. Schematic of the Canonical Wnt Pathway. With the presence of low-density lipoprotein 5/6 (LRP 5/6), interaction between Frizzled (FZ) and Wnt signals the canonical Wnt pathway. Dishevelled (DSH) is recruited to the membrane where it interacts with the scaffolding protein axin, as well as casein kinase 1 (CK1), glycogen synthase kinase 3β (GSK-3β), and adenomatous polyposis coli (APC). This interactions allows the accumulation and subsequent nuclear localization of β-catenin (β-cat) and the transcription of Wnt target genes.

Upon binding to FZ or VANG, DSH is in its active phosphorylated state where it has the ability to interact with tissue specific downstream effectors (Shafer et al., 2011; Singh et al., 2010). Downstream effectors in the the fly wing include Inturned and Fuzzy (Bayly and Axelrod, 2011; Gao and Chen, 2010; Goodrich and Strutt, 2011; Gray et al., 2011; Vladar et al., 2009). During convergent extension and neurogenesis in vertebrates, DSH interacts with the downstream effectors RHO-A and RAC evoking cytoskeleton re-arrangements (Bayly and Axelrod, 2011; Gao and Chen, 2010; Goodrich and Strutt, 2011; Gray et al., 2011; Vladar et al., 2009). In some cases the DSH-FZ complex is internalized via a β-arrestin dependent mechanism (Chen et al., 2003; Gao and Chen, 2010). An endocytotic DSH-FZ complex provides an opportunity for effector proteins to interact with DSH thereby enhancing its signal as seen in human embryonic kidney 293 cells (Chen et al., 2003; Gao and Chen, 2010).

DAAM and DGO are two proteins that interact with DSH-FZ to amplify the PCP induced signal regardless of the DSH-FZ complex location (Gao and Chen, 2010; Jenny et al., 2005). DAAM is found in vertebrates and is a formin homology adaptor protein (Gao and Chen, 2010). DAAM can bind to the PDZ domain of DSH increasing the binding affinity of RHO-A and RAC to DSH (Gao and Chen, 2010; Habas et al., 2001). DAAM1 is required for the non-canonical PCP pathway activation of RHO-A and for proper polarization during *Xenopus* gastrulation (Habas et al., 2001). DGO is a cytoplasmic protein with six amino terminal ankyrin repeats (Jenny et al., 2005). DGO binds to the PDZ region of DSH and promotes the phosphorylation of DSH to amplify the effects on downstream effectors (Jenny et al., 2005).

PRKL also has the ability to bind to the PDZ domain of DSH(Jenny et al., 2005). PRKL is a cytoplasmic protein that is localized to the proximal membrane following the symmetry breaking event (Axelrod, 2009; Goodrich and Strutt, 2011; Ma et al., 2003; Tree et al., 2002; Vladar et al., 2009). PRKL is composed of a PET domain, three LIM domains and a C-terminal CAAX motif (Fujimura et al., 2009; Okudra et al., 2007). A PET domain is important for protein-protein interactions, while LIM domains are double zinc finger motifs found to be important for many developmental pathways (Fujimura et al., 2009; Okudra et al., 2007). The C-terminal CAAX motif increases PRKL membrane association: an important characteristic that enables PRKL to interact in the PCP pathway (Mapp et al., 2011). There is evidence that PRKL acts as an antagonist to DSH, regulating its localization and phosphorylation (Fujimura et al., 2009; Jenny et al., 2005).

PRKL competes with DGO to bind with cytoplasmic DSH thereby sequestering DSH to the distal side of the membrane and preventing a proximal localization and function of DSH (Axelrod, 2009; Fujimura et al., 2009; Goodrich and Strutt, 2011; Jenny et al., 2005; Tree et al., 2002; Vladar et al., 2009). It has been shown in *Drosophila* pupal wing cells that cytoplasmic and proximally located PRKL regulates the localization of DSH by binding with the DSH DEP domain (Tree et al., 2002). The binding of PRKL with DSH prevents DSH membrane association ultimately leading to the disruption of DSH localization and function in the PCP pathway (Tree et al., 2002). Further evidence that PRKL antagonises DSH localization can be found in zebrafish, where mutations in PRKL disrupt the asymmetrical localization of DSH during gastrulation and neuronal migration (Carreira-Barbosa et al., 2003). In a PRKL mutant, the interaction between PRKL and

DSH that prevents FZ from interacting with DSH on the proximal side of the cell is absent resulting in failed branciomotor neuron migration and improper convergent extension (Carreira-Barbosa et al., 2003).

After the symmetry breaking event, PRKL is recruited to the proximal membrane by VANG where it interacts and binds with the C-terminal of VANG (Bastock et al., 2003; Ciruna et al., 2006; Shafer et al, 2011; Taylor et al., 1998; Vladar et al., 2009). VANG is a four pass transmembrane protein that contains a C-terminal PDZ binding motif: ESAV (Bastock et al., 2003; Torban et al., 2004). The localization and binding of PRKL to VANG creates a feedback loop in PCP signalling (Tree et al., 2002); PRKL induces E3 ubiquitin ligase activity and regulates DSH activity through ubiquitination as seen in human liver cancer HCC cells as well as in C1300 murine neuroblastoma cells (Chan et al., 2006; Fujimura et al., 2009). PRKL antagonizes DSH through phosphorylation and degradation; improper DSH function in C1300 murine neuroblastomas cells results in an increase in neurites (Fujimura et al., 2009). VANG also has the ability to bind to DSH preventing a proximal localization and forcing a distal localization so that it may interact with FZ as demonstrated during zebrafish gastrulation (Park and Moon, 2002; Torban et al., 2004; Yin et al., 2008).

A key conclusion from recent planar cell polarity studies is that the critical proximal-distal asymmetries of the core proteins are a result of intracellular feedback between the protein complexes and intercellular connections (Figure 2). These complex feedback mechanisms of the core proteins are responsible for the polarization of cells within a sheet of cells. An improper localization of the core proteins affects the

feedback system and creates a domineering non-autonomous effect as can be seen in the fly wing (Figure 1C and 1D) (Adler et al., 2000; Vladar et al., 2009). In fly wings where the PCP pathway is not functioning properly wild type cells will orient the cell hairs either towards or away from a mutant cell clone depending on which core protein is absent (Figure 1C and 1D) (Adler et al., 2000; Vladar et al., 2009). A lack of either feedback or intercellular communication results in a loss of polarity and can produce severe developmental defects.

1.1.1.2 Farnesyltransferase

A protein can be modified at any point during its creation as a means to control its function. Post-translational modification is one method in which a cell controls the activity of a protein by modifying the protein after translation from RNA. There are many types of post-translational modifications such as phosphorylation, ubiquitination, methylation, acetylation, glycosylation, oxidation and palmitoylation. The post-translational attachment of a 15 to 20 carbon group to a protein is known as protein prenylation and is catalyzed by protein prenyltransferases (Maurer-Stroh et al., 2003).

There are three different protein prenyltransferases in vertebrates: farnesyltransferase (FT), geranylgeranyltransferase-I (GGT-I) and geranylgeranyltransferase-II (GGT-II) (Maurer-Stroh et al., 2003). Each of the three prenyltransferases are composed of a heterodimeric structure that is composed of an α and a β subunit (Maurer-Stroh et al., 2003). The α subunits serve as regulatory units and are composed of seven tetratricopeptide repeats formed by pairs of helices stabilized by conserved intercalating residues. The repeats form a right-handed

superhelix that fits the $(\alpha\text{-}\alpha)_6$ barrel of the β subunit. The β subunits are necessary for proper function as they contain the substrate- and lipid-binding pockets (Maurer-Stroh et al., 2003). The protein prenyltransferases each have specific and different α and β subunits with the exception of FT and GGT-1, which share a common α subunit: farnesyltransferase α-subunit (FNTA) (Maurer-Stroh et al, 2003). The FNTA subunit is responsible for recognition of a CAAX prenylation motif at the C-terminal end of target proteins where "C" is cysteine, "A" is an aliphatic amino acid and "X" is a variable amino acid. Although FT and GGT-I both use FNTA, it is the identity of X that determines the target protein's affinity to GGT-I or FT and subsequent geranylgeranylation (20-C) or farnesylation (15-C) (Maurer-Stroh et al., 2003; Mulligan et al., 2010).

FT is responsible for initiating a series of steps that will end with the attachment of a 15-C farnesyl group to a protein containing the CAAX motif (Figure 3) (Long et al., 2002; Maurer-Stroh et al., 2003). After binding a 15-C farnesyl-phosphate, FT recognizes the CAAX motif (Figure 3) (Long et al., 2002; Maurer-Stroh et al., 2003). The cysteine of the CAAX motif and Zn^{2+} forms a complex that enables transference of the lipid anchors (Long et al., 2002; Maurer-Stroh et al., 2003). Addition of the 15-C farnesyl group is followed by the proteolytic cleavage of the terminal AAX amino acids and the methylation of the cysteine (Figure 3) (Mulligan et al., 2010). The resulting farnesylated protein has increased hydrophobicity, which is necessary for membrane insertion and interactions with other hydrophobic proteins (Maurer-Stroh et al., 2003; Mulligan et al., 2010).

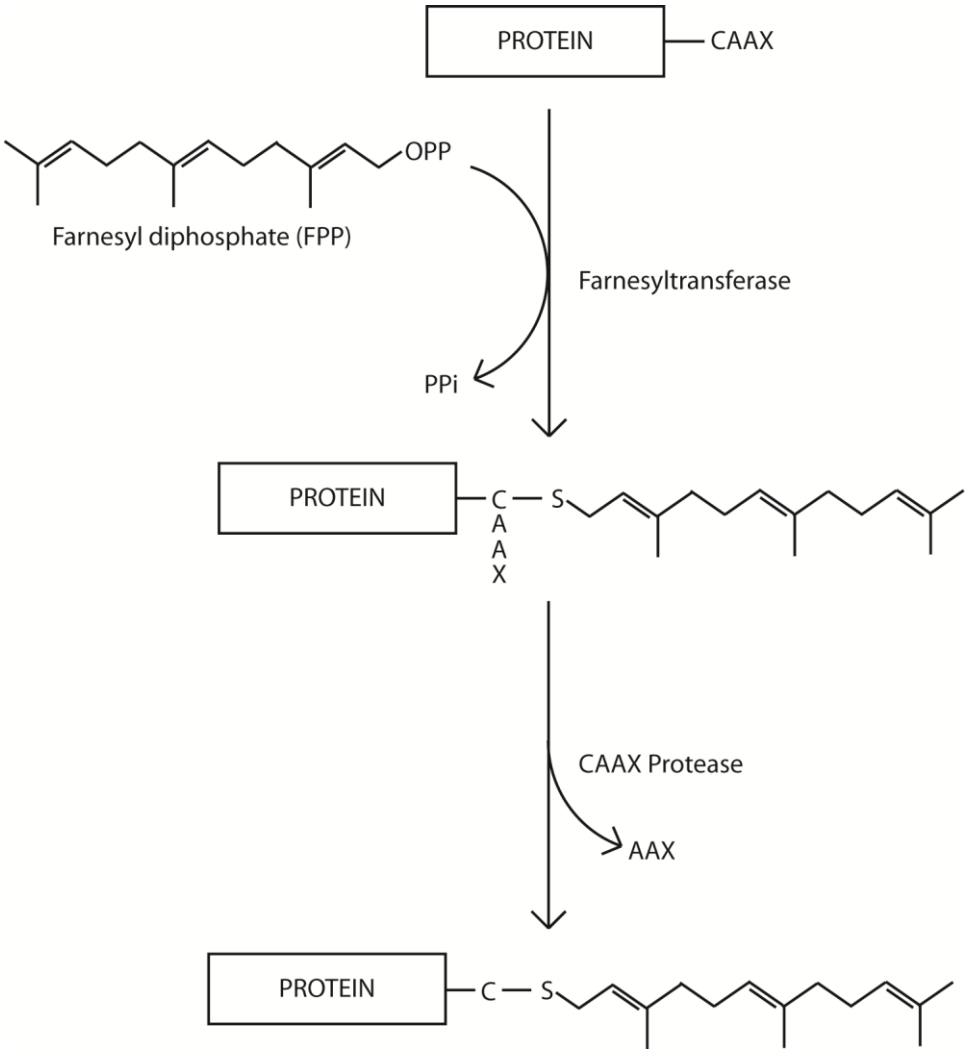

Figure 4. Schematic of farnesylation. Farnesylation begins with Farnesyltransferase binding with FPP. Farnesyltransferase then recognizes a CAAX motif of a target protein and binds with that protein for the addition of FPP. The CAAX motif is then cleaved by a CAAX protease yielding a farnesylated protein. Protein farnesylation increases hydrophobicity of the protein enabling easier interaction with cell membranes.

Many proteins have the CAAX prenylation motif. Targets for GGTIs include many small RHO GTPases including RHO-A, RAC1, and CDC42 (Maurer-Stroh et al., 2003). Targets for FT include the RAS superfamily of small GTPases, nuclear lamina proteins, kinetochore proteins as well as subunits of G-proteins (Hara and Han, 1995; Kyathanahalli and Kowluru, 2011; Maurer-Stroh et al., 2003). Considering that FT regulates the activity of their target proteins and the oncogenetic nature of the RAS superfamily of proteins, FT presents an opportunity for a targeted approach to control many types of cancers through the use of FT inhibitors (FTIs) (Sebti, 2005). However, it is important to consider side effects of FTIs as primary mouse hepatocellular cultures with FT knockouts have demonstrated severe hepatocellular disease (Yang et al., 2012). FT has also been implicated in Alzheimer's disease as patients with Alzheimer's disease have demonstrated an increased amount of farnesyl-phosphates in grey and white matter suggesting a specific targeting of isoprenoid regulation (Eckert et al., 2009).

FT has also been shown to be important for farnesylation of the core PCP pathway component PRKL (Mapp et al., 2011). PRKL has a C-terminal CAAX motif and requires an association with the membrane as well as other proteins in order to properly function; therefore, PRKL is an ideal candidate for farnesylation by FT. Zebrafish have two Prickle 1 isoforms: ZPrkl1a and ZPrkl1b (Mapp et al., 2011). It has been shown that Zebrafish Vang2, Prkl1a and 1b, Fz, Celsr, and Scrib are all required for the characteristic tangential migration of the facial branchiomotor neurons (FMBNs) through the segmented hindbrain (Bingham et al., 2010; Mapp et al., 2011). While ZPrkl1b is important for proper FMBN migration in an FT dependent manner, it

functions in a nuclear fashion, independent of the PCP pathway (Mapp et al., 2011). FT is required for the nuclear localization and function of ZPrkl1b in neuronal migration of FMBNs (Mapp et al., 2011). The CAAX domain proves to be even more important for proper function and localization than the nuclear localization signals for ZPrkl1b (Mapp et al., 2011). Since ZPrkl1b has been shown to also interact with Vang2, it is possible that Vang2 removes ZPrkl1b from the nucleus, thereby terminating the tangential migration of the FMBNs (Bingham et al., 2010; Mapp et al., 2011). Through studying FMBN tangential migration in Zebrafish, it was determined that FT is responsible for the farnesylation of PRKL; a component of the PCP pathway.

1.1.2 Extracellular Polarity Cues

The asymmetrical localization of the core proteins is critical for the correct function of the planar cell polarity pathway and proper polarization. As the PCP pathway continues to be researched, the mechanisms of the core components are becoming better explained; however, the inducing signal of the symmetry breaking event remains controversial. The symmetry breaking event is essential for proper polarity and is believed to be a response to an asymmetrically distributed extracellular cue (Axelrod, 2009; Bayly and Axelrod, 2011; Goodrich and Strutt, 2011; Ma et al., 2003; Vladar et al., 2009). These cues have the ability to interact with PCP transmembrane proteins, or at a minimum, they have the ability to influence the localization of PCP transmembrane proteins (Axelrod, 2009; Bayly and Axelrod, 2011; Goodrich and Strutt, 2011; Ma et al., 2003; Vladar et al., 2009). As FZ and VANG are transmembrane receptors for the PCP pathway, proteins that interact with FZ and VANG are prime

candidates for global PCP cues. Several candidate cues that are being studied intensively include the Wnt ligands and cadherins such as Fat and Daschous (DS).

Wnts were first considered to be an extracellular positional cue because Fz belongs to the Wnt receptor family (Axelrod, 2009; Bhanot et al., 1996). Wnts are secreted glycoproteins that can act over long distances (Logan and Nusse 2004; Prasad and Clark, 2006). They have been demonstrated to control many developmental processes such as asymmetric cell division, cell fate determination, axonal guidance and tissue polarity (Prasad and Clark, 2006). Wnts are palmitoylated, which is important for forming lipid rafts, packaging for secretion as well as associating with lipoprotein particles (Panakova et al., 2005; Zhai et al., 2004). There are numerous Wnt homologues for both invertebrates and vertebrates. While all Wnt ligands have the ability to interact with Fz receptors, the majority of Wnt homologues function to activate the canonical Wnt/Fz pathway(ref) (Logan and Nusse, 2004; Montcouquiol et al., 2006). As of recently, only a few homologues have been discovered to interact with Fz in vertebrate PCP pathways: Wnt11, Wnt7a and Wnt5a (Keller, 2002; Le Grand et al., 2009; Montcouquiol et al., 2006; Moon et al., 1993; Qian et al., 2007; Tada and Smith, 2000; Vivancos et al., 2009).

Wnt 11 has been proven to play a role in convergent extension (CE), a critical process of embryogenesis that determines the body plans of organisms (Keller, 2002; Tada and Smith, 2000). CE occurs during gastrulation and is a result of several rounds of medio-laterally directed cell intercalation resulting in a closure of the blastophore and simultaneous elongation of the AP axis (Keller, 2002). Cells first elongate and intercalate

radially within the plane of the tissue (Keller, 2002). This is followed by a convergence and extension of medio-lateral intercalation cells to form a narrower but longer sheet (Keller, 2002). CE is partially controlled by the PCP pathway as over-expression or removal of the core PCP proteins Dsh, Vang, Fz, and Prkl results in a failure of CE (Keller, 2002). Through over-expression and inhibition experiments, *Xenopus larvae* Wnts have also been included in the PCP pathway for controlling CE movements (Tada and Smith, 2000).

Xenopus larvae Wnt11 (XWnt11) is expressed in many tissues throughout convergent extension. A dominant negative protein XWnt11 displays the same phenotypes as a Dsh knockout in *Xenopus larvae* embryos indicating the possible interaction of XWnt11 in the PCP pathway (Tada and Smith, 2000). Further analysis reveals that XWnt11 CE defects can be rescued by a non-canonical specific signalling Dsh protein providing convincing evidence for XWnt11 involvement in activating the PCP pathway (Tada and Smith, 2000). Mutations in Wnt5a also results in a failure of convergent extension as well as mouse inner ear development (Moon et al., 1993; Qian et al., 2007).

Hearing defects and deafness in mice can be a result of an improper functioning PCP pathway (Axelrod, 2009; Vladar et al., 2009; Wang and Nathans, 2007). Mutations in Vang, Fz, Dsh and Prkl all lead to inner ear defects in the Organ of Corti (Vladar et al., 2009). These defects are a result and characteristic of the PCP pathways involvement in CE and hair orientation (Wang and Nathans, 2007). Over-expression or lack of expression of Wnt5a also results in cochlear defects (Qian et al., 2007). Wnt5a

knockouts *in vivo* and *in vitro* results in a shortened and widened cochlear duct consistent with and indicative of CE defects (Qian et al., 2007). Wnt5a knockouts also display imperfect stereocilia bundle alignment within the Organ of Corti as well as an extra, but incomplete, row of stereocilia bundles (Qian et al., 2007). Not only do the Wnt5a cochlear CE and hair cell defects implicate Wnt5a involvement in the PCP pathway, but Vangl2 protein localization is also affected in Wnt5a knockouts (Qian et al., 2007). In wild type mice cochlea, Vangl2 is localized to the junctions between hair cells and supporting cells on the medial side of the hair cells (Qian et al., 2007). Absence of such localization In Wnt5a knockout mice further implicates and confirms a role for Wnt5a as a global PCP cue.

Vangl2 localization is also affected by Wnt7a in mouse satellite stem cells (Le Grand et al., 2009). Mouse satellite stem cells represent a small population of the muscle cells and are responsible for maintaining their population through self-renewal (Le Grand et al., 2009). Acting through Fz7 receptor, Wnt7a activates the PCP pathway and controls localization of PCP proteins, such as Vangl2 protein, to ensure proper function of mouse satellite stem cells grown in culture (Le Grand et al., 2009). Through studies in mice and frogs, Wnts (in particular Wnt7a, Wnt5a and Wnt11) have been demonstrated to act as a global PCP cue.

Although Wnts are involved in the PCP pathway and Fz is a member of the wnt receptor family, controversy remains over the role of Wnts as a global PCP cue. This controversy stems from the fact that while Wnts have been shown in some systems to act upstream and activate Fz in a PCP pathway dependent manner, experiments in other

systems have disproven Wnts as a global PCP cue (Chen et al., 2008; Goodrich and Strutt, 2011; Lawrence et al., 2002). Notably, in the original and classical example of the PCP pathway, the fly wing and eye, there is no evidence to date that Wnts play a role in activating the PCP pathway (Lawrence et al., 2002). Experiments including single and multiple knockouts of Wnts have no effect on polarity in the fly wing or the eye (Lawrence et al., 2002). This has led to the discovery of other possible activators of the PCP pathway including the Fat/Dachous (Ds) pathway; whose function is best exemplified in the *Drosophila* eye.

The *Drosophila* compound eye formation is a result of many cell fate and morphogenetic mechanisms leading to the formation of highly precise and complex patterning of ommatidia (Carthew, 2007; Strutt and Mlodzik, 1995; Strutt and Strutt, 2002; Zheng et al., 1995). The development occurs over a period of 2 days in which unorganized and freely dividing cells pass through an anteriorly migrating morphogenetic furrow to become highly polarized and form complex rows of ommatidia (Figure 1E) (Carthew, 2007; Strutt and Mlodzik, 1995; Strutt and Strutt, 2002; Zheng et al., 1995). As the ommatidia emerge from the furrow they rotate up to 90 degrees away from the anterio-posterior axis (Figure 1E) (Carthew, 2007; Strutt and Mlodzik, 1995). Dorsal and ventral ommatidia rotate in opposite directions establishing a dorso-ventral midline known as the equator (Figure 1E) (Carthew, 2007; Strutt and Mlodzik, 1995). Another characteristic of dorsal and ventral ommatidia is their chirality. During rotation, the ommatidia lose symmetry and adopt one of two chiral forms defined by the asymmetric packing of eight photoreceptors (Figure 1E) (Carthew, 2007; Cooper and

Bray, 1999; Strutt and Mlodzik, 1995; Wang and Nathans, 2007; Zheng et al., 1995). The differences in rotation and chirality between the dorsal and ventral ommatidia create mirror images between the dorsal and ventral sides of the eye (Carthew, 2007; Cooper and Bray, 1999; Strutt and Mlodzik, 1995; Wang and Nathans, 2007; Zheng et al., 1995).

Polarity in the *Drosophila* eye is a result of both the rotational direction and the chirality of ommatidia. This polarity is defined by the differentiation of the R3/R4 photoreceptor cells (Axelrod, 2009; Cooper and Bray, 1999; Vladar et al., 2009; Zheng et al., 1995). Fz is thought to receive a signal from the equator that affects the Notch signaling in the equipotent R3/R4 pair forming a Notch gradient (Axelrod, 2009; Cooper and Bray, 1999; Zheng et al., 1995). This competition for Notch signaling leads to an equatorial differentiation of the R3 photoreceptor and a polar R4 photoreceptor (Axelrod, 2009; Cooper and Bray, 1999). Mutations in PCP components such as Fz and Dsh result in a loss of the DV equator due to random rotational directions as well as random selection of chiralities by the ommatidia (Figure 1F) (Cooper and Bray, 1999; Strutt and Strutt, 2002; Zheng et al., 1995). Mutations in the atypical cadherins Fat and Ds also result in polarity defects of ommatidia in an R3/R4 differentiation dependent manner (Axelrod, 2009; Strutt and Strutt, 2002).

Fat and Ds are non-classic cadherins in that they contain an abnormally large amount of extracellular cadherin repeats and they are located apically but not within the adheren junctions (Ma et al., 2003; Matakatsu and Blair, 2004; Tepas et al., 2000). It is proposed that Fat cadherins function either directly or indirectly as receptors for Ds cadherins (Ma et al., 2003; Matakatsu and Blair, 2004). Fat is uniformly distributed

throughout tissues while Ds has a definite gradient (Axelrod, 2009, Ma et al., 2003; Matakatsu and Blair, 2004; Strutt and Strutt 2002). Upon interaction with a golgi resident transmembrane protein Four-jointed (Fj), also found in a gradient, Fat becomes receptive to Ds creating more Fat-Ds heterodimers in one orientation resulting in a Fat-Ds gradient (Axelrod, 2009; Ma et al., 2003). It is this interaction between the Fj sensitive Fat and the Ds gradient that creates a polarized environment, ensuring proper cellular orientation (Axelrod, 2009; Ma et al., 2003; Strutt and Strutt, 2002).

Several experiments implicate the Fat/Ds pathway as a global PCP cue (Ma et al., 2003; Matakatsu and Blair, 2004; Simon, 2004; Strutt and Strutt, 2002). Loss-of-function studies in *Drosophila* have shown that mutations in Fat, Ds or Fj result in a loss of polarity in the eye (Ma et al., 2003). In addition, mutations in the Fat/Ds pathway also affect PCP core protein localizations (Ma et al., 2003; Matakatsu and Blair, 2004; Simon, 2004; Yang et al., 2002). Although loss-of-function phenotypes from Fat/Ds pathway mutation experiments suggest interaction with the PCP core proteins, the mechanism of interaction is still unknown. There are also several experiments that can refute the possibility of the Fat/Ds pathway acting as a global PCP cue (Casal et al., 2006; Ma et al., 2003; Yang et al., 2002).

Mutations within the Fat/Ds pathway result in a loss of polarity in the *Drosophila* eye; however, they are not exactly similar to PCP loss-of-function phenotypes (Casal et al., 2006; Lawerence et al., 2007; Ma et al., 2003; Yang et al., 2002). PCP loss-of-function phenotypes results in a loss of cell fate differentiation between the R3/R4 photoreceptor and subsequent disorientation along the tissue axes (Cooper and Bray,

1999; Yang et al., 2002; Zheng et al., 1995). Fat/Ds pathway loss-of-function phenotypes demonstrate that ommatidia have correctly polarized R3/R4 photoreceptors; however, the ommatidia are oriented in a random direction with regards to the tissue axes (Yang et al., 2002). As well, in core PCP loss-of-function mutants, an over-expression of Fat/Ds pathway components can be sufficient to restore proper polarity suggesting interaction between the Fat/Ds pathway and similar downstream effectors (Casal et al., 2006). With the addition of an unknown interacting mechanism between the Fat/Ds and PCP pathway, these challenges demonstrate the controversy and uncertainty behind the role of the Fat/Ds pathway as a global PCP cue.

1.2 Neuronal Polarity

Neuronal polarization refers to the specification and differentiation between axons and dendrites. Axons are typically long, thin and propagate signals through use of neurotransmitters while dendrites are typically short, highly branched, and receive and relay signals postsynaptically (Arimura and Kaibuchi, 2005; Craig and Banker, 1994; Ou and Shen, 2011). While it is possible to study the growth of neurons *in situ,* most knowledge of neuronal polarization comes from studying cultured hippocampal neurons (Craig and Banker, 1994; Dotti et al., 1988). Hippocampal neurons grown in culture develop through five morphologically distinct stages to produce a single axon and several dendrites. These five stages of development are highly dynamic and have been used as a model for neuronal polarization. Stage one of neuronal development is defined by the appearance of lamellipodia around the circumference of the neuronal

cell body (Arimura and Kaibuchi, 2005; Craig and Banker, 1994; Dotti et al., 1988). These lamellipodia are small, thin, flat extensions in constant motion and mainly composed of actin filaments (Dotti et al., 1988). The lamellipodia transform with time into small neurites, which is characteristic of stage two of neuronal development (Dotti et al., 1988). The neurites in stage two are approximately equal in length and all appear to have growth cones at their tips suggesting that an axon has yet to be defined (Arimura and Kaibuchi, 2005; Craig and Banker, 1994; Dotti et al., 1988). During stage three of neuronal development one neurite breaks symmetry and rapidly extends becoming the axon and polarizing the neuron (Arimura and Kaibuchi, 2005; Craig and Banker, 1994; Dotti et al., 1988). Several days after the differentiation of the axon, stage four of neuron development occurs: the remaining neurites elongate and acquire dendritic properties (Arimura and Kaibuchi, 2005; Craig and Banker, 1994; Dotti et al., 1988). Stage five of neuronal development is the continued maturation of the already defined axon and dendrites into a mature neuron with synaptic connections to other neurons (Arimura and Kaibuchi, 2005; Craig and Banker, 1994; Dotti et al., 1988). It is clear that the initial stages of neuron development are a result of major polarization events occurring within the neuron. While the polarization of neurons is controlled primarily by external signalling cues, evidence in developing rat hippocampal neurons suggests the presence of an internal neuronal polarization mechanism (Arimura and Kaibuchi, 2005; Bradke and Dotti, 2000; Craig and Banker, 1994).

1.2.1 Intracellular Mechanism

In order to determine the intracellular polarizing mechanism of neuron development, the basic composition of a growing axon must be understood. A developing axon is rich in actin filaments and microtubules that are undergoing constant rearrangements (Arimura and Kaibuchi, 2005; Bradke and Dotti, 1999; Bradke and Dotti, 2000). As microtubules are located within the site of the axon, it is logical to suspect the involvement of microtubule associated proteins (MAPs) as well as tau in the polarization of the neuron. MAPs are known to regulate microtubule stability, while tau has been demonstrated to preferentially bind to microtubules in an emerging axon, thus promoting stability and growth (Halpain and Dehmelt, 2006; Mandell and Banker, 1996). Although the asymmetrical localization of MAPs and tau are important in the developing neuron, their distributions are uniform until the fourth stage suggesting that they do not play an important role in determining neuronal polarization (Caceres et al., 1986; Dotti et al., 1987; Dotti et al., 1988; Mandell and Banker, 1996). Actin filaments are also capable of regulating microtubule organization (Bradke and Dotti, 2000; Halpain and Dehmelt, 2006). Since actin filament rearrangement is needed for axonal growth, the major actin and cytoskeleton regulators of the Rho GTPase family are strongly implicated as being necessary for axonal development (Arimura and Kaibuchi, 2005). Indeed RhoA, Rac1 and Cdc42 have been found to be important not only in axonal development, but also in neuronal polarization (Arimura and Kaibuchi, 2005; Govek et al., 2005). RhoA has typically been found to be involved in neurite retraction through the Rho Kinase ROCK pathway, while Rac1 and Cdc42 have been discovered to promote

neurite extension (Govek et al., 2005). Interestingly, although an overexpression of Rac1 or Cdc42 in neurons increases the quantity and length of extending neurites, it results in fewer mature neurons (Arimura and Kaibuchi, 2005; Govek et al., 2005; Nishimura et al., 2005). Therefore a balance of GDP- and GTP-bound Rac1 and Cdc42 is required for the polarization of one single mature axon (Arimura and Kaibuchi, 2005). The activation of Rac1 has also been identified to activate an important enzyme for neuronal polarization: PI-3 kinase (Arimura and Kaibuchi, 2005; Govek et al., 2005).

A developing neuron undergoes a major internal polarization event during the second and third stage that differentiates the future axon and dendrites. The internal polarization event begins with the accumulation of an enzyme and its lipid product at the site of the future axon. Through studying Akt-pleckstrin homology (PH) domain GFP, it was determined that along with its phospholipid product PIP_3, PI-3 kinase is activated and localized to one side of the cell during stage 1 of cultured hippocampal neuron development (Menager et al., 2004; Shi et al., 2003) . During the second and third stage, both PI-3 kinase and PIP_3 were found to be located in the differentiated axon (Menager et al., 2004). The involvement of PI-3 kinase (PI3-K) in determining the polarity of a neuron is multifold.

PI3-K is important for the axonal localization of a polarity complex consisting of PAR-3, PAR-6 and atypical protein kinase C (aPKC) (Arimura and Kaibuchi, 2005; Nishimura et al., 2005). PAR-3 and PAR-6 are scaffolding proteins which bind to each other, thereby forming a PAR complex (Nishimura et al., 2005). This complex is then transported to the distal tips of neurites by a kinesin-2 motor protein: KIF3 (Nishimura

et al., 2005). At the distal tip of neurites, PI3-K activated Cdc42 binds directly to a PAR-6/PAR-3 complex resulting in the recruitment and activation of aPKC (Arimura and Kaibuchi, 2005; Nishimura et al., 2005). Once formed, the PAR complex has the ability to effect cytoskeleton re-arrangements and regulate axonal growth through effectors (Arimura and Kaibuchi, 2005; Govek et al., 2005; Halpain and Dehmelt, 2006; Nishimura et al., 2005). Upon activation, aPKC has the ability to regulate the phosphorylation activity of GSK-3β (Etienne-Manneville and Hall, 2003; Goold et al., 1999; Gordon-Weeks et al., 1993). The PAR complex is suspected to regulate the stability of microtubules (MT) at the site of future axon growth through a GSK-3β MAP1B pathway (Etienne-Manneville and Hall, 2003; Goold et al., 1999; Gordon-Weeks et al., 1993). The PAR complex is also important for the development of a neurite into an axon because it controls an important positive feedback loop resulting in further growth (Arimura and Kaibuchi, 2005; Nishimura et al., 2005). The PAR complex has the ability to activate Rac1 through the Rac-GEF Tiam1/STEF pathway; Rac1 has the ability to interact with actin filaments as well as to activate PI3-K (Arimura and Kaibuchi, 2005; Menager et al., 2004; Nishimura et al., 2005). Rac-1 induced activation of PI3-K positively reinforces activation of Cdc42 and the PAR complex.

PI3-K also affects neuronal polarization through the Akt/GSK-3β signalling pathway (Arimura and Kaibuchi, 2005). GSK-3β is a constitutively active kinase that phosphorylates proteins such as MAP1B and adenomatous polyposis coil gene product (APC) leading to the destabilization of microtubules (Arimura and Kaibuchi, 2005; Etienne-Manneville and Hall, 2003; Goold et al., 1999). GSK-3β also phosphorylates

collaspin response mediator protein (CRMP-2) thereby inhibiting association between CRMP-2 and tubulin heterodimers as well as CRMP-2 and NUMB (Arimura et al., 2003; Arimura and Kaibuchi, 2005; Nishimura et al., 2003). An expression of constitutively active GSK-3β prevents axon formation through destabilizing microtubules and preventing the endocytosis of adhesion molecules respectively (Arimura and Kaibuchi, 2005; Nishimura et al., 2003). The activity of GSK-3β can be suppressed by an active form of Akt (Arimura and Kaibuchi, 2005). $PIP_{3,}$ the product of PI3-K, is necessary for recruiting Akt to the plasma membrane where it becomes phosphorylated and activated by phosphoinositide-dependent kinase (PDK) (Arimura and Kaibuchi, 2005; Menager et al., 2004). PDK activated Akt phosphorylates GSK-3β preventing its kinase activity (Arimura and Kaibuchi, 2005). Suppressed GSK-3β activity allows CRMP-2, MAP1B, and APC to promote MT stability resulting in axon differentiation and elongation.

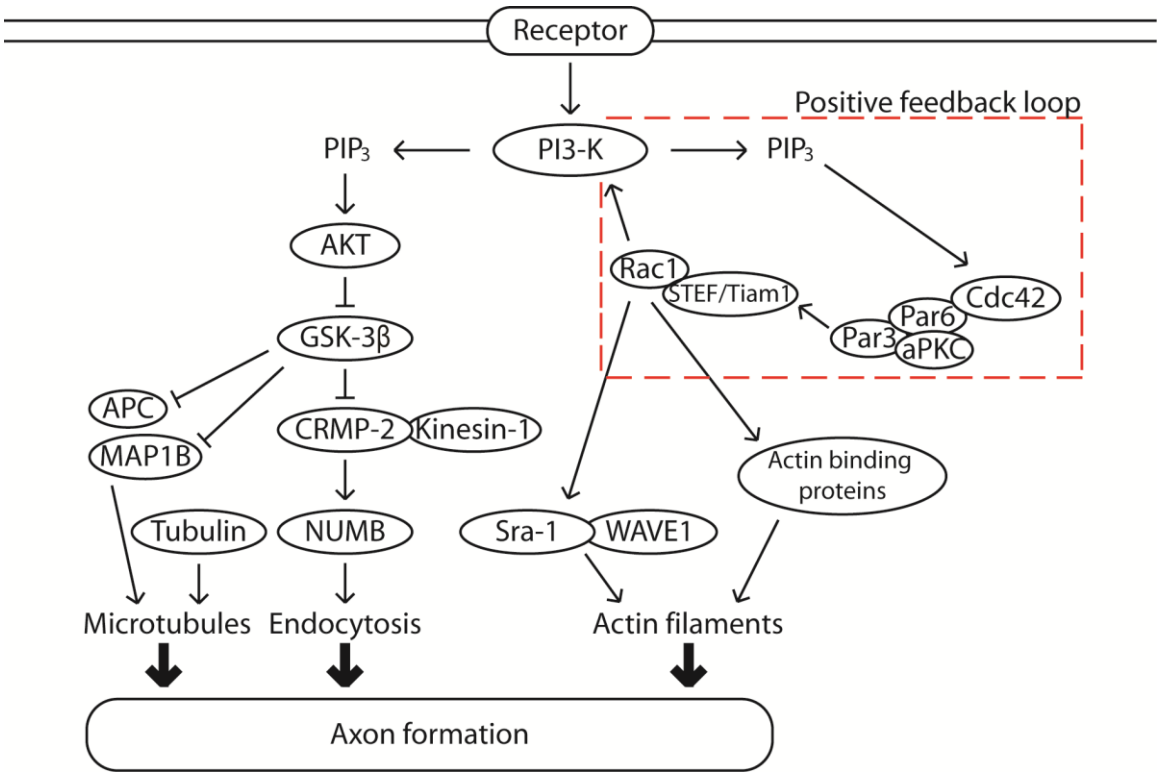

Figure 5. Schematic of molecular mechanism for axon formation. Activation of phosphoinositide 3-kinase (PI3-K) from a receptor at the site of future axon growth leads to an accumulation of phosphatidylinositol (3,4,5)-triphosphate (PIP_3). PIP_3 can promote axon formation through interacting with Cdc42 or the AKT pathway. Cdc42 and the PAR complex create a positive feedback loop resulting in more localized PIP_3 to further destabilize actin filaments creating axon formation. The AKT pathway inhibits GSK-3β resulting in microtubule formation and endocytosis, which are necessary for axon formation.

1.2.2 Planar Cell Polarity Genes Involved in Neuronal Polarity

A developing hippocampal neuron grown in culture has an internal polarization mechanism, but one cannot ignore that the polarity of neurons developing *in vivo* may also be regulated by extrinsic morphogenic factors. Several PCP genes are involved in axonal guidance, cytoskeleton rearrangements and epithelial cell polarity; therefore, the products of planar polarity genes would be good candidates to function as morphogenic factors inducing neuronal polarization. Indeed, several PCP genes have recently been implicated in neuronal polarity (Andersson et al., 2008; Stuebner et al., 2010; Zhang et al., 2007).

Dishevelled is the hub of the planar cell polarity pathway and as such an excellent starting point to discuss the PCP pathway's involvement in neuronal polarity. Dvl has been known to accumulate at the tip of growing axons and at the site of axon formation in isolated cultured hippocampal neurons (Zhang et al., 2007). Although Dvl is involved in the canonical pathway and therefore interacts directly with GSK-3β to inhibit kinase activity, overexpression of Dvl proves to have little effect on the phosphorylation of GSK-3β (Zhang et al., 2007). Rather, overexpression of Dvl results in an increase of activated aPKC, an integral part of the PAR complex that is critical for neuronal polarity (Zhang et al., 2007). Since Dvl has been shown to influence neuronal polarity independent of the canonical Wnt pathway, other PCP genes have since been implicated in neuronal polarity.

In mice and Drosophila, Wnt5a is suggested to be involved in neuronal polarity (Andersson et al., 2008). *In vivo* studies with dopamine neurons in mice have proven

that Wnt5a, acting through Rac1, is important for determining neuronal polarity (Andersson et al., 2008; Blakely et al., 2011). Dopamine neurons form the nigrostriatal, mesocortical and mesolimbic pathways as they are located within the ventral midbrain and project to the striatum and prefrontal cortex (Andersson et al., 2008; Blakely et al., 2011; Stuebner et al., 2010). In Wnt5a knockout mice, PCP defects were observed in A9-A10 dopaminergic neurons in mice between embryonic day 10.5 and 13.5 (Andersson et al., 2008; Blakely et al., 2011). Fz3 knockout mice also display morphogenetic defects in dopamine neurons; however, there are subtle differences in Wnt5a defects and consequently Fz3 is not believed to transduce the Wnt5a PCP-like signal (Stuebner et al., 2010). Other PCP components, including the other Wnt ligands, should be examined to completely rule out a PCP mechanism for the Fz3 morphogenetic defects in the dopaminergic neurons. While Fz3 does not appear to be involved with Wnt5a PCP-like signaling, it is not surprising that both Dvl and Rac1 were discovered to function in the same pathway as Wnt5a, strengthening a role for the involvement of the planar cell polarity pathway during neuronal polarity (Andersson et al., 2008; Blakely et al., 2011; Zhang et al., 2007). Similarly in *Drosophila*, Wnt5a is involved in the neuronal polarity of mushroom body neurons where it acts genetically with the other PCP genes including *fz, dsh,* and *stbm* (Shimizu et al., 2011).

Prkl is concentrated at high levels in the brain especially early in development (Okuda et al., 2007). Prkl is primarily expressed in the cerebral cortex and hippocampus and is important for regulating neurite outgrowth during neuronal development (Okuda et al., 2007). A Prkl knockdown in isolated mice neuroblastoma neuro2a cells yields less

neurite bearing cells suggesting that Prkl is important for the proper differentiation and polarization of neurons (Okuda et al., 2007). The involvement of Prkl in neuronal polarization provides strong evidence towards the importance of PCP signalling during neuronal development. While all the polarity genes have been demonstrated to be important, the mechanism by which polarity is influenced by the PCP pathway is still relatively unknown and therefore more research in this area is required (Montcouquiol et al., 2006).

1.3 *Caenorhabditis elegans*

Caenorhabditis elegans is an excellent choice for a model organism because of its simplicity. When compared to most model organisms, the nematode *C. elegans* has a relatively simple body plan comprising 959 somatic cells forming many of the same organs as higher functioning vertebrates such as the gastrointestinal tract, muscles, an epidermis, as well as a nervous system (Jorgensen and Mango, 2002). The worm also has a simple and rapid life cycle; developing from egg to adult in approximately three days, living up to three weeks, and laying up to 300 eggs in a lifetime (Jorgensen and Mango, 2002). The translucent nature of *C. elegans* makes it relatively easy to view each of the 959 somatic cells at a very high resolution and provides a unique rare opportunity to track cells throughout development (Jorgensen and Mango, 2002). Studying the effects of biological processes *in vivo* provides a better understanding for external interactions that are often difficult to attain through *in vitro* studies.

C. elegans is ideal for studying genetic interactions due to its completely sequenced genome and ease of genetic manipulation. Although the genome is relatively small, consisting of approximately 20 000 genes, much of it is highly conserved in higher order vertebrates (Jorgensen and Mango, 2002). Worms are easy to handle and manipulate genetically. They can be grown on petri dishes or in liquid culture and the hermaphroditic nature of the worm ensures that singular clones maintain the genome throughout future generations (Jorgensen and Mango, 2002). Males provide an opportunity to incorporate new DNA and select mutations into existing genomes (Jorgensen and Mango, 2002). The genome of *C. elegans* can also be easily mutated randomly with a chemical mutagen making them an excellent tool for genetic screens to dissect genetic pathways (Jorgensen and Mango, 2002).

1.3.1 Planar Cell Polarity in *Caenorhabditis elegans*

The planar cell polarity pathway is a conserved pathway important for the development of many organisms including *C. elegans. C. elegans* contains five Wnt ligands (*lin-44, egl-20, cwn-1, cwn-2* and *mom-2*), four Frizzled receptors (*lin-17, mig-1, cfz-2,* and *mom-5*), one Flamingo ortholog (*fmi-1)*, one Van Gogh receptor (*vang-1), three* Dishevelled orthologs (*dsh-1, dsh-2, mig-5*), and one Prickle ortholog (*prkl-1)* (Green et al., 2008; Hawkins et al., 2005; Hilliard and Bargmann, 2006; Hoffmann et al., 2010; Prasad and Clark, 2006; Sanchez-Alvarez et al., 2011; Wu and Herman, 2006; Wu and Herman, 2007). Although the mechanisms and relationships between PCP genes are not entirely understood, it is clear that these PCP genes interact differently to govern different processes in *C. elegans* including cell migration, organogenesis, axon

migration and neuron polarity (Hawkins et al., 2005; Hilliard and Bargmann, 2006; Hoffmann et al., 2010; Prasard and Clark, 2006; Sanchez-Alvarez et al., 2011; Spencer et al., 2001).

1.3.1.1 Blastomere Polarity

Planar polarity genes are important for regulating asymmetric cell divisions and determining cell fate during the development of *C. elegans*. At the four-cell stage of development, the embryo of *C. elegans* is composed of four blastomeres: P2, EMS, ABp and ABa (Walston and Hardin, 2006). EMS cells divide to produce E and MS daughter cells; the E cell will generate all of the endoderm and the MS cell will generate a large portion of the mesoderm (Goldstein, 1993; Goldstein, 1995; Walston and Hardin, 2006). An important interaction in the embryo occurs at the four-cell stage of the embryo in which the EMS cell contacts P2 (Goldstein 1993). With the absence of P2 contact, the EMS cell produces two MS daughter cells, but generates no endoderm (Goldstein, 1993; Walston and Hardin, 2006). Furthermore, when the P2 cell is relocated to the anterior side of the EMS cell, the result is an anterior born E cell rather than a wild type (wt) posterior born E cell (Goldstein, 1993). Therefore P2 induces the polarity of the EMS cell through cell-cell interaction (Goldstein, 1993; Goldstein, 1995a). Examining the division of EMS more closely it is also possible to distinguish a separate polarizing event: the mitotic spindle (Goldstein, 1995b). Cell-cell contact between P2 and EMS polarizes the mitotic spindle, thereby controlling the axis of division of the EMS cell (Goldstein, 1995b). Cell fate and mitotic spindle polarization are believed to be separate events controlled by separate pathways; experiments where P2 is allowed to contact EMS only

after the spindle is oriented still results in gut formation (Goldstein 1995b). Genetic screening has highlighted the importance of PCP genes *mom-2*, *mom-5, dsh-2* and *mig-5* not only for proper spindle orientation but also for the generation of endoderm (Rocheleau et al., 1997; Thorpe et al., 1997). At first, the polarity genes involved in cell fate specification of EMS appear to act through the canonical pathway, as was discovered by the lack of endoderm found in *wrm-1/b-catenin*, and *pop-1/tcf/lef* mutant worms (Rocheleau et al., 1997; Thorpe et al., 1997). This is difficult to discern though as the localization of *pop-1* could be a secondary effect to spindle orientation and not directly involved in the same pathway as the planar polarity genes, as is evidenced by the increase in POP-1 nuclear localization in the MS cell compared to the E cell (Hawkins et al., 2005; Rocheleau et al., 1997; Thorpe et al., 1997; Wu and Herman, 2005). The polarity genes involved in spindle orientation appear to act in a non-canonical fashion as transcription of *pop-1* is not required for proper spindle polarization (Bei et al., 2002; Schlesslinger et al., 1999). It is possible that the separate pathways for gut induction and spindle alignment converge, which could explain the difficulty in determining the mechanisms (Walston et al., 2004)

1.3.1.2 B Cell Polarity

B cell polarity in *C. elegans* is dependent on proper localization and function of PCP pathway components (Wu and Herman, 2006; Wu and Herman, 2007). The B cell in *C. elegans* divides to generate a large anterior dorsal daughter, B.a., and a small posterior ventral daughter B.p (Wu and Herman, 2006). Through translational GFP reporter genes it was discovered that LIN-17/FZ is localized asymmetrically to the

anterior cortex and cytoplasm of B cells (Wu and Herman, 2007). Additionally, the localization becomes symmetrical in a LIN-44/WNT and MIG-5/DSH mutant background (Wu and Herman, 2007). Similar to the *Drosophila* classical PCP pathway, MIG-5/DSH localization is also asymmetrical and dependent upon the proper localization of LIN-17/FZ (Wu and Herman, 2007). Mutations in either of these PCP genes results in a changed polarity of the B cell, which alters the fate of the daughter B cell (Wu and Herman, 2006; Wu and Herman, 2007). Mutations in *mig-5* also result in migration defects of several cells including dorsal and ventral hypodermal cells, Q neuroblasts and the distal tip gonadal cells (Walston et al., 2006). The PCP proteins involved with B cell polarization appear to function in a non-canonical manner as B-catenin homologs WRM-1 and BAR-1 as well as SGG-1/GSK3-B, PRY-1/AXIN and DSH-2 are not involved (Wu and Herman, 2006). Planar polarity genes function in a RHO-1/RHO-A and LET-502/ROCK dependent manner providing further evidence that non-canonical PCP signalling is involved in cytoskeleton rearrangements and *C. elegans* B cell polarization (Wu and Herman, 2006).

1.3.1.3 Vulva Organogenesis

Planar cell polarity components are also important for cell orientation during organogenesis (Green et al., 2008; Hoffman et al., 2010). The *C. elegans* vulva is derived from three precursor cells P5.p, P6.p, and P7.p aligned from anterior to posterior along the ventral epithelium (Green et al., 2008). P6.p undergoes three symmetric divisions that generate primary vulva cells while P5.p and P7.p divide three times to produce secondary vulva cells that display mirror-image symmetry in the anterior-posterior (AP)

plane by orienting towards the anterior and posterior direction respectively (Green et al., 2008). There appears to be two pathways involving planar polarity genes, both regulating the orientation of the secondary vulva cells. There is a non-canonical long range signalling pathway in which *egl-20/wnt,* expressed from the tail hypodermal cells in a gradient, instructively polarizes the vulva cells to orient in the posterior direction through *vang-1* and *ror/cam-1* (Green et al., 2008). Less clear are the downstream effectors of the second short range pathway in which *lin-44* and *mom-2* act redundantly through *lin-17* to re-orient the vulva cells towards the centre of the vulva forming the mirror-symmetry (Green et al., 2008). Although the mechanisms and interactions between the pathways are largely unknown, the involvement of the polarity genes suggests a PCP-like mechanism responsible for cell orientation during organogenesis.

1.3.1.4 VC Neuronal Polarity

Cultured hippocampal cells are an important neuronal polarity model; however, studying neuronal polarization *in vitro* makes it difficult to study the effects of extracellular polarization cues on the internal polarization mechanisms of neurons. Given its relatively simple neuronal system, *C. elegans* is a good model to study the effects of extracellular cues on neuronal polarization *in vivo* (Ou and Shen, 2011). The worm has several neurons with simple morphology that are ideal to study neuronal polarization including the ventral cord type C (VC) neurons.

A

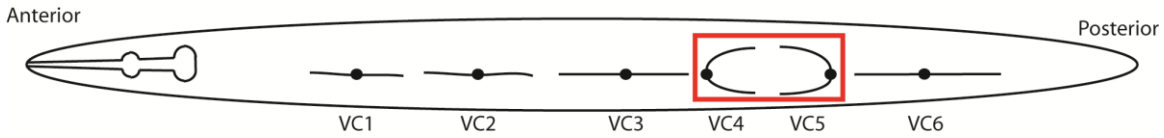

B

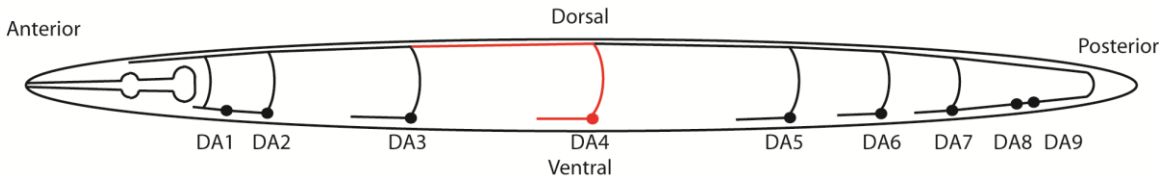

Figure 6. *C. elegans* VC and DA neuron schematic. (A) VC1-3 and VC6 each extend two neurites along the ventral cord. VC4 and VC5 each extend two neurites around the vulva in the medio-lateral plane. The image is a ventral view of the worm. **(B)** The location of DA neurons. Each DA neuron sends an axon to the dorsal side of the worm where it extends anteriorly to innervate dorsal muscles and provide backwards locomotion. DA5 is located immediately posterior to the vulva. The image is a lateral view of the worm.

VC neurons are a set of six peripheral motor neurons that mediate egg laying behaviour (Figure 4A) (White et al., 1986). All six VC neurons are bipolar neurons that are located along the ventral cord in the AP axis (White et al., 1986). The distal neurons VC1-3 and VC6 extend neurites along the AP axis, whereas VC4 and VC5 extend processes in the medio-lateral (ML) axis to surround the left and right sides of the vulva (Figure 4A) (Sanchez-Alvarez et al., 2011). The ML polarization of VC4 and VC5 ensures that connections are formed with the vm2 vulva muscles as well as with the HSN neuron which also mediates egg laying behaviour (White et al., 1976). VC4 and VC5 provide an excellent model to study neuronal polarity *in vivo* as they have simple morphologies that differ from the other VC neurons. While the directional cues that polarize VC4 and VC5 to innervate the vulva are not known, Sanchez-Alvarez et al. (2011) have discovered that polarity genes are involved in the polarization of VC4 and VC5.

Genetic interactions between *vang-1* and *prkl-1* negatively regulate neurite formation in VC4 and VC5 (Sanchez-Alvarez et al., 2011). Worms with mutations in *vang-1, prkl-1* or *dsh-1* display the presence of an ectopic neurite in VC4 and VC5, extending anteriorly and posteriorly, respectively (Sanchez-Alvarez et al., 2011). Furthermore, over-expression analysis of *prkl-1* results in a suppression of the wild-type medio-lateral neurite outgrowth in VC4 and VC5, transforming the bi-polar morphology of VC4 and VC5 neurons to mono-polar (Sanchez-Alvarez et al., 2011). Through the use of double mutants, *vang-1* and *prkl-1* were demonstrated to interact in the same pathway (Sanchez-Alvarez et al., 2011). Interestingly, none of the WNTS or FZs appear to be involved with the polarity of the VC neurons including *lin-44/wnt, egl-20/wnt*, and

lin-17/fz (Sanchez-Alvarez et al., 2011). While knockout mutations in *lin-44, egl-20,* and *lin-17* all create polarity defects in the ALM and PLM neurons, no such polarity defects arise in VC4 and VC5 suggesting an alternative PCP-like pathway may be involved in neuronal polarization (Prasad and Clark, 2006; Sanchez-Alvarez et al., 2011).

1.4 Summary and Rational

While planar cell polarity components have been shown to regulate neuronal polarity, the complete picture of the pathway has yet to be determined (Prasad and Clark, 2006; Sanchez-Alvarez et al., 2011). The polarity of VC4 and VC5 in *C. elegans* is partially regulated by VANG-1 and PRKL-1 cooperating to suppress neurite outgrowth and by DSH-1 (Sanchez-Alvarez et al., 2011). The mechanism of action of the polarity components in VC4 and VC5 are still unknown and this mechanism does not appear to be identical to that of the classical *Drosophila* PCP pathway. Therefore, utilizing the genetic characteristics of *C. elegans,* a genetic screen may discover more polarity components involved in regulating neuronal polarity of VC4 and VC5. The discovery of additional PCP components would provide further insight into the unknown polarity mechanism.

An over-expression of *prkl-1* specifically expressed in neurons results in a suppression of neurite extension and a mono-polar phenotype of VC4 and VC5 (Sanchez-Alvarez et al., 2011). In addition to mono-polar VC4 and VC5 neurons, one of the consequences of *prkl-1* over-expression in motor neurons is that worms display an

inability to move backwards (Sanchez-Alvarez et al., unpublished data). Since *vang-1* has been known to function upstream in the same pathway as *prkl-1*, backwards locomotion should be restored by introducing a *vang-1* null mutant into the over-expressed *prkl-1* transgenic animals. If the polarity gene *vang-1* can rescue the *prkl-1* defect by restoring backwards locomotion, then it stands to reason that it is possible to rescue backwards locomotion with other polarity genes involved in neuronal polarity. Using an integrated transgenic worm line, a *prkl-1* suppressor screen was conducted in this study looking for restored backwards locomotion to find novel polarity genes involved in VC4 and VC5 polarization.

The *prkl-1* suppressor screen identified a relatively new polarity component: *fntb-1.* FNTB-1 is the β-subunit for farnesyltransferase. FNTB-1 is responsible for attaching the farnesyl group to the recognized protein containing a CAAX motif that is bound to the FNTA subunit. Interestingly enough PRKL-1 in *C. elegans* has a CAAX motif at its C-terminus: CTVS. The role of *fntb-1* has not yet been studied and characterised in *C. elegans* neuronal polarization; therefore this study also attempts to characterize the role of *fntb-1* in regulating VC4 and VC5 polarization.

1.5 Objectives

I. Determine if the *prkl-1* over-expression induced backwards locomotion defect can be used as an assay to screen for new polarity genes.

II. To conduct a *prkl-1* suppressor screen to discover new polarity genes that can restore backwards locomotion and regulate VC4 and VC5 polarity.

III. To characterize the role of *fntb-1* in VC4 and VC5 polarization

1.6 Hypothesis

1. It will be possible to discover novel PCP genes involved in polarizing VC4 and VC5 by conducting a *prkl-1* suppressor screen.

2. The novel polarity gene *fntb-1* is responsible for farnesylating *prkl-1* to negatively regulating neurite outgrowth in VC4 and VC5.

CHAPTER 2

METHODS

2.1 Strains

2.1.1 Strains used in this study

The *C. elegans* worms in this study were handled, cultured and manipulated as per the techniques defined by Brenner (1974). The worms used in the study were grown on nematode growth medium (NGM) plates that were streaked with *Escherichia coli OP50*. The *C. elegans* wild type strain used in this study was the N2 Bristol strain and all experiments were performed at 20°C unless otherwise stated. The following strains and transgenic lines were used in this study and acquired from the *C. elegans* Genetic Centre unless otherwise stated:

Linkage Group (LG) IV: *prkl-1 (ok3182), fntb-1 (e6.1), fntb-1 (AS24)*

LG X: *vang-1 (tm1422)*

N2; *punc-4::gfp::prkl-1*

N2*; punc-129::gfp*

N2; *punc-129::gfp; punc-4::gfp::prkl-1*

N2; *cyIs4 (pcat-1::gfp; rol-6 (su1006))*

punc-4::gfp::prkl-1; vang-1 (tm1422)

punc-129::gfp; punc-4::gfp::prkl-1; vang-1 (tm1422)

vang-1 (tm1422); cyIs4

prkl-1 (ok3182); cyIs4

fntb-1 (e6.1); cyIs4

fntb-1 (AS24); cyIs4

Ex[pfntb-1::gfp]; N2

Ex[pprkl-1::gfp]; N2

fntb-1 (e6.1); prkl-1 (ok3182); cyIs4

fntb-1 (AS24); prkl-1 (ok3182); cyIs4

Ex[pfntb-1::fntb-1 (40 ng μl^{-1}); podr-1::rfp (40 ng μl^{-1})]; fntb-1 (e6.1); cyIs4

Ex[punc-4::fntb-1 (40 ng μl^{-1}); podr-1::rfp (40 ng μl^{-1})]; fntb-1 (e6.1); cyIs4

Ex[punc-4::fntb-1 (40 ng μl^{-1}); podr-1::rfp (40 ng μl^{-1})]; fntb-1 (AS24); cyIs4

Ex[pcol-10::fntb-1 (40 ng μl^{-1}); podr-1::rfp (40 ng μl^{-1})]; fntb-1 (e6.1); cyIs4

Ex[pcol-10::fntb-1 (40 ng μl^{-1}); podr-1::rfp (40 ng μl^{-1})]; fntb-1 (AS24); cyIs4

Ex[punc-4::gfp::prkl-1 (40 ng μl^{-1}); podr-1::rfp (40 ng μl^{-1})]; prkl-1 (ok3182); cyIs4

Ex[pcol-10::gfp::prkl-1a (40 ng μl^{-1}); podr-1::rfp (40 ng μl^{-1})]; prkl-1 (ok3182); cyIs4

Ex[pcol-10::gfp::prkl-1b (40 ng μl^{-1}); podr-1::rfp (40 ng μl^{-1})]; prkl-1 (ok3182); cyIs4

Ex[punc-4::gfp::prkl-1a ΔCAAX (40 ng μl^{-1}); podr-1::rfp (40 ng μl^{-1})]; prkl-1 (ok3182); cyIs4

Ex[punc-4::gfp::prkl-1a CNIM (40 ng μl^{-1}); podr-1::rfp (40 ng μl^{-1})]; prkl-1 (ok3182); cyIs4

Ex[punc-4::gfp::prkl-1 (40 ng μl^{-1}); podr-1::rfp (40 ng μl^{-1})]; fntb-1 (e6.1); cyIs4

Ex[punc-4::gfp::prkl-1 (40 ng μl^{-1}); podr-1::rfp (40 ng μl^{-1})]; fntb-1 (AS24); cyIs4

Ex[punc-4::gfp::prkl-1α ΔCAAX (40 ng μl^{-1}); podr-1::rfp (40 ng μl^{-1})]; fntb-1 (e6.1); cyIs4

Ex[punc-4::gfp::prkl-1α ΔCAAX (40 ng μl^{-1}); podr-1::rfp (40 ng μl^{-1})]; fntb-1 (AS24); cyIs4

Ex[punc-4::gfp::prkl-1α CNIM (40 ng μl^{-1}); podr-1::rfp (40 ng μl^{-1})]; fntb-1 (e6.1); cyIs4

Ex[punc-4::gfp::prkl-1α CNIM (40 ng μl^{-1}); podr-1::rfp (40 ng μl^{-1})]; fntb-1 (AS24); cyIs4

Ex[punc-4::gfp::prkl-1 (40 ng μl^{-1}); podr-1::rfp (40 ng μl^{-1})]; fntb-1 (e6.1); prkl-1 (ok3182); cyIs4

Ex[punc-4::gfp::prkl-1 (40 ng μl^{-1}); podr-1::rfp (40 ng μl^{-1})]; fntb-1 (AS24); prkl-1 (ok3182); cyIs4

Ex[punc-4::gfp::prkl-1α ΔCAAX (40 ng μl^{-1}); podr-1::rfp (40 ng μl^{-1})]; fntb-1 (e6.1); prkl-1 (ok3182); cyIs4

Ex[punc-4::gfp::prkl-1α ΔCAAX (40 ng μl^{-1}); podr-1::rfp (40 ng μl^{-1})]; fntb-1 (AS24); prkl-1 (ok3182); cyIs4

Ex[punc-4::gfp::prkl-1α CNIM (40 ng μl^{-1}); podr-1::rfp (40 ng μl^{-1})]; fntb-1 (AS24); prkl-1 (ok3182); cyIs4

Ex[punc-4::gfp::prkl-1 (40 ng μl^{-1}); podr-1::rfp (40 ng μl^{-1})]; prkl-1 (ok3182); plin-11::rfp

Ex[punc-4::gfp::prkl-1α ΔCAAX (40 ng μl^{-1}); podr-1::rfp (40 ng μl^{-1})]; prkl-1 (ok3182);

plin-11::rfp

Ex[punc-4::gfp::prkl-1 (40 ng μl^{-1}); podr-1::rfp (40 ng μl^{-1})]; prkl-1 (ok3182); fntb-1 (AS24); plin-11::rfp; cyIs4

Ex[punc-4::gfp::prkl-1α ΔCAAX (40 ng μl^{-1}); podr-1::rfp (40 ng μl^{-1})]; prkl-1 (ok3182); fntb-1 (AS24); plin-11::rfp; cyIs4

2.1.2 Transgenic strains created

Transgenic animals used in this study were created by the use of standard micro-injections techniques and genetic crosses (Brenner, 1974; Mello et al., 1991; Mello and Fire, 1995). To introduce extra-chromosomal (Ex) DNA into the nematode genome, young adults were first placed in hydrocarbon oil and embedded on air-dried 2% agarose gel pads. Capillary glass needles used to perform the injections were created by using a Sutter P-97 microelectrode needle puller and loaded with an injection mix of the desired extra-chromosomal DNA, a co-injection marker to identify transgenic animals, and a pSK carrier vector. Using a Ziess Axiovert microscope with a 40X objective and an Eppendorf FemtoJet Microinjector equipped with a micro-manipulator, the desired plasmids were injected into the gonads of young adult worms. After injection, a drop of M9 solution (22 nM KH_2PO_4, 22 mM Na_2HPO_4, 85 mM NaCl, and 1 mM $MgSO_4$) was placed on top of the hydrocarbon oil to hydrate and dislodge the worms from the agarose pad. The worms were then placed in M9 on an NGM plate seeded with *E. coli OP50* and allowed to recover. Using a fluorescence Ziess Stemi SV II Apo Stereomicroscope, the progeny of the injected worms (F1 population) were screened for

the presence of the co-injection marker (*podr-1::rfp)* and cloned to a NGM plate seeded with *E. coli OP50*. The F2 generation was screened again to ensure inheritance of the extra-chromosomal DNA.

After the first transgenic animals were created via microinjection, subsequent transgenic animals were created by crossing the extra-chromosomal DNA into different backgrounds and selecting for homozygous animals based on genotyping and expression of the co-injection marker. The genetic crosses ensure similar transgenic expression between different genetic lines.

2.1.3 Genotyping

Strains in this study were genotyped based on visual confirmation and polymerase chain reaction (PCR) analysis. Both *fntb-1* mutant alleles used in this study are closely linked to the VC4 and VC5 marker *cyIs4* allowing *fntb-1*$^{-/-}$ animals to be identified by using a fluorescence Ziess Stemi SV II Apo Stereomicroscope to visualize GFP expression. All other mutants were genotyped based on PCR analysis. Approximately ten to twenty worms were placed in PCR tubes containing a 10 µl solution of lysis buffer (50 mM KCl, 10 mM Tris-HCl pH 8.2, 2.5 mM MgCl2, 0.45% NP-40, 0.45% Tween-20, 0.01% gelatine, 60 µg/ml proteinase K). The PCR tubes were frozen in a Thermoforma -80°C fridge for 30 min. After freezing, the genotyping samples were then incubated in a BioRad PCR machine at 60°C for 1 hour followed by 95°C for 15 min. Following lysis, a 20 µl PCR reaction was performed using 1 µl of the lysate as the DNA template and a mixture consisting of 2 µl of 10X New England Biolabs PCR Buffer, 0.75 µl of 10 pmol for each of the primers (Appendix A), 0.88 µl of 2 mM dinucleotide triphosphates (dNTP), 0.1 µl of

New England Biolabs *Taq* DNA Polymerase, and molecular grade H_2O to 20 µl. The general PCR reaction for genotyping was as follows: 94°C for 2 min, a 5 to 10 cycle repeat of 94°C for 10 sec, 63°C stepping down 1°/cycle to 52°C for 30 sec, and 68°C for 30 sec, 25 cycles of 94°C for 10 sec, 52°C for 30 sec, and 68°C for 30 sec followed by 7 min holding at 68°C. The PCR samples then underwent gel electrophoresis on a 1% agarose gel to determine homozygous worm lines. The specific primers for genotyping reactions, the melting temperatures and recognition band sizes can be found in Appendix A.

2.2 Genetic Screen

2.2.1 Ethyl Methanesulfonate Mutagenesis

The Ethyl methanesulfonate mutagenesis was performed as described in Jorgensen (2002). The transgenic *punc-4::gfp::prkl-1* worms were synchronized on several NGM plates seeded with *E. coli OP50* until the L4 developmental stage. Each plate was washed with approximately 2 ml of M9 and collected into a 15 ml falcon tube. The 15 mL falcon tube containing the *punc-4::gfp::prkl-1* worms was centrifuged at 1000 rpm for 30 sec. After centrifugation, the liquid supernatant was aspirated without disturbing the worm pellet at the bottom and the washing process was repeated. Following washing, the worms were re-suspended in 4 ml of M9 and 20 µl of EMS was added so that the final concentration of EMS was 0.05 M. Ethyl methanesulfonate is a chemical mutagen that induces mutations at an approximate rate of one mutation per gene for every 2 000 genomes screened (Jorgensen, 2002). The *punc-4::gfp::prkl-1* worms were left in the EMS solution on a rotator for 4 hours before being washed twice

with M9. The worms were then placed on NGM *E. coli OP50* seeded plates using sterilized glass Pasteur pipettes and allowed to recover. After 30 min of recovery, L4 worms were transferred to new plates where they laid eggs for up to three days. The L4 mutagenized worms are known as the P0 population and their progeny the F1 population. The F1 population was transferred to new NGM *E. coli OP50* seeded plates, five worms per plate, and allowed to lay eggs. The F2 population was then screened using a Leica M60 Dissecting Microscope for recovery of backwards locomotion (Figure 5C).

2.2.2 Phenotype Analysis

2.2.2.1 Locomotion

Backwards locomotion in *C. elegans* is controlled by the A-type neurons: DA and VA (Figure 6A) (White et al., 1992). The DA and VA neurons innervate dorsal and ventral muscles respectively (Miller and Niemeyer, 1995; White et al., 1992). The complimenting muscle innervation of the A-type neurons results in a smooth, sinusoidal and undulating type of backwards locomotion. Touching the head of the worm elicits a behaviour response to tactile stimulation resulting in backwards locomotion; therefore, backwards locomotion was assessed by gently prodding the worms on the head with a platinum tipped wire and observing the response using a Leica M60 Dissecting Microscope.

There are many ways in which locomotion can be quantified in *C. elegans* including measuring the amplitude and the distance between successive peaks in the

path of the worm (Tavernarakis et al., 1997). Since the screen in this study focuses on the recovery of backwards locomotion, not all worms will display backwards locomotion; therefore, we decided to simplify the categorization of backwards locomotion into three categories: wild type, partial, and no backwards locomotion (Figure 5B). Wild type backwards locomotion is defined by the smooth, sinusoidal and undulating backwards movement. No backwards locomotion is defined by the worm curling into a ball and displaying no backwards movement. Partial backwards locomotion includes all types of backwards movement that is not wild type.

2.2.2.2 DA neurons

There are nine DA neurons located in the *C. elegans* ventral cord (Figure 4B) (White et al., 1992). Each DA neuron sends a commissure to the dorsal side of the worm where it extends in the anterior direction to innervate dorsal muscles important for backwards locomotion (Figure 4B) (Miller and Niemeyer, 1995; White et al., 1992). The DA neurons can be visualized with a DA and DB neuron specific marker: *punc-129::gfp*. Similar to DA neurons, DB neurons extend a commissure to the dorsal side of the worm; however, the DB axon extends in the posterior direction after the commissure to innervate dorsal muscles important for forwards locomotion. Since the marker illuminates DA and DB neurons, it was necessary to study DA neurons that could be easily identified using a landmark of the worm. DA5 is located just posterior to the vulva, making it the easiest to identify. DA and DB neurons alternate positionally along the ventral cord so that DB neurons are located anterior to the DA neurons. For example, DA5 is located just posterior to the vulva while DB5 is located immediately

anterior to the vulva. The alternating characteristics of the DA and DB neurons allow for easy identification of DA4 and DA3; therefore, DA3, DA4, and DA5 were chosen to study DA morphology defects. DA morphology defects were analyzed using an LED Colibri epifluorescent Zeiss AxioImager M2 Microscope with various objective lenses.

2.2.2.3 VC4 and VC5 neurons

VC4 and VC5 extend two neurites in the ML plane to each side of the vulva innervating vm2 vulva muscles and the HSN (White et al., 1976). An LED Colibri epifluroescent Zeiss AxioImager M2 Microscope with a 63x objective lens was used to visualize and classify the polarity of the VC4 and VC5 neurons in transgenic animals expressing the VC4 and VC5 neuron specific marker *cyIs4 (pcat-1::gfp)*. In this study, a neurite is defined as a protrusion from the cell body that is at least the length of the cell body. A change of polarity in the VC4 and VC5 neuron is defined as any difference in the number and location of neurites from wild type. The ectopic neurite defect is defined as any VC4 or VC5 neuron that extends a neurite in the AP direction including bi-polar AP neurons and tri-polar neurons. For each independent genomic line, a single worm was cloned to three separate plates and their progeny was scored for neurite defects. A X^2 test was then performed to determine significant differences of neurite defects.

2.3 Molecular Cloning and Creation of DNA constructs

DNA constructs used in this study were created by fusion PCR and standard molecular cloning techniques (Fire et al., 1990). The vector backbone used for all plasmids was pPD95.77. Digestion and ligation reaction mixtures and temperatures

were specific to each plasmid created and can be found below. A rapid and an overnight ligation were performed for each vector to increase the probability of proper ligation. The insert to vector ratio for all ligations was calculated using the following equation: Insert mass (mg) = ratio x [insert size (bp)/vector size (bp)] x vector mass (mg). Competent DH5α cells were used for transformation of all plasmids. The general transformation procedure begins by adding 2 µl of plasmids from the rapid ligation and 2 µl of plasmids from the overnight ligation to an eppendorf tube containing 40 µl of competent DH5α cells and placing on ice for 30 min. The DH5α cells were then heat shocked at 42°C for 1 min followed by 2 min on ice. After the two minutes on ice, 1 ml of Luria-Bertani (LB) solution (5 g yeast extract, 10 g tryptone and 10 g NaCl per L) was added and the solution was incubated at 37°C in a shaking incubator for 1 hour. The transformed DH5α cells were streaked onto an LB medium plate containing 50 µg/ml Ampicillin (Amp) and incubated overnight in a 37°C incubator. Colony PCR was performed to verify the presence of the insert and then a QIAprep Spin Miniprep Kit was used to extract DNA plasmids from the transformed bacteria (Qiagen Inc., Toronto, ON). Following DNA extraction, restriction enzymes were used to verify the correct sequence of the plasmids. The DNA constructs created in this study and the method of construction is as follows:

pfntb-1::fntb-1

pfntb-1::fntb-1 was created using standard PCR techniques to amplify 2.8 KB upstream of *fntb-1* and includes the 3'UTR. *pfntb-1* was amplified using N2 genomic

DNA as a template. *fntb-1* was cloned from cosmid F23B12. The primers used can be found in Appendix A.

pfntb-1::gfp

pfntb-1::gfp was created using standard PCR and cloning techniques. 2.8 KB of *fntb-1* promoter was amplified and inserted into a *gfp* backbone vector.

pprkl-1::gfp

pprkl-1::gfp was created by Sanchez-Alvarez et al. (2011) using standard PCR and cloning techniques.

punc-4::fntb-1

punc-4::fntb-1 was created using fusion PCR techniques. The *unc-4* promoter was amplified from *punc-4::gfp::prkl-1*, a plasmid created by Sanchez-Alvarez et al. (2011), and fused to *fntb-1*, which was amplified from an *fntb-1* cDNA plasmid created by Anna Su (Sanchez-Alvarez et al., 2011).

pcol-10::fntb-1

pcol-10::fntb-1 was created using fusion PCR techniques. The *col-10* promoter was amplified from a plasmid created by Sanchez-Alvarez et al. (2011) and fused to *fntb-1*, which was amplified from an *fntb-1* cDNA plasmid created by Anna Su (Sanchez-Alvarez et al., 2011).

punc-4::gfp::prkl-1a

punc-4::gfp::prkl-1a was previously created by Sanchez-Alvarez et al. (2011).

pcol-10::gfp::prkl-1a

pcol-10::gfp::prkl-1a was previously created by Sanchez-Alvarez et al. (2011).

pcol-10::gfp::prkl-1b

pcol-10::gfp::prkl-1b was created using standard cloning techniques. The *col-10* promoter was first amplified from a plasmid created by Sanchez-Alvarez et al. (2011). The *col-10* promoter was then digested with PstI and SphI at 37°C for 2.5 hours in a 20 µl reaction consisting of 2 µl of fermentas B Buffer, 10 µl of *pcol-10*, 0.5 µl SphI, 1 µl PstI and 6.5 µl of molecular grade H_2O. *punc-4::gfp::prkl-1b*, a plasmid from Sanchez-Alvarez et al. (2011), was also digested at 37°C for 2.5 hours in a 20 µl reaction consisting of 2 µl of fermentas B Buffer, 2 µl *punc-4::gfp::prkl-1b*, 0.5 µl SphI, 1 µl PstI and 14.5 µl of molecular grade H_2O. Both insert and vector were gel purified and two ligations were performed at different ratios. The 3:1 ratio ligation reaction consisted of 3 µl of digested *punc-4::gfp::prkl-1b*, 2.2 µl digested *pcol-10*, 4 µl of 5x fermentas T_4 ligase buffer, 1 µl of T_4 ligase and 9.8 µl of molecular grade H_2O. The 6:1 ratio ligation reaction consisted of 3 µl of digested *punc-4::gfp::prkl-1b*, 4.4 µl digested *pcol-10*, 4 µl of 5x fermentas T_4 ligase buffer, 1 µl of T_4 ligase and 9.8 µl of molecular grade H_2O. Both ligation reactions were incubated at RT for 30 min. Following ligation the general transformation procedure was used to create *pcol-10::gfp::prkl-1b*.

punc-4::gfp::prkl-1a ΔCAAX

punc-4::gfp::prkl-1a ΔCAAX was created by Sanchez-Alvarez et al. (2011).

punc-4::gfp::prkl-1a CNIM

punc-4::gfp::prkl-1a CNIM was created using fusion PCR and standard cloning techniques. 2.4 kb of *prkl-1a* was first amplified from a plasmid created by Sanchez-Alvarez et al. (2011) and fused to a 980 bp ending of *prkl-1a* that includes the *mig-2* C-terminal with the 3'UTR. The *prkl-1a CNIM* was then digested with XbaI and Bam HI at 37°C for 2.5 hours in a 20 µl reaction consisting of 2 µl of fermentas Bam HI Buffer, 10 µl of *prkl-1a CNIM*, 0.5 µl Bam HI, 1 µl XbaI and 6.5 µl of molecular grade H_2O. A plasmid from Sanchez-Alvarez et al. (2011), *punc-4::gfp::prkl-1a*, was also digested at 37°C for 2.5 hours in a 20 µl reaction consisting of 2 µl of fermentas Bam HI Buffer, 2 µl *punc-4::gfp::prkl-1a*, 0.5 µl Bam HI, 1 µl XbaI and 14.5 µl of molecular grade H_2O. Both insert and vector were gel purified and two ligations were performed at different ratios. The 3:1 ratio ligation reaction consisted of 3 µl of digested *punc-4::gfp::prkl-1a*, 4 µl digested *prkl-1a CNIM*, 4 µl of 10x fermentas T_4 ligase buffer, 1 µl of T_4 ligase and 8 µl of molecular grade H_2O. The 6:1 ratio ligation reaction consisted of 3 µl of digested *punc-4::gfp::prkl-1a*, 8 µl digested *prkl-1a CNIM*, 4 µl of 10x fermentas T_4 ligase buffer, 1 µl of T_4 ligase and 4 µl of molecular grade H_2O. Both ligation reactions were incubated at RT for 30 min. Following ligation the general transformation procedure was used to create *punc-4::gfp::prkl-1a CNIM*.

2.4 Fluorescent microscopy and imaging

Worms grown at 20°C were placed in an immobilization solution (15% w/v Levamnisole (Sigma) in M9) on a glass slide mounted with a 2% agarose gel pad. Fluorescent images were taken using an LED Colibri Epifluroescent Zeiss AxioImager M2

Microscope affixed with a Zeiss AxioCam MRm and viewed with AxioVision software version 4.8. Images were initially taken as Z-stacks with an interval of 0.200 µm between each captured image. The Z-stack was then collapsed into a single image using the AxioVision software version 4.8.

2.5 Localization analysis

Localization of PRKL-1A and PRKL-1A ΔCAAX in VC4 and VC5 was analyzed by capturing images of transgenic worms expressing *punc-4::gfp::prkl-1a* and *punc-4::gfp::prkl-1a ΔCAAX* at various developmental stages with an LED Colibri Epifluroescent Zeiss AxioImager M2 Microscope 63x objective affixed with a Zeiss AxioCam MRm. The developmental stage of the worm was determined based on vulva development, visible with the help of the *zyIs1 (plin-11::rfp)* marker. *lin-11* encodes a transcription factor expressed in VC1 to VC6 and in vulva cells. The images of the worms were initially taken as Z-stacks with an interval of 0.200 µm between each image and then collapsed into a single image using AxioVision software version 4.8. The punctae counted in this study can be defined by a visual change in GFP intensity.

CHAPTER 3

RESULTS

3.1 Backwards locomotion defect

3.1.1 Backwards locomotion can be restored with other PCP genes

A mutation in the *prkl-1* gene results in the growth of an ectopic axon from VC4 and VC5 (Sanchez-Alvarez et al., 2011). Conversely, *prkl-1* over-expression results in a suppression of neurite outgrowth and a monopolar phenotype of VC4 and VC5 (Sanchez-Alvarez et al., 2011). Interestingly, *prkl-1* over-expression from an *unc-4* promoter, a neuronal specific promoter, also resulted in another defect: the inability of a worm to move backwards. When touched lightly on the head with a platinum tipped wire a *wt* worm will move backwards in a smooth, sinusoidal, and undulating wave pattern, which is an appropriate behavioural response to the tactile stimulation (Figure 5A and 5B). When touched lightly on the head, a *punc-4::gfp::prkl-1* transgenic worm does not respond with the normal avoidance response to the stimulus. Instead, a *punc-4::gfp::prkl-1* transgenic worm curls into a ball and pauses before continuing to move forward (Figure 5A and 5B). While characterizing the backwards locomotion defect in *punc-4::gfp::prkl-1* transgenic worms, another locomotion phenotype was observed: a partial ability to move backwards. Worms with a partial ability to move backwards have the ability to move backwards when touched lightly on the head; however, backwards locomotion is severely handicapped. Partial backwards locomotion does not follow the

smooth, sinusoidal, and undulating patterning of *wt* movement, but is an uneven bending resulting in a circular movement of the worm (Figure 5B). Since *vang-1* has been known to interact with *prkl-1*, an attempt to restore the backwards locomotion was made by introducing a *vang-1 (tm1422)* deletion allele into the *punc-4::gfp::prkl-1* transgenic worm line (Figure 5A). Indeed we observed a recovery of backwards locomotion in the *punc-4::gfp::prkl-1; vang-1 tm1422* line where *wt* and partial backwards locomotion combined resulted in a 81% ± 2.6 rescue of backwards locomotion (Figure 5A). This recovery of backwards locomotion demonstrates that *vang-1* genetically interacts with *prkl-1*. This result also suggests that it may be possible to recover the backwards locomotion defect with mutations in other PCP genes; therefore, a *punc-4::gfp::prkl-1* transgenic worm line could be used in a *prkl-1* suppressor screen to discover new planar cell polarity components.

3.1.2 Backwards locomotion defects are a result of DA neuron defects

Backwards locomotion is controlled by the A-type class of motor neurons: VA and DA (White et al., 1992). There are 12 VA neurons and 9 DA neurons located in the ventral cord (White et al., 1992). All A-type neurons receive the same synaptic input from a common set of interneurons (AVA, AVD and AVE) and extend axonal processes in the anterior direction (Figure 6A) (Miller and Niemeyer, 1995; White et al., 1992). The VA neurons innervate ventral muscles and function complementary to the DA neurons, which send commissures to the dorsal cord thereby innervating dorsal muscles (Figure 4B) (Miller and Niemeyer, 1995; White et al., 1992).

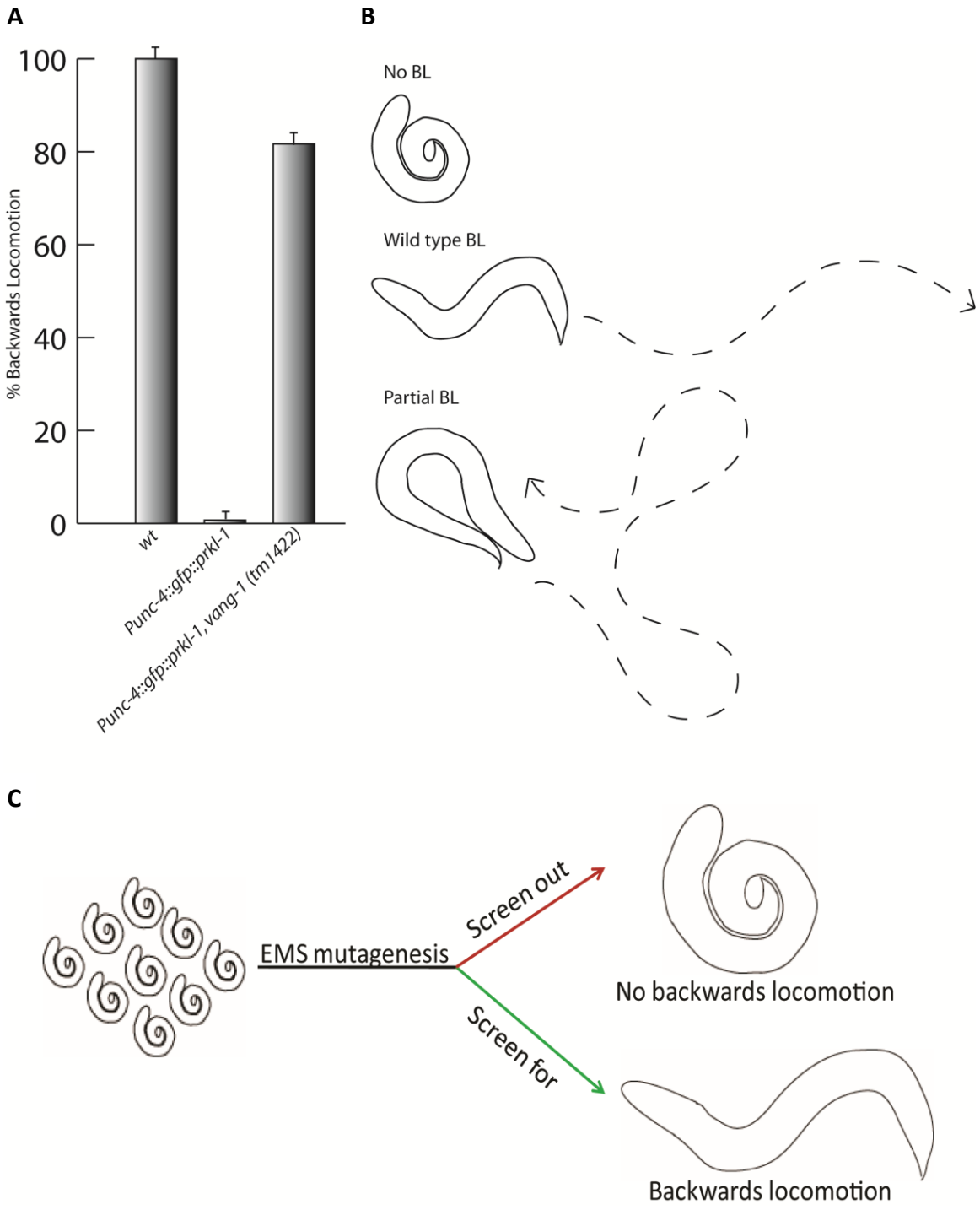

Figure 7. Backwards locomotion defect classification, rescue and screen. (A) The backwards locomotion defect in *punc-4::gfp::prkl-1* is severe and can be rescued by disrupting *vang-1* function. n>150 for all bars. Error bars represent a 95% confidence interval of proportions. **(B)** The classification of backwards locomotion (BL) into three categories. **(C)** Worms were mutated using ethyl methanesulfonate and screened for recovery of backwards locomotion.

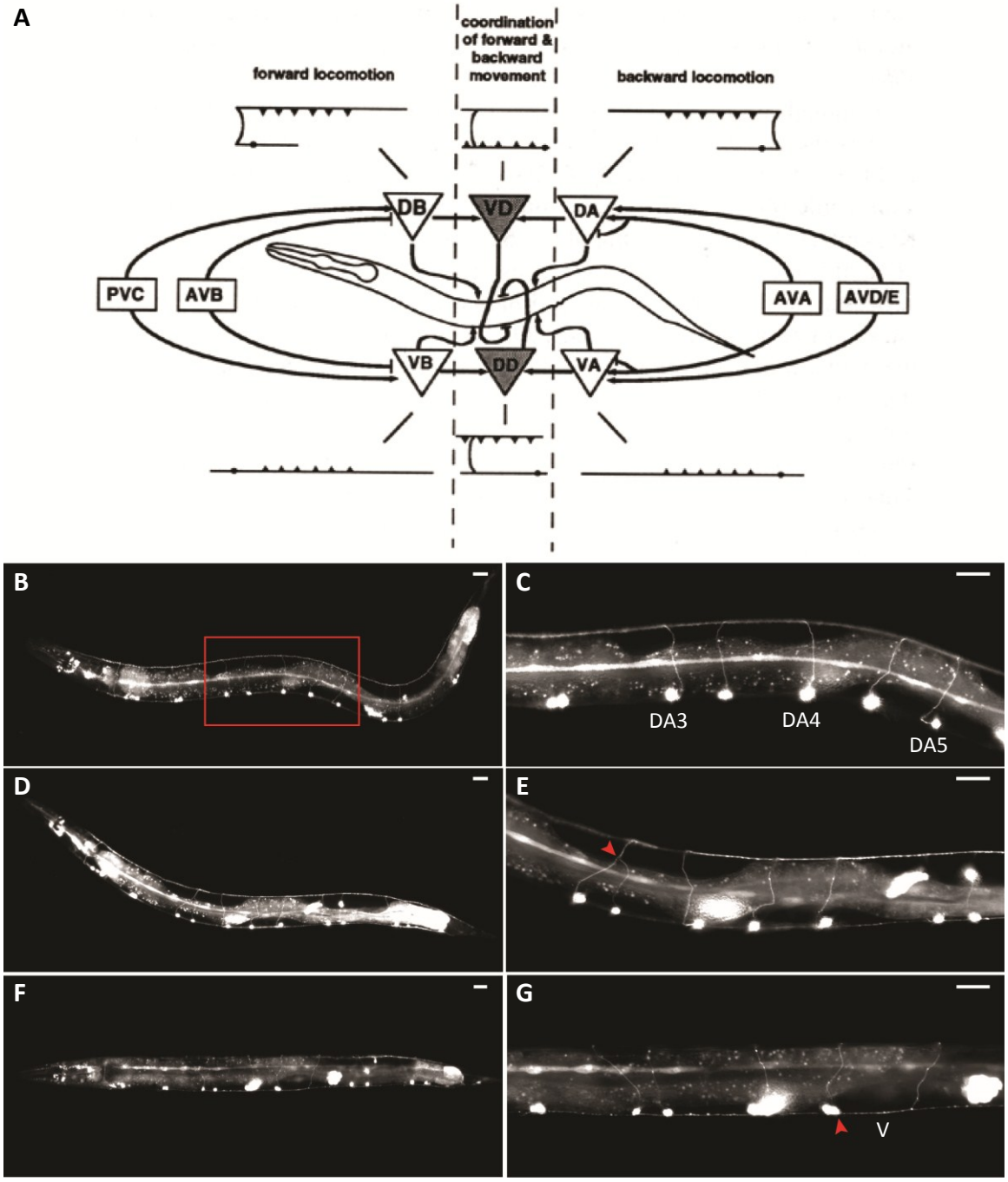

Figure 8. DA neuron defects. (A) The neuronal wiring for locomotion in *C. elegans*. Figure taken with permission from Cold Spring Harbor Laboratory Press, 1997. **(C, E, G)** Magnification of DA3, DA4 and DA5 neurons from **(B, D, F)** respectively. **(B, C)** Images of *wt* worms showing typical DA neuron morphology and axon guidance. **(D, E)** Images of worms with *prkl-1* over-expression (*punc-4::gfp::prkl-1a).* Red arrow point to axon guidance defect in DA3. **(F, G)** Images of *punc-4::gfp::prkl-1a; vang-1 (tm1422)* worms showing rescue of axon guidance defects. Red arrow points to DA5 migration defect. V represents location of the vulva. All worms express *punc-129::gfp*. Scale bars for all images, 20µm.

Interestingly, the *unc-4* gene is expressed in the VC neurons as well as in the DA and VA motor neurons (Miller et al., 1992; Miller and Niemeyer, 1995; White et al., 1992). *unc-4* encodes for a homeodomain protein that determines the pattern of synaptic input to specific motor neurons (Miller et al., 1992; Miller and Niemeyer, 1995; White et al., 1992). In null *unc-4* mutant animals, the VA neurons are transformed so that they receive the same synaptic inputs as their sister VB neurons. The VB neurons are involved in forward locomotion and receive inputs from the PVC and AVB interneurons (Figure 6A) (Miller et al., 1992; Miller and Niemeyer, 1995; White et al., 1992). The backwards locomotion defect in *unc-4* mutants could be rescued by a VA specific expression of *unc-4* (Miller et al., 1992; Miller and Niemeyer, 1995; White et al., 1992). These findings suggest that the *unc-4* gene is expressed in the backwards locomotion neurons and is important for the cell fate determination of VA but not DA neurons (Miller et al., 1992; Miller and Niemeyer, 1995; White et al., 1992).

Since *unc-4* is expressed in the VA and DA neurons, we examined the DA neurons for polarity defects in the *punc-4::gfp::prkl-1* transgenic worm lines. The DA neurons were chosen over the VA neurons because it would be difficult to visualize individual VA axon tracts as they are bundled in the ventral cord. The *unc-129::gfp* transgenic marker is expressed in DA and DB neurons (Colavita et al., 1998). DA3, DA4 and DA5 neurons were examined because they are easy to identify and exhibit the stereotypical DA neuron phenotype (Figure 4B). In wt *unc-129::gfp* transgenic worms, the position of the DA5 cell body is located immediately posterior to the vulva (Figure 4B, 6B, and 6C). DA4 and DA3 are located anterior to DA5 with DB neurons located in between (Figure 6B and

6C). *punc-4::gfp::prkl-1* transgenic worms display axon guidance defects in DA3 neurons (Figure 6D and 6E). These defects suggest that backwards locomotion is impeded by improper innervation of the DA neurons. As expected, introducing a *vang-1 (tm1422)* deletion background rescues the axon guidance defects of DA3, which correlates with the recovered backwards locomotion phenotype (Figure 6F and 6G). Interestingly, the induction of *vang-1 (tm1422)* deletion allele also creates a cell positioning defect of DA5 (Figure 6F and 6G). DA5 in wt and over-expressed *prkl-1* worms is located posterior to the vulva (Figure 4B 6B and 6C). Upon introducing the *vang-1 (tm1422)* deletion allele to the *punc-4::gfp::prkl-1* transgenic line, the position of DA5 was located anterior to the vulva (Figure 6F and 6G). While the location of DA5 in a *punc-4::gfp::prkl-1*; *vang-1 (tm1422)* mutant is changed, the axon guidance of DA5 is unaffected as the commissure occurs posterior of the vulva and backwards locomotion is recovered suggesting proper guidance and innervations (Figure 5A, 6F and 6G).

3.2 A *prkl-1* suppressor genetic screen

The *punc-4::gfp::prkl-1* transgenic worms provide an opportunity to use recovery of backwards locomotion as a screening assay to find new PCP genes that affect VC4 and VC5 polarity (Figure 5C).

A semi-clonal screen was performed with two *prkl-1* over-expression integrated transgenic worm lines, *punc-4::gfp::prkl-1* line 5 and line 13, looking for the recovery of backwards locomotion (Table 1 and Figure 5C). The *punc-4::gfp::prkl-1* transgene is located on different chromosomes for line 5 and line 13: IV and V respectively. Approximately 38, 950 genomes were screened and 125 mutants that displayed

backwards locomotion were recovered. In addition to the semi-clonal screen, a clonal screen (one mutated worm per plate) of approximately 6, 300 genomes was performed and 23 mutants that displayed backwards locomotion were recovered.

Although 148 mutants recovered backwards locomotion, not all were mutations in genes. A recovery of backwards locomotion can be caused by either a disruption of components in the *prkl-1* pathway or a change in the expression of *prkl-1* on the transgenic array. An EMS-induced disruption in the *punc-4::gfp::prkl-1* transgene can alter *gfp::prkl-1* expression and result in the recovery of backwards locomotion. The *prkl-1* transgene also contains a co-injection marker: *odr-1::rfp*. *odr-1::rfp* results in the expression of RFP in a pair of sensory neurons in the head. Any change that disrupts the *prkl-1* transgene will also affect expression of *odr-1::rfp*; therefore, the 148 mutants were screened for GFP and RFP intensity. There were 81 mutants that displayed either no GFP or RFP. 61 mutants showed strong GFP and RFP expression suggesting normal function of the *punc-4::gfp::prkl-1* transgene.

SCREEN TYPE	GENOMES SCREENED	MUTANTS DISCOVERED
SEMI-CLONAL	38, 950	125
CLONAL	6, 300	23
TOTAL	45, 250	148

Table 1. The *prkl-1* suppressor screen . The semi-clonal and clonal screens totalled approximately 45, 250 genomes and discovered 148 mutants of which 61 were mutations not in the integrated transgenic array.

Since we were concerned with finding new PCP components that affect the polarization of VC4 and VC5, the reporter transgene *cyIs4 (pcat-1::gfp)* was used to visualize VC4 and VC5. Wild type worms display a low penetrance of ectopic VC4 and VC5 neurites (approximately 4.0%) (Figure 7 and 8A). In contrast, *vang-1 (tm1422)* deletion worms display approximately 76% ectopic VC4 and VC5 neurites (Figure 7 and 8C). Complementation tests with *vang-1 (tm1422)* confirmed the discovery of twelve new alleles of *vang-1*, all with similar penetrance of VC4 and VC5 defects (Table 2). A previous genetic screen by Sanchez-Alvarez et al. (2011) identified *fntb-1* as a PCP gene involved in VC4 and VC5 neurite formation (unpublished data). *fntb-1 e6.1* mutant worms display approximately 73% ectopic VC4 and VC5 neurites (Figure 7 and 8D). Complementation tests with the remaining 55 mutants and the *fntb-1 e6.1* allele led to the discovery of a new *fntb-1* allele: *I2-68* (Table 2).

In summary, the backwards locomotion screen led to the discovery of twelve new alleles of *vang*-1, one new allele of *fntb*-1, five mutations in unknown genes that affect VC4 and VC5 polarity, and forty-three uncharacterized mutants (Table 2).

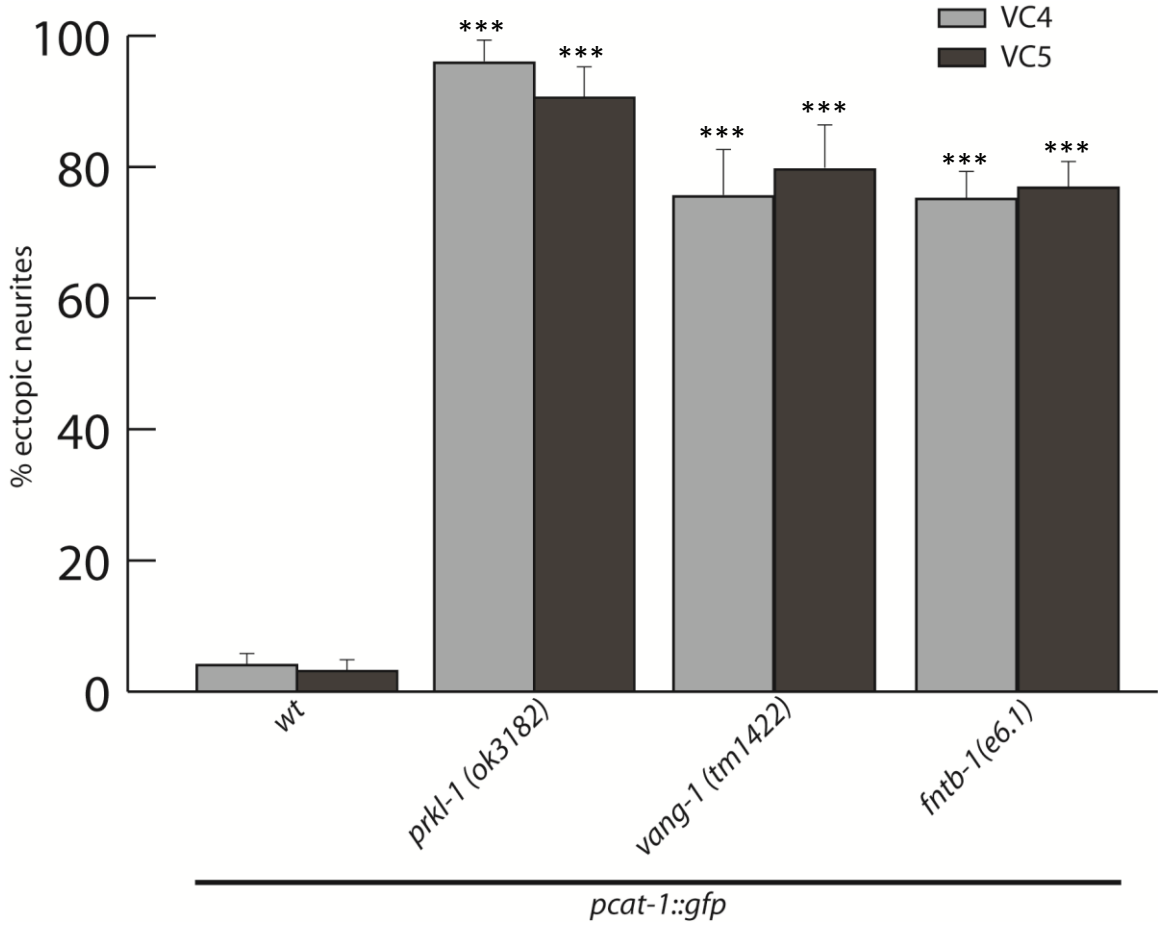

Figure 9. VC5 and VC5 ectopic neurite frequencies in *wt, prkl-1, vang-1* and *fntb-1* mutants. Compared to *wt*, PCP defective genes *prkl-1, vang-1* and *fntb-1* display strong ectopic neurite defects. n>150 for all lines. Error bars represent a 95% confidence interval of proportions . ***p<0.0001, χ^2 test.

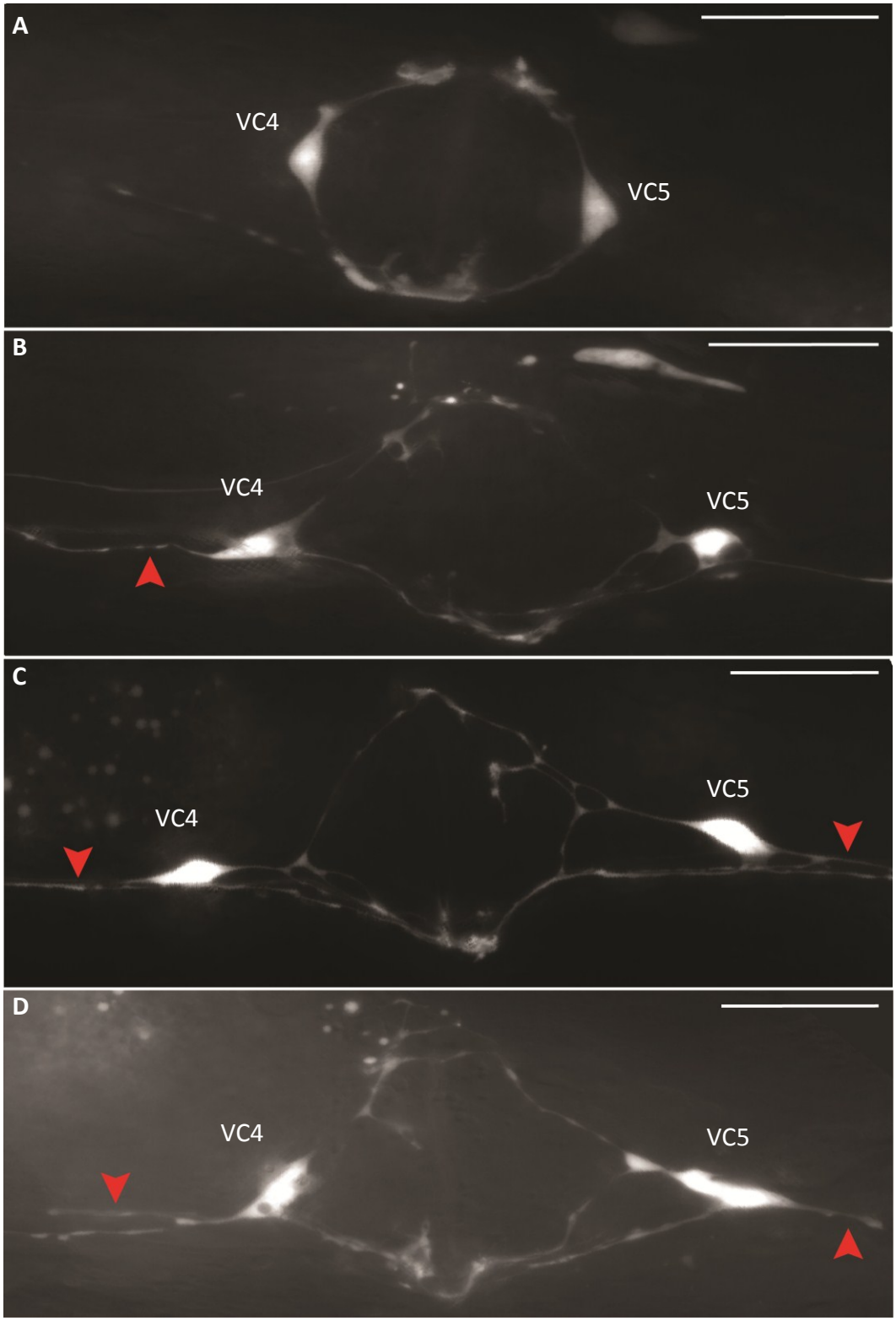

Figure 10. VC4 and VC5 phenotypes in *wt, prkl-1, vang-1* and *fntb-1* mutants. (A) *wt* VC morphology. VC4 and VC5 display ectopic neurites in **(B)** *prkl-1 (ok3182),* **(C)** *vang-1 (tm1422)* and **(D)** *fntb-1 (e6.1)* mutants. Arrows indicate ectopic neurites. All worms express *cyIs4 (pcat-1::gfp).* Scale bars, 20 µm.

IDENTITY	MUTANTS	ALLELES
vang-1	12	*1-60, 3-18, 3-69, GG1-44, I3-3, I3-30, M1-39, N2-31, P2-54, P3-89, Q3-18, T1-11*
fntb-1	1	*I2-68*
Unknown	5	*EE3-25, FF3-13, J1-8, J4, T1-42*
Undefined	43	

Table 2. Identification of mutants from the *prkl-1* suppressor screen. The results from complementation tests with *vang-1 (tm1422)* and *fntb-1 (e6.1)* are shown. The five unknown mutants did not compliment *vang-1 (tm1422)* or *fntb-1 (e6.1)*. Complementation tests between the unknown alleles will establish complementation groups to identify the number of genes discovered. There are 43 mutants that have either not undergone complementation tests with *vang-1 (tm1422)* and *fntb-1 (e6.1)*, have not been counted, or did not display significant VC4/VC5 ectopic neurites.

3.3 *fntb-1* characterization

The *C. elegans* ortholog of f*arnesyltransferase β-subunit*, *fntb-1*, is located on chromosome V (Figure 9A) and is approximately 1.9 KB unspliced. FNTB-1 is a 401 amino-acid protein that it is highly conserved across species (Figure 9B). Although *fntb-1* has previously been identified to affect the polarity of VC4 and VC5 (Sanchez-Alvarez et al., unpublished data), the role of FNTB-1 and FT has yet to be defined in the polarization of VC4 and VC5.

3.3.1 Mutations in *fntb-1* result in VC4 and VC5 neuronal polarization defects

The *prkl-1* suppressor screen resulted in the discovery of a new allele of *fntb-1*: *I2-68*. *fntb-1 (I2-68)* displays a very weak penetrance of VC4 and VC5 ectopic neurites: 8% ± 2.3 and 8.7% ± 2.4 respectively. The two alleles, *fntb-1 (e6.1)* and *fntb-1 (AS24)*, previously identified by Sanchez-Alvarez et al. (unpublished) display strong VC4 and VC5 ectopic neurite defects. Since *fntb-1* genomic rescue of the VC4 and VC5 ectopic neurites had not been completed, a genomic rescue of *fntb-1 (e6.1)* was performed. *fntb-1 (e6.1)* displays approximately 73% ectopic VC neurites, while *fntb-1 (AS24)* displays approximately 76% ectopic VC neurites. Since both alleles of *fntb-1* are not significantly different, we created two independent lines in an *fntb-1 (e6.1)* mutant background that carried a genomic rescuing clone of *fntb-1*. Both independent *Ex(pfntb-1::fntb-1); fntb-1 (e6.1)* lines rescue the VC4 and VC5 ectopic neurite defect (Figure 10). *Ex(pfntb-1::fntb-1); fntb-1 (e6.1)* line 1 displays an ectopic neurite penetrance of 9.3% ± 1.9 in VC4 (Figure 10C) and 11.3% ± 1.3 in VC5 (Figure 10D).

Ex(pfntb-1::fntb-1); fntb-1 (e6.1) line 2 displays an ectopic neurite penetrance of 11.3% ± 6.2 in VC4 (Figure 10C) and 36% ± 7.9 in VC5 (Figure 10D).

The ability of the extra-chromosomal genomic constructs to rescue the VC4 and VC5 ectopic neurite defects demonstrates that the observed defects are caused by mutations in *fntb-1* and can be rescued by the *fntb-1* gene. Since the new allele of *fntb-1* (I2-68) was discovered from a *prkl-1* suppressor screen we suspected an interaction between *fntb-1* and *prkl-1*. Indeed *fntb-1* has previously been shown to interact with *prkl-1* in the process of FMBN tangential migration during zebrafish development (Mapp et al., 2011). For this reason, we investigated the possibility that *fntb-1* interacts with *prkl-1* in the neuronal polarization of VC4 and VC5.

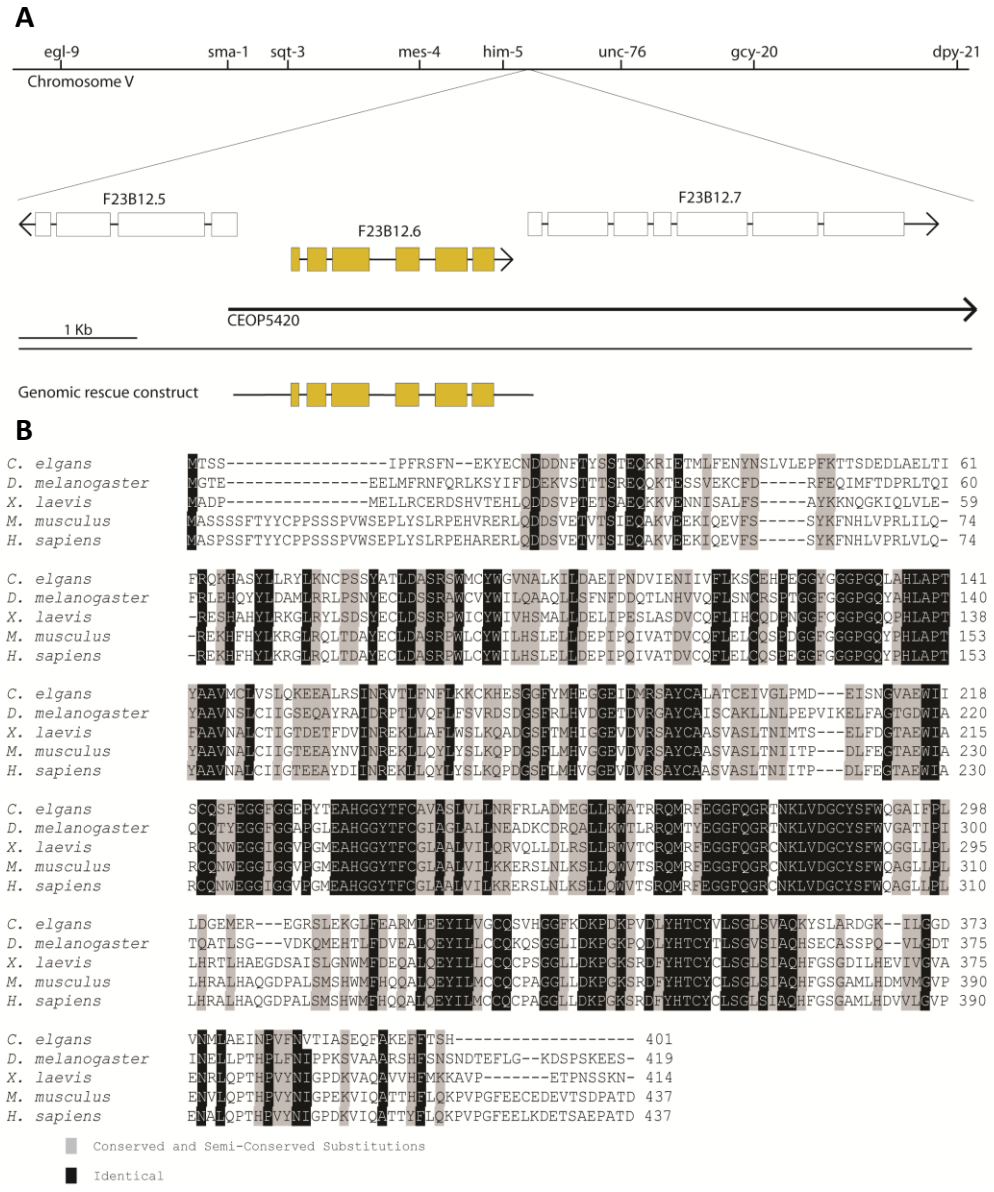

Figure 11. *fntb-1* alignment. (A) The genomic location and rescue construct for *fntb-1*. **(B)** An alignment of the FNTB-1 amino acid sequence with other organisms confirms that *fntb-1* is highly conserved.

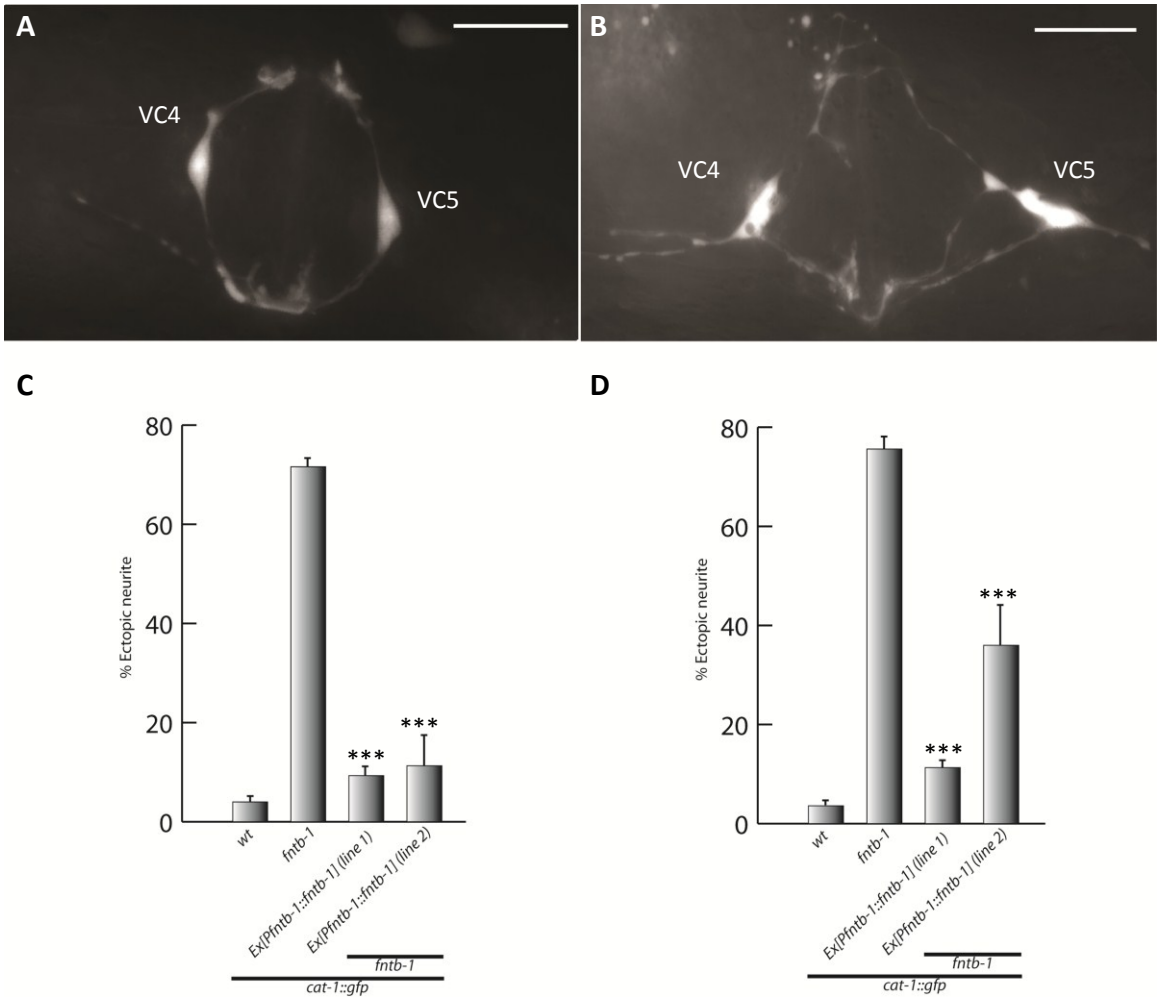

Figure 12. Genomic rescue of *fntb-1*. (A) *wt* VC4 and VC5 phenotype. Scale bar, 20µm. **(B)** *fntb-1 (e6.1)* mutant VC4 and VC5 phenotype. Scale bar, 20 µm. **(C)** The genomic rescue of VC4 ectopic neurite. **(D)** The genomic rescue of VC5 ectopic neurites. n>150 for all lines. Error bars represent a 95% confidence interval of proportions. ***p<0.001, χ^2 test.

3.3.2 The *fntb-1* and *prkl-1* promoters are expressed in the same cells

The transcriptional expression of *fntb-1* was analyzed during various stages of the worm life cycle by visual cell identification (Figure 11). The *fntb-1* promoter is widely expressed in many cells in the worm throughout all stages of development; however, it is most strongly expressed in the head, vulva and rectal regions (Figure 11 and Table 3). Due to strong GFP-intensity, it is difficult to identify individual cells in the head and rectal regions; however, a list of identified cells that display *fntb-1* promoter activity can be found in Table 3. Since *fntb-1* is involved in the polarization of VC4 and VC5, it was important to analyze the transcriptional expression of *fntb-1* in the VC neurons (Figure 12). The VC neurons are born at the L1 stage of development. Expression of *pfntb-1* in the VC neurons is detectable during the L3 stage of development and continuing into adulthood (Figure 11 and 12). Interestingly, *pfntb-1* is also expressed in the rest of the egg-laying organ: the HSN, the vulva cells and the uterine cells (Figure 12). There is stronger promoter activity of *fntb-1* in the vulva and uterine cells during the L3-L4 stage than during adulthood.

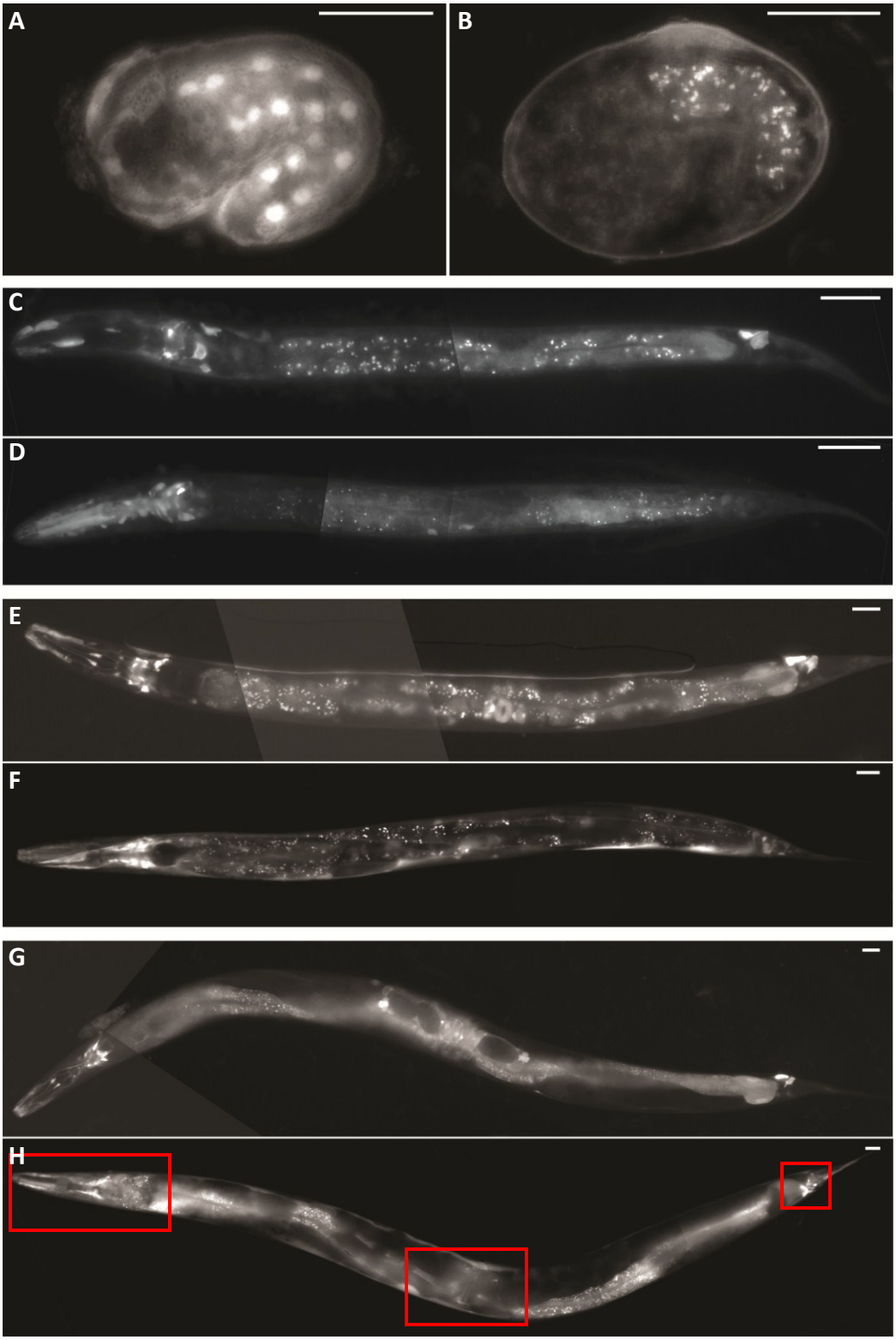

Figure 13. Transcriptional expression of *fntb-1* compared to *prkl-1*. (A, C, E, G) *pprkl-1::gfp* worms displaying location of *prkl-1* promoter activity. **(B, D, F, H)** *pfntb-1::gfp* worms displaying location of *fntb-1* promoter activity. **(A,B)** 1.5 fold stage. **(C, D)** L2 stage. **(E, F)** L4 stage. **(G, H)** Adult worms. *fntb-1* and *prkl-1* promoters are expressed at high levels in the head, rectum and vulva regions. Scale bars, 20 µm.

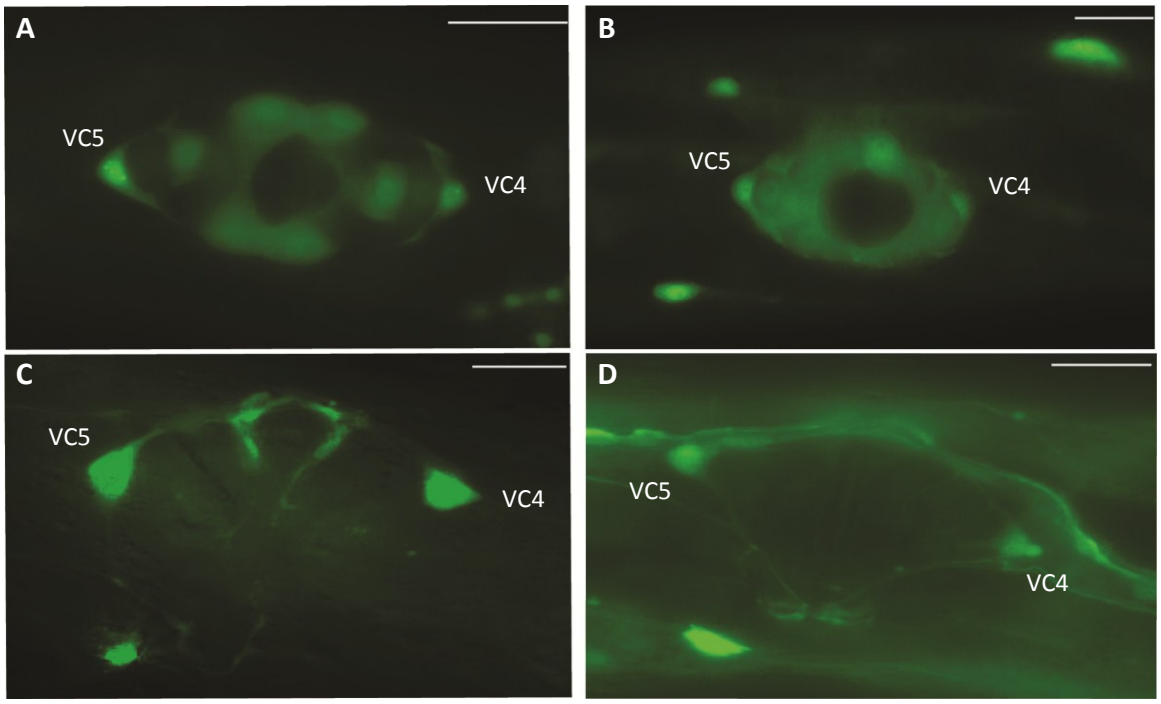

Figure 14. VC4 and VC5 transcriptional expression of *fntb-1* compared to *prkl-1*. All images are pictures taken at greater magnifications from the worms in **Figure 11E-H**. **(A, C)** *pprkl-1::gfp* worms displaying *prkl-1* promoter activity in VC4, VC5, the vulva and uterine cells at the **(A)** L4, and **(C)** Adult life stages. **(B, D)** *pfntb-1::gfp* worms displaying *fntb-1* promoter activity in VC4, VC5, the vulva and uterine cells at the **(A)** L4, and **(C)** Adult life stages. *fntb-1* and *prkl-1* both display promoter activity in VC4 and VC4 throughout development. Scale bars, 20 µm.

CELL SYSTEM	*fntb-1* expression	*prkl-1* expression
Alimentary	pm1-8 Intestinal cells Intestinal-rectal valve Somatic muscle Sphincter muscle Rectal gland	Rectal epithelial cells B, U, F and Y
Coelomocytes	ccDL/R ccPL/R ccAL/R	
Reproductive	Vulva cells Uterine cells	Vulva cells Uterine cells
Neurons	Many head neurons Many ventral cord neurons VC1-6 ALNL, PLNL DVB CAN SDQL ALM, PLM ADAL, ADAR RMEU AVG	Many head neurons VC1-6 IL1DL/R IL1VL/R IL1L/R I1L/R

Table 3. Location of *fntb-1* and *prkl-1* transcriptional expression. Cells that express *fntb-1* and *prkl-1* are shown. Cell identification was done visually by studying *fntb-1* and *prkl-1* driven GFP expression in pictures. The cells listed should not be considered an exhaustive list as many cells were unable to be identified due to high levels of GFP expression in the head, rectum, and ventral cord.

The transcriptional expression of *prkl-1* has been defined previously by Sanchez-Alvarez et al. (2011). A list of identified cells that express the *prkl-1* promoter throughout development can be found in Table 3. As expected, *pfntb-1* and *pprkl-1* are expressed in the same cells throughout development (Figure 11 and Table 3). Specifically, *prkl-1* promoter activity in the VC neurons is noticeable beginning at the L3 stage of development and continuing into adulthood (Figure 11 and 12). Also, *pprkl-1* has a stronger expression in the vulva cells at stage L4 than the vulva and uterine cells during adulthood (Figure 12). Unlike the *fntb-1* promoter, the *prkl-1* promoter is only expressed in the primary vulva precursor cells during the L3 stage of development and is not expressed in the HSN.

3.3.3 *fntb-1* acts cell and non-cell autonomously

To determine *fntb-1* function in regulating VC4 and VC5 polarity we conducted rescue experiments using a neuronal and hypodermal cell specific promoter. The *unc-4* promoter is expressed in the VC neurons from birth and is therefore a good choice to gauge the cell autonomous rescue capabilities of *fntb-1.* Two independent *Ex(punc-4::fntb-1)* arrays were created and crossed into both *fntb-1 (e6.1)* and *fntb-1 (AS24).* Neuronal specific expression of *fntb-1* significantly rescued the VC4 and VC5 ectopic neurite defects in both *fntb-1 (e6.1)* and *fntb-1 (AS24)* (Figure 13). It is evident that *fntb-1* functions in a cell-autonomous manner as both *fntb-1 (e6.1)* and *fntb-1 (AS24)* were rescued by a neuronal specific promoter.

To resolve if *fntb-1* functions non-cell autonomously in VC neuronal polarization, the *col-10* promoter was used to drive *fntb-1* expression specifically in hypodermal cells.

col-10 is a collagen gene that is expressed in hypodermal cells, including the vulva precursor cells. Two independent *Ex(pcol-10::fntb-1)* arrays were created and crossed into both *fntb-1 (e6.1)* and *fntb-1 (AS24)*. The hypodermal specific expression of *fntb-1* significantly rescued the VC4 and VC5 ectopic neurite defects in both *fntb-1 (e6.1)* and *fntb-1 (AS24)* (Figure 13). Interestingly, the VC4 and VC5 hypodermal specific rescues for both *fntb-1* alleles are similar to the neuronal specific rescues (Figure 13). The non-neuronal specific rescue results suggest that *fntb-1* also functions non-cell autonomously to regulate neuronal polarity.

3.3.4 *prkl-1* acts cell and non-cell autonomously

Previous experiments have shown that *fntb-1* interacts with *prkl-1* (Mapp et al., 2001). In this study we discovered that *fntb-1* functions both cell and non-cell autonomously to regulate VC4 and VC5 neuronal polarity; however, *prkl-1* has previously been found to act only cell autonomously (Sanchez-Alvarez et al., 2011). To confirm that *prkl-1* acts only cell autonomously, we conducted *prkl-1a* rescue experiments using neuronal and hypodermal specific promoters: *punc-4* and *pcol-10* respectively. Two independent *Ex(punc-4::gfp::prkl-1a)* and *Ex(pcol-10::gfp::prkl-1a)* arrays were created and crossed into *prkl-1 (ok3182)*. As expected, the neuronal specific expression of *prkl-1a* significantly rescued the VC4 and VC5 ectopic neurite defects in *prkl-1 (ok3182)* worms (Figure 14). This result confirms that *prkl-1* functions cell autonomously to regulate neuronal polarity. With the exception of VC5 from *Ex(pcol-10::gfp::prkl-1a); prkl-1 (ok3182)* line 2, the hypodermal specific expression of *prkl-1a* displayed a weak but significant rescue of the VC4 and VC5 ectopic neurite

defects in *prkl-1 (ok3182)* worms (Figure 14). This result suggests that *prkl-1* also functions non-cell autonomously to regulate neuronal polarity.

PRKL-1 is present in two different isoforms in *C. elegans*: PRKL-1A and PRKL-1B. The non-cell autonomous function of *prkl-1b* in the regulation of neuronal polarity has yet to be defined. Only one viable *Ex(pcol-10::gfp::prkl-1b),* hypodermal specific, cell line was obtained and displayed a VC4 and VC5 ectopic neurite penetrance of 81.3% ± 3.5 and 72.7% ± 4.7 respectively (Figure 14). The hypodermal specific expression of *prkl-1b* displayed a mild but significant rescue of the VC4 and VC5 ectopic neurite defects in *prkl-1 (ok3182)* worms (Figure 14). This result also suggests that *prkl-1* functions non-cell autonomously to regulate neuronal polarity.

3.3.5 *fntb-1* and *prkl-1* interact genetically

Since PRKL-1 has a CAAX motif, it is possible that FNTB-1 and PRKL-1 act in the same pathway to regulate VC4 and VC5 polarity. We created *fntb-1* and *prkl-1* double mutants to determine if *fntb-1* and *prkl-1* interact genetically in the same or parallel pathway. If *fntb-1* and *prkl-1* act in a common pathway, then we would predict that the penetrance of VC4 and VC5 ectopic neurites would not increase in double mutants. When compared with *prkl-1 (ok3182)*, both *fntb-1* and *prkl-1* double mutants displayed similar VC4 and VC5 ectopic neurite frequencies (Figure 15). These results suggest that *fntb-1* and *prkl-1* act in the same pathway to regulate neuronal polarity.

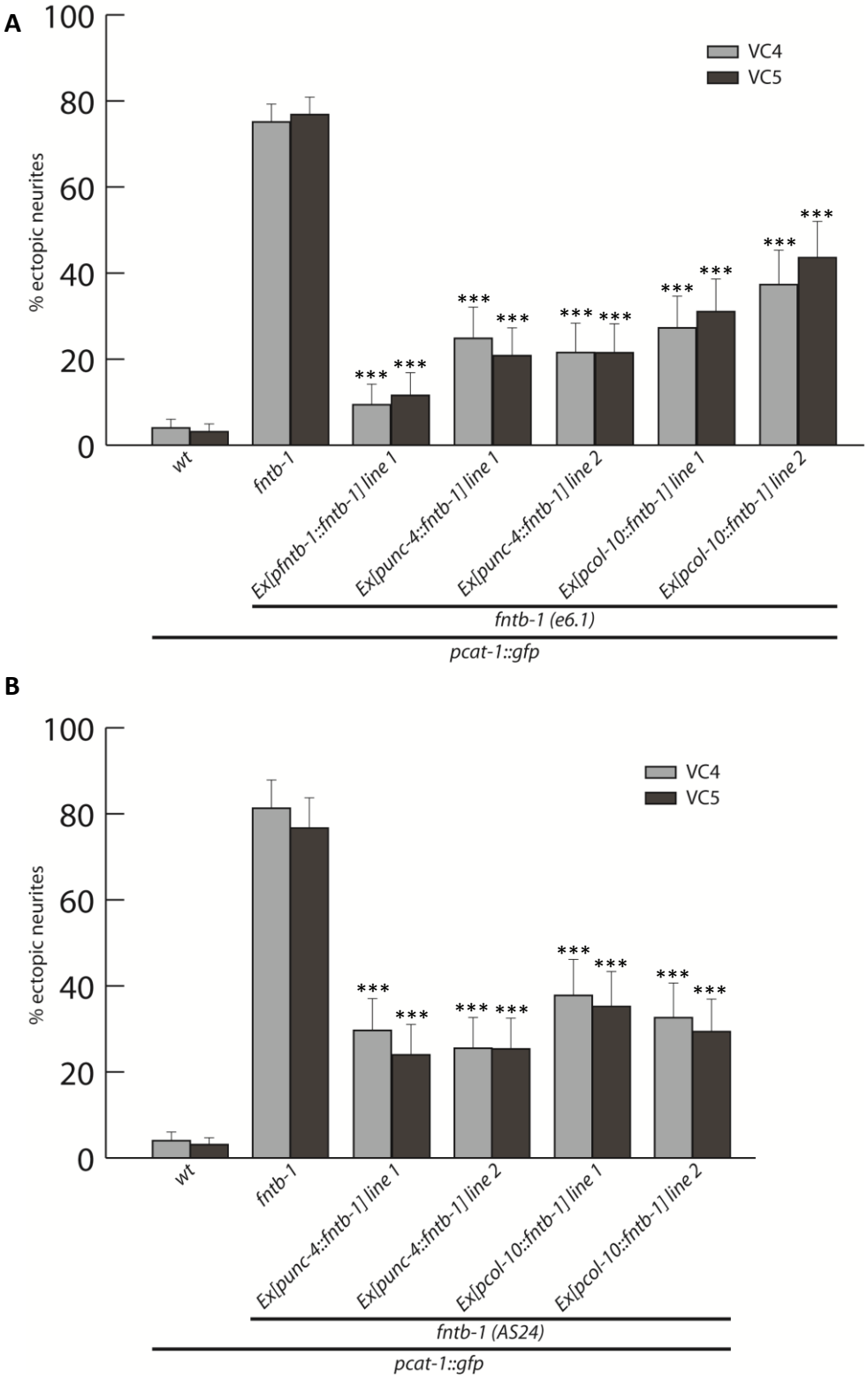

Figure 15. Cell and non-cell autonomous rescue of *fntb-1*. (A) Neuronal- and hypodermal-specific rescue of *fntb-1 (e6.1)*. **(B)** Neuronal- and hypodermal-specific rescue of *fntb-1 (AS24)*. n>150 for all lines. Error bars represent a 95% confidence interval of proportions. ***p<0.001, χ^2 test.

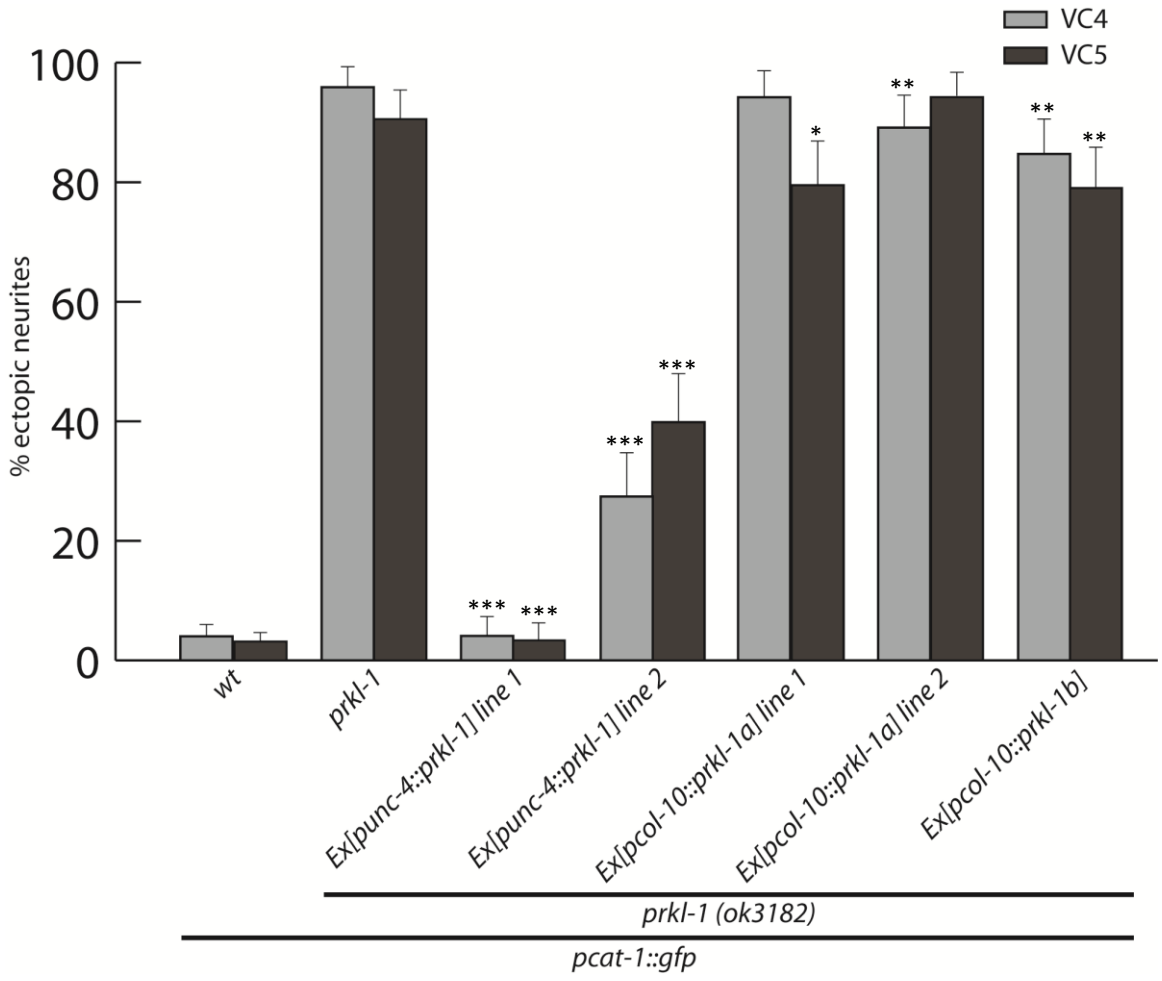

Figure 16. Cell and non-cell autonomous rescue of *prkl-1*. Neuronal- and hypodermal-specific rescue of *prkl-1 (ok3182)*. When compared to *prkl-1 (ok3182)* both *prkl-1a* and *prkl-1b* rescues non-cell autonomously. n>150 for all lines. Error bars represent a 95% confidence interval of proportions. ***p<0.001, **p<0.01, *p<0.05, χ^2 test.

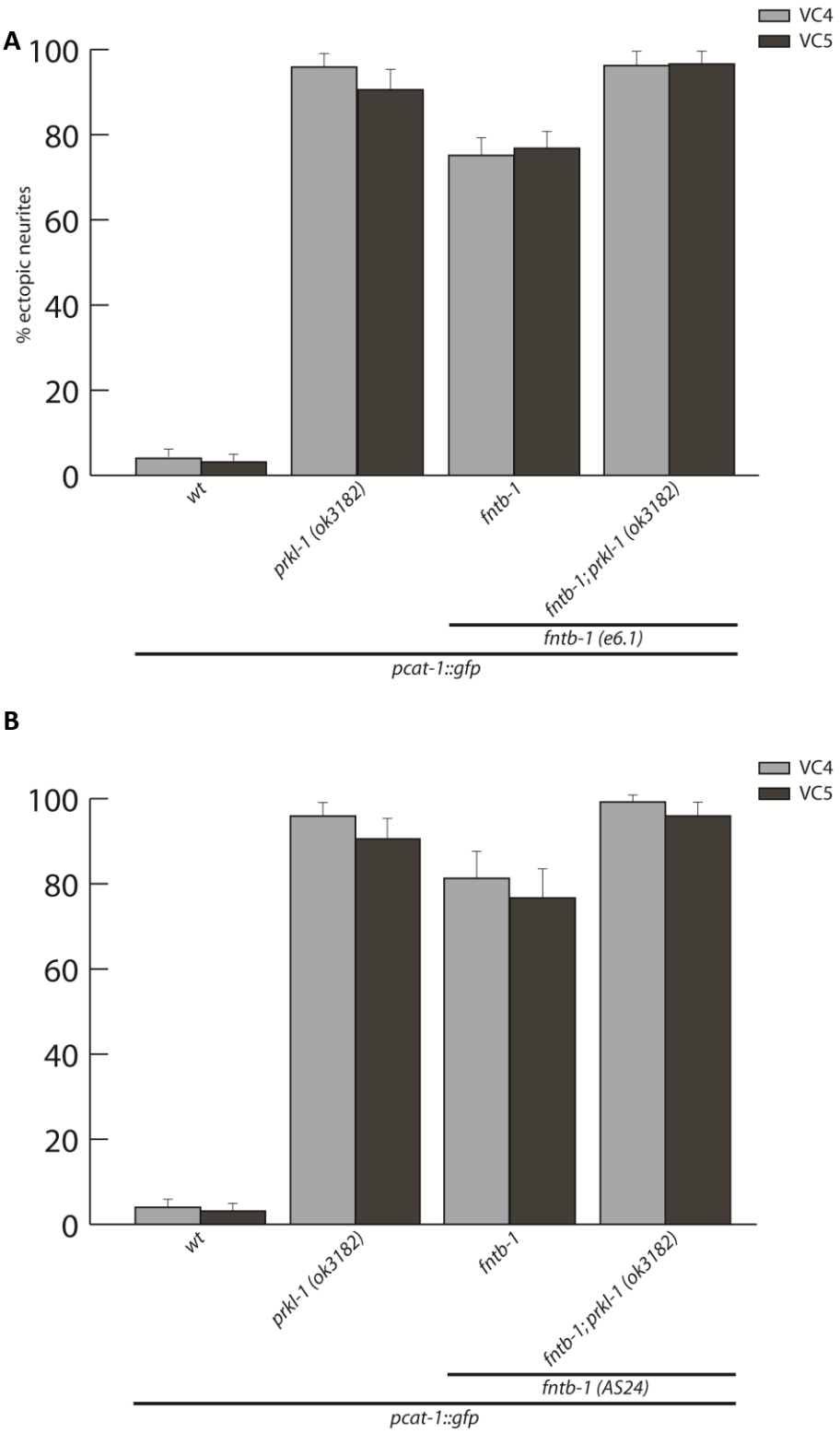

Figure 17. *prkl-1* and *fntb-1* single and double mutant analysis. The *prkl-1;fntb-1* double mutant analysis using **(A)** *fntb-1 (e6.1)* and **(B)** *fntb-1 (AS24)* suggests that *fntb-1* is in the same pathway as *prkl-1*. Counts were n>150 for all lines. Error bars represent a 95% confidence interval of proportions.

3.3.6 The CAAX domain is important for *prkl-1* function and *fntb-1* interaction

The CAAX motif has been shown to be important for PRKL-1 farnesylation (Mapp et al., 2011). To determine the relevance of the CAAX motif for PRKL-1 function, we deleted the PRKL-1 CAAX motif: CTVS. Two independent *Ex(punc-4::gfp::prkl-1α ΔCAAX)* arrays were created and crossed into *prkl-1 (ok3182)* worms. Interestingly, expression of *prkl-1α ΔCAAX* displayed a mild but significant rescue of VC4 and VC5 ectopic neurite defects in *prkl-1 (ok3182)* animals (Figure 16). Since *prkl-1α ΔCAAX* displays mild rescue of ectopic VC neurites, it suggest that the CAAX motif may not be necessary for some PRKL-1 function. However, the difference between *prkl-1α* and *prkl-1α ΔCAAX* rescue suggests that the CAAX motif is required for proper function of PRKL-1A and polarity of VC4 and VC5.

To further determine the importance of the CAAX motif for PRKL-1 function in regulating neuronal polarity, we modified the CAAX motif of PRKL-1. FT is one of three prenyltransferases. FT shares its α-subunit with GGT-I, which is important for the recognition of the CAAX motif. Since the identity of X determines farnesylation or geranylgeranylation, the farnesylation signal in PRKL-1A (CTVS) was replaced with the geranylgeranylation signal of MIG-2: CNIM. *mig-2* encodes a 195 AA protein that is part of the Rho family GTPases important for neuronal migration and axon guidance (Zipkin et al., 2007). Similar to PRKL-1, MIG-2 localizes to the cell membrane (Zipkin et al., 2007; Sanchez-Alvarez et al., 2011). MIG-2 is predicted to be geranylgeranylated by GGT-I; therefore, *punc-4::gfp::prkl-1α CNIM* should rescue VC4 and VC5 ectopic neurite defects in *prkl-1 (ok3182)*. Two independent *Ex(punc-4::gfp::prkl-1α CNIM)* arrays were

created and crossed into *prkl-1 (ok3182)* worms. Expression of *prkl-1a CNIM* displays a strong rescue of VC4 and VC5 ectopic neurite defects in *prkl-1 (ok3182)* animals (Figure 16). These results suggest that any CAAX motif is important for prenylation and PRKL-1 function.

3.3.7 High levels of *prkl-1* expression can rescue *fntb-1* mutants

VC4 and VC5 ectopic neurite defects in *fntb-1* mutants could be due to a loss of *prkl-1* function. We attempted to rescue VC4 and VC5 ectopic neurite defects by expressing high levels of *prkl-1a* in *fntb-1* mutants. Two independent *Ex(punc-4::gfp::prkl-1a)* arrays were created and crossed into both *fntb-1 (e6.1)* and *fntb-1 (AS24)* worms. Expression of *prkl-1a* displayed a significant rescue of VC4 and VC5 ectopic neurite defects in both *fntb-1* alleles (Figure 17). While *punc-4::gfp::prkl-1a* expression did not rescue the VC4 and VC5 ectopic neurite defects as well as *punc-4::fntb-1* expression, the results suggest that *prkl-1* can function independently of *fntb-1* and that high expression levels of *prkl-1* can rescue *fntb-1* VC4 and VC5 ectopic neurite defects.

To determine the importance of the CAAX motif for the *fntb-1* independent functions of *prkl-1*, we expressed *prkl-1a ΔCAAX* and *prkl-1a CNIM* at high levels in *fntb-1* mutants and assessed VC4 and VC5 polarity. Two independent *Ex(punc-4::gfp::prkl-1a ΔCAAX)* and *Ex(punc-4::gfp::prkl-1a CNIM)* arrays were created and each was crossed into both *fntb-1 (e6.1)* and *fntb-1 (AS24)* animals. Interestingly, expression of *prkl-1a ΔCAAX* and *prkl-1a CNIM* both displayed a significant and similar rescue of VC4 and VC5 ectopic neurite defects in both *fntb-1* alleles (Figure 17). Also, while expression of *prkl-*

1a ΔCAAX and *prkl-1a CNIM* did not rescue VC ectopic neurite defects as well as *punc-4::fntb-1*, expression of both *prkl-1a ΔCAAX* and *prkl-1a CNIM* resembled the *prkl-1a* rescue (Figure 17). These results show that the high levels of *prkl-1* are capable of rescuing *fntb-1* mutant VC4 and VC5 ectopic neurite defects independent of the presence or absence of the CAAX motif.

3.3.8 *fntb-1* is required for proper *prkl-1* function

Since high levels of *prkl-1* retain some function independent of the presence or absence of the CAAX motif, rescue experiments were performed in the *fntb-1(AS24)* and *prkl-1* double mutant. Two independent *Ex(punc-4::gfp::prkl-1a)* lines were created and crossed into *fntb-1(AS24); prkl-1 (ok3182)* animals. Expression of *Ex(punc-4::gfp::prkl-1a)* significantly rescued the *fntb-1(AS24); prkl-1 (ok3182)* VC4 and VC5 ectopic neurite defects (Figure 18). This result suggests that *prkl-1* retains some function independent of *fntb-1*.

To determine the importance of the CAAX motif and confirm that the *punc-4::gfp::prkl-1a* result is not due to high levels of expressed *prkl-1*, we performed rescue experiments with the PRKL-1 CAAX deletion and with the modified PRKL-1 CAAX motif. Two independent *Ex(punc-4::gfp::prkl-1a ΔCAAX)* and *Ex(punc-4::gfp::prkl-1a CNIM)* arrays were created and each was crossed into *fntb-1 (AS24); prkl-1 (ok3182)* animals. Interestingly, expression of *prkl-1a ΔCAAX* and *prkl-1a CNIM* both displayed a significant and similar rescue of VC ectopic neurite defects in *fntb-1 (AS24); prkl-1 (ok3182)* worms (Figure 18). Since high expression levels of *prkl-1a*, *prkl-1a ΔCAAX,* and *prkl-1a CNIM* all display similar rescues of ectopic VC neurites, it suggests that *prkl-1* may retain the

ability to interact with other PCP proteins independently of both the CAAX motif and *fntb-1*. Also, since high expression levels of *prkl-1* did not fully rescue the *fntb-1* VC ectopic neurites, it suggests that *fntb-1* may be interacting with other proteins important for neuronal polarization and that is important, if not essential, for proper *prkl-1* function.

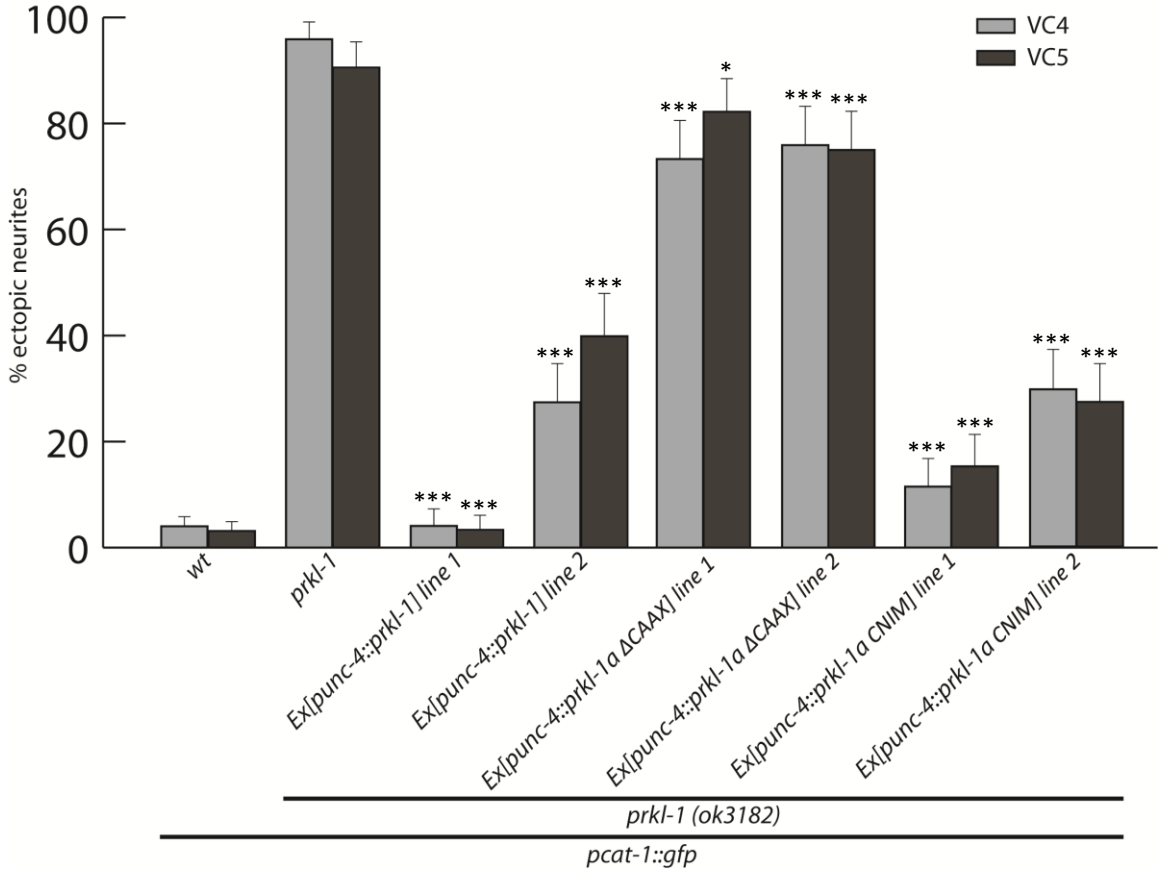

Figure 18. Rescue of *prkl-1* mutants with *prkl-1CAAX* mutants. Expression of the CAAX deleted *prkl-1* construct displays a weak but significant rescue of VC4 ectopic neurites. Expression of *prkl-1 CNIM* displays a strong rescue of ectopic neurites. n<150 for all lines. Error bars represent a 95% confidence interval of proportions. ***p<0.001, *p<0.05, χ^2 test.

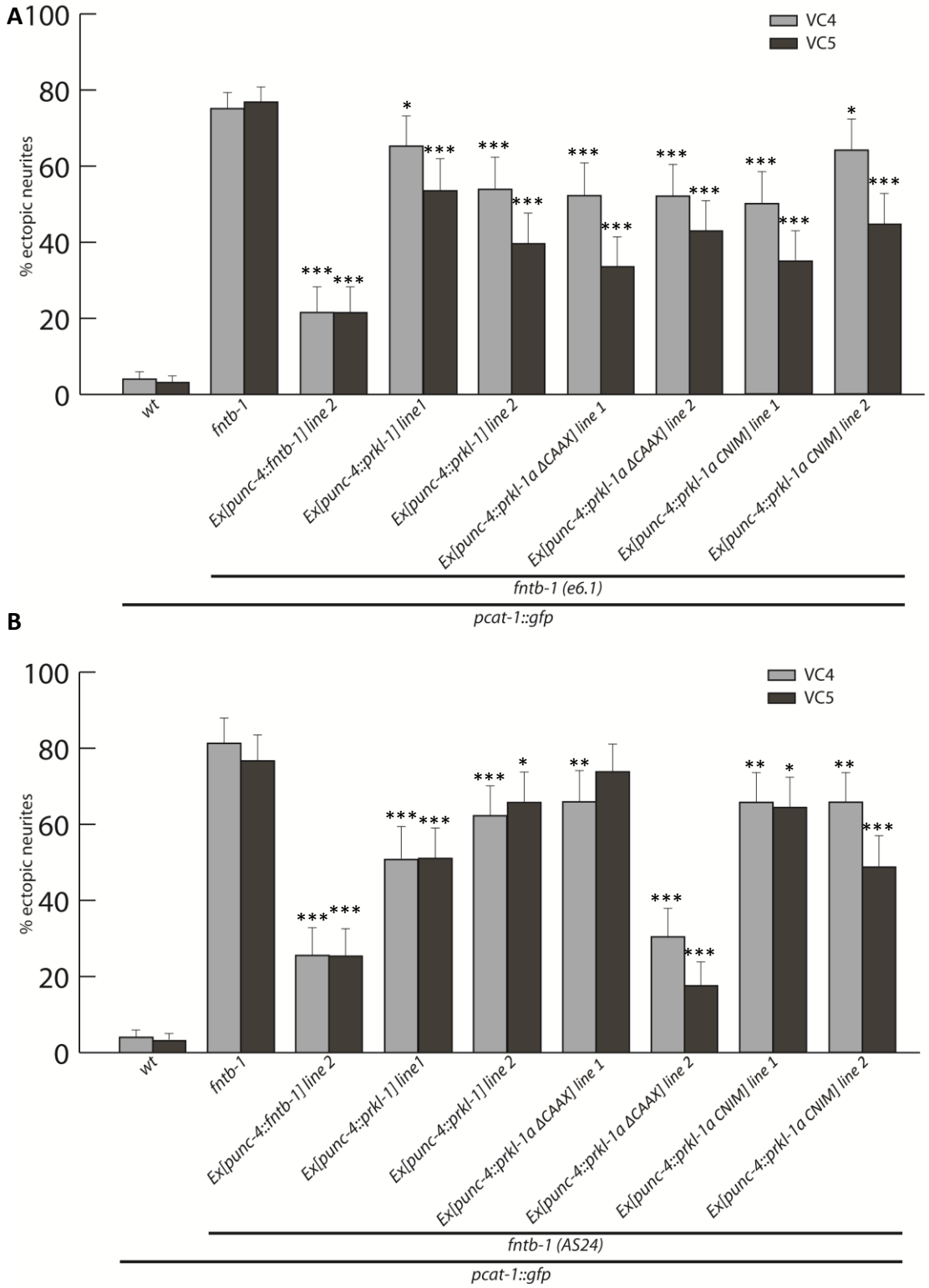

Figure 19. Rescue of *fntb-1* mutants with genetically modified *prkl-1* constructs. Expression of genetically modified *prkl-1* displays a weak but significant rescue for both the **(A)** *fntb-1 (e6.1)* and **(B)** *fntb-1 (AS24)* mutant VC4 and VC5 ectopic neurites. n>150 for each line. Error bars represent a 95% confidence interval of proportions. ***p<0.001, **p<0.01, *p<0.05, χ^2 test.

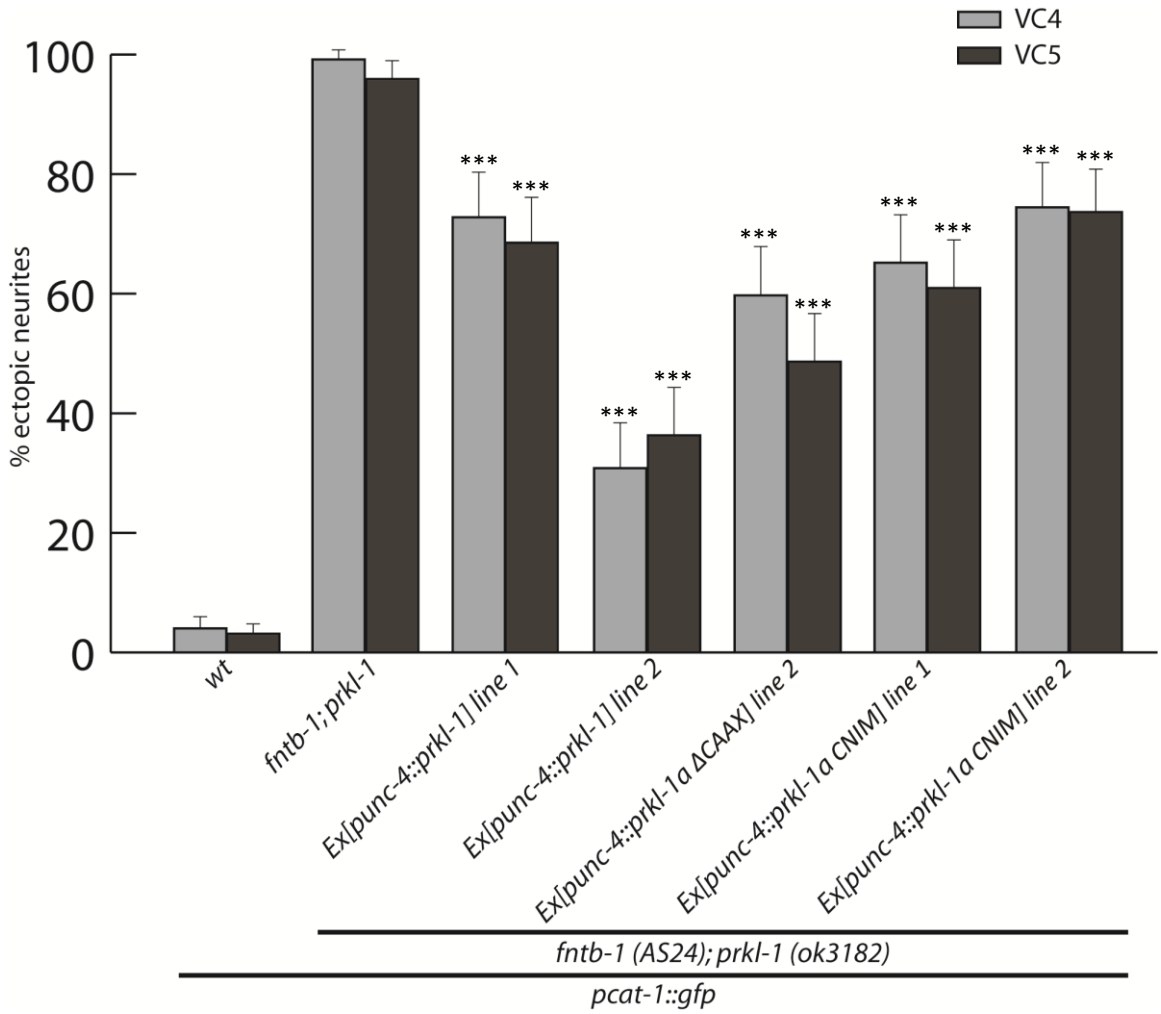

Figure 20. Rescue of *fntb-1; prkl-1* double mutant with modified *prkl-1* constructs. Expression of genetically modified *prkl-1* displays a weak but significant rescue of the *fntb-1; prkl-1* double mutant VC4 and VC5 ectopic neurites. n>150 for each line. Error bars represent a 95% confidence interval of proportions. ***p<0.001, χ^2 test.

3.3.9 PRKL-1 localization is affected by FNTB-1 and the CAAX motif

The rescue experiments performed with *fntb-1* and *prkl-1* confirmed that FNTB-1 is important for the farnesylation of PRKL-1. Since the farnesylation of proteins is important for membrane insertion and protein interaction (Maurer et al., 2003; Mulligan et al., 2010), the localization of PRKL-1A and PRKL-1A ΔCAAX in a wild type and FNTB-1 mutant background was studied to determine whether FNTB-1 effects the localization of PRKL-1.

In an attempt to simulate wild type localization of PRKL-1, a *prkl-1 (ok3182)* worm background was used in order to avoid *prkl-1* over-expression. Two independent *Ex(punc-4::gfp::prkl-1a)* and *Ex(punc-4::gfp::prkl-1a Δcaax)* arrays were created and each crossed into *prkl-1 (ok3128).* Since polarization of VC4 and VC5 occurs around the L3/L4 stage, pictures of the four genetic lines at the L3 and L4 stages were taken and examined for differences in the localization of PRKL-1A and PRKL-1A ΔCAAX (Figure 19 and 20). Since *punc-4::gfp::prkl-1a* and *punc-4::gfp::prkl-1a Δcaax* displayed significantly different rescues, we expected to observe a difference in the localization of PRKL-1A and PRKL-1A ΔCAAX. Qualitative analysis confirmed this; PRKL-1A displayed many, small GFP punctae that appeared around the membrane of VC4 and VC5 (Figure 19A, 19B, 20A and 20B) while PRKL-1A ΔCAAX displayed fewer, but larger GFP punctae around the membrane of VC4 and VC5 (Figure 19C, 19D, 20C and 20D). Also, there appeared to be no developmental differences in the number of GFP::PRKL-1A and GFP::PRKL-1A ΔCAAX punctae as both L3 and L4 stages displayed similar phenotypes (Figure 19 and 20). The difference in the amount and the size of punctae between *punc-4::gfp::prkl-1a; prkl-1*

(ok3182) and *punc-4::gfp::prkl-1a Δcaax; prkl-1 (ok3182)* suggests that the CAAX motif is important for proper localization of PRKL-1A.

Since both FNTB-1 and the CAAX motif are important for the farnesylation of PRKL-1A, whether or not the difference in the localization of PRKL-1A and PRKL-1A ΔCAAX was independent of FNTB-1 was investigated. In order to determine whether PRKL-1A localization is affected by FNTB-1, the two independent *Ex(punc-4::gfp::prkl-1a)* and *Ex(punc-4::gfp::prkl-1a Δcaax)* arrays from previous experiments were each crossed into an *fntb-1 (AS24); prkl-1 (ok3182)* mutant background. Since *cyIs4* linked to *fntb-1*, GFP expression from the *cyIs4* array was unavoidable. The presence of *cyIs4*, a VC4 and VC5 cytoplasmic marker, would impede the ability to view PRKL-1A localization in VC4 and VC5 at the mid L4 stage; therefore, we analyzed VC4 and VC5 at an early L4 stage when *cyIs4* was not active. We expected to see a change in the wild type PRKL-1A localization but not the PRKL-1A ΔCAAX. Indeed a change in wild type PRKL-1A punctae was observed (Figure 19E, 19F, 20E and 20F). Both *punc-4::gfp::prkl-1a; prkl-1 (ok3182); fntb-1; cyIs4; zyIs1* and *punc-4::gfp::prkl-1a Δcaax; prkl-1 (ok3182); fntb-1; cyIs4; zyIs1* lines displayed fewer GFP punctae (Figure 19E-H and 20E-H). Similar to the wild type *prkl-1 (ok3182)* single mutant background experiments, there were no differences in the respective *prkl-1 (ok3182); fntb-1 (AS24)* mutant lines in the number or size of punctae for both VC4 and VC5. The change of PRKL-1A localization, but not PRKL-1A ΔCAAX localization, in an *fntb-1 (AS24)* mutant background suggests that FNTB-1 recognizes the CAAX motif and that FNTB-1 affects PRKL-1 localization.

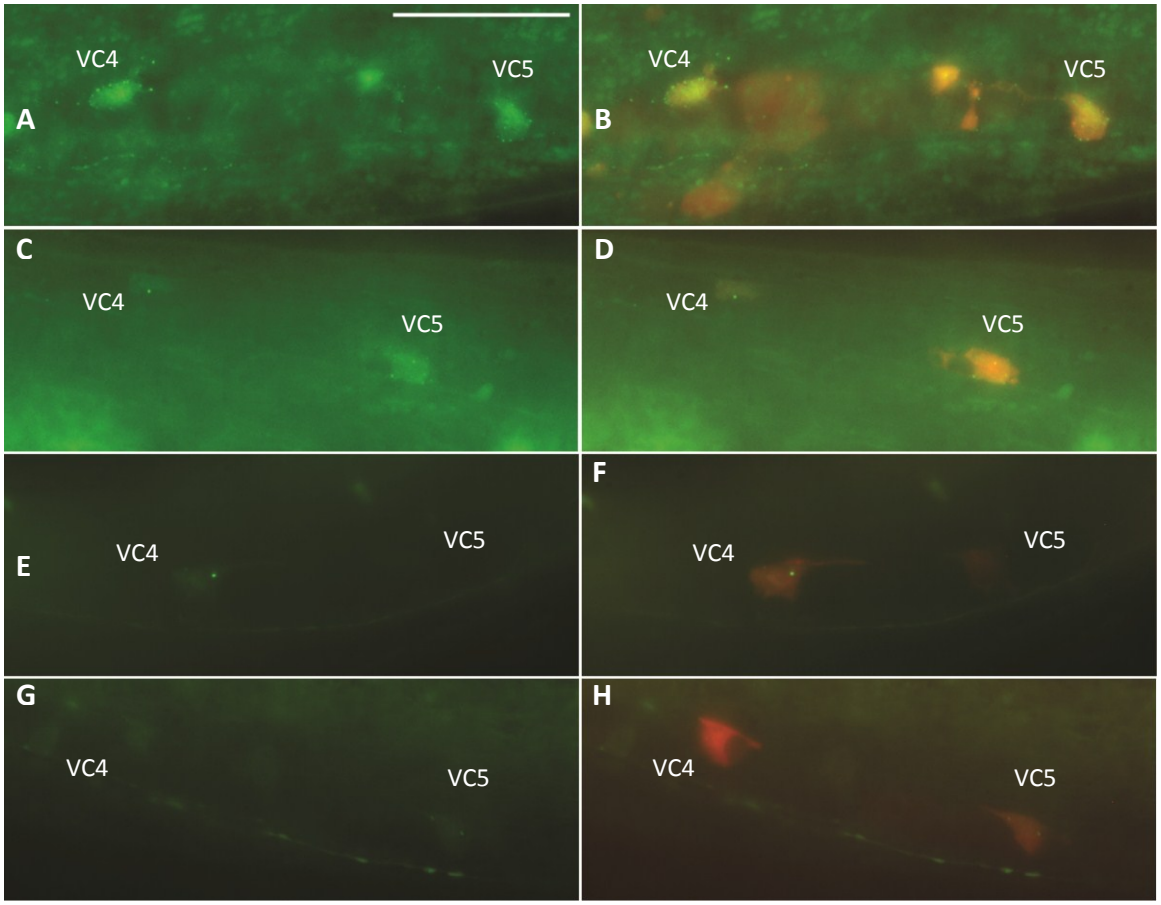

Figure 21. Localization of PRKL-1 in L3 *wt* and *fntb-1* mutant VC4 and VC5 neurons. (A, B) *Ex(punc-4::gfp::prkl-1a); prkl-1 (ok3182)* worms displaying GFP-PRKL-1 punctae on VC4 and VC5 membrane. **(C, D)** *Ex(punc-4::gfp::prkl-1a ΔCAAX); prkl-1 (ok3182)* worms displaying few GFP-PRKL-1 punctae on VC membrane. **(E, F)** *Ex(punc-4::gfp::prkl-1a); fntb-1 (AS24); prkl-1 (ok3182)* worms displaying few GFP-PRKL-1 punctae. **(G, H)** *Ex(punc-4::gfp::prkl-1a ΔCAAX); fntb-1 (AS24); prkl-1 (ok3182)* worms displaying few GFP-PRKL-1 punctae. **(B, D, F, H)** are the same images as **(A, C, E, G)** respectively merged with *plin-11::rfp* images to show VC neuron cytoplasm and vulva cells. Scale bars, 20 µm.

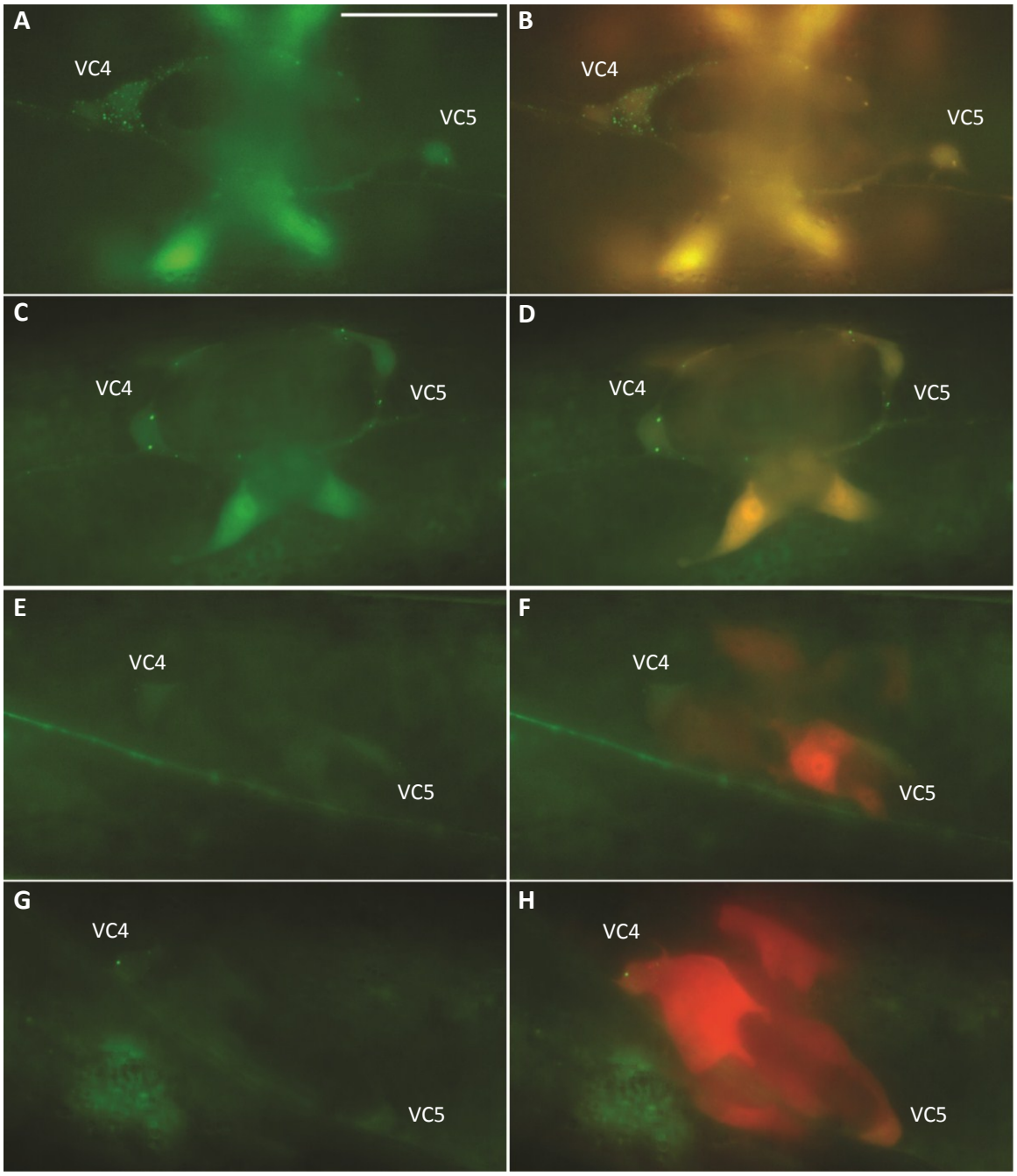

Figure 22. Localization of PRKL-1 in L4 *wt* and *fntb-1* mutant VC4 and VC5 neurons. (A, B) *Ex(punc-4::gfp::prkl-1a); prkl-1 (ok3182)* worms displaying GFP-PRKL-1 punctae on VC4 and VC5 membrane. **(C, D)** *Ex(punc-4::gfp::prkl-1a ΔCAAX); prkl-1 (ok3182)* worms displaying few GFP-PRKL-1 punctae on VC membrane. **(E, F)** *Ex(punc-4::gfp::prkl-1a); fntb-1 (AS24); prkl-1 (ok3182)* worms displaying few GFP-PRKL-1 punctae. **(G, H)** *Ex(punc-4::gfp::prkl-1a ΔCAAX); fntb-1 (AS24); prkl-1 (ok3182)* worms displaying few GFP-PRKL-1 punctae. **(B, D, F, H)** are the same images as **(A, C, E, G)** respectively merged with *plin-11::rfp* images to show VC neuron cytoplasm and vulva cells. Scale bars, 20 µm.

CHAPTER 4

DISCUSSION

4.1 A novel genetic screen discovered new components in VC4 and VC5 polarity

Genetic screens are excellent tools for identifying and dissecting new components of genetic pathways. Many of the core PCP components have been identified through genetic screens in *Drosophila melanogaster* (Gubb and Garcia-Bellido, 1982). The PCP core complex is an internal signalling module that receives external signals from PCP global cues to induce polarity (Bayly and Axelrod, 2011; Goodrich and Strutt, 2011; Lapebie et al., 2011; Vladar et al., 2009). An excellent advantage of *C. elegans* is that it is relatively easy to perform genetic screens. The *prkl-1* suppressor screen was a novel approach designed to search for new PCP components. An over-expression of *prkl-1* in motor neurons creates a backwards locomotion defect. Since the locomotion defect can be restored by mutations in other PCP genes that interact with *prkl-1*, it was logical to use suppression of the backwards locomotion phenotype as a screen to identify new PCP genes that regulate the polarity of VC4 and VC5.

The VC neurons in *C. elegans* provide an excellent opportunity to study neuronal polarity as they display differences in the orientation and growth of neurites relative to the AP axis and the vulva. VC1 to VC3 and VC6 extend two neurites each along the ventral nerve cord in the AP direction, while VC4 and VC5 extend two neurites mediolaterally around the vulva. Ablation of the vulva results in VC4 and VC5 adopting

an AP polarity similar to the rest of the VC neurons implying that the default polarity of the VC neurons is in the AP direction (Li and Chalfie, 1990). The vulva ablation experiments suggest that a long-range, extra-cellular polarity signal gradient polarizes the VC neurons in the default AP plane, while the vulva emits a stronger polarity signal that re-polarizes VC4 and VC5 in the ML plane to surround the vulva. This re-polarization of VC4 and VC5 is similar to the re-polarization of the vulva cells during organogenesis. In vulva organogenesis, *egl-20*/wnt orients the vulva cells in the posterior direction while *lin-44* and *mom-2* are secreted from primary vulva cells to re-polarize the cells towards the vulva (Green et al., 2008). Studying the PCP pathway in VC4 and VC5 becomes complex because mutations in confirmed downstream effectors of the PCP pathway, such as the RAS superfamily of small GTPases, create neuronal polarity defects and vulva defects in *C. elegans* (Arimura and Kaibuchi, 2005; Govek et al., 2005; Hara and Han, 1995). The complexities of the PCP pathway effectors and vulva development make it extremely difficult to differentiate between mutations in the core PCP module and mutations that affect vulva development with secondary VC4 and VC5 polarity defects. The *prkl-1* suppressor screen was a vulva independent screen that could therefore identify additional polarity components that may not have been discovered otherwise.

The *prkl-1* suppressor screen was validated through the discovery of twelve new alleles of *vang-1* and one new allele of *fntb-1*. Additionally the screen discovered five new mutations that affect the polarization of VC4 and VC5. Since the ectopic neurite defects of VC4 and VC5 were relatively low in the five discovered genetically mutated

worm lines, it is challenging to determine the quantity and identity of genes that were mutated. It is also unknown whether the mutated genes function in the PCP pathway rather than a parallel pathway that regulates neuronal polarity such as PI-3 kinase and PIP_3 related pathways (Arimura and Kaibuchi, 2005; Menager et al., 2004; Nishimura et al., 2005). It is possible that a mutation in any gene that affects expression levels or localization of RhoA, Rac1 or Cdc42 will affect neuronal polarity (Arimura and Kaibuchi, 2005; Govek et al., 2005; Nishimura et al., 2005). However, due to the efficiency of the screen and the quantity of mutants that displayed backwards locomotion defects, there may be more than the five newly discovered mutations because other mutants that display a recovery of backwards locomotion have yet to be analyzed for VC4 and VC5 defects.

4.2 Characterization of *fntb-1*

4.2.1 Non-cell autonomous function of *fntb-1* and *prkl-1*

Previous studies in *Drosophila* and zebrafish have defined an interaction and cell-autonomous function for the cytoplasmic proteins FNTB-1 and PRKL-1 (Lin and Gubb, 2009; Mapp et al., 2011). In our study, *fntb-1* displayed a non-cell autonomous rescue of the ectopic neurite defects in VC4 and VC5. The ectopic neurite defects were also mildly rescued non-cell autonomously with both isoforms of *prkl-1*. The mild rescue of the ectopic neurite defects leads to uncertainty in the non-cell autonomous function of *prkl-1* in VC neuronal polarity. Previous studies have indicated conflicting results

concerning the non-cell autonomous function of *prkl-1* (Gubb et al., 1999; Lin and Gubb, 2009; Sanchez-Alvarez et al., 2011). In *Drosophila* wing cells, *prkl-1* functions in a cell and non-cell autonomous manner (Gubb et al., 1999; Lin and Gubb, 2009). A cloned wing cell expressing *prkl-1* displays occasional non-cell autonomous rescue of *prkl-1* mutant defects in neighbouring cells (Gubb et al., 1999). Furthermore, an over-expression of *prkl-1* with a deleted PET domain interferes with the polarization of neighbouring wing cells in wild type *Drosophila* indicating a non-cell autonomous function of *prkl-1* in the PCP pathway that is dependent on the PET domain (Lin and Gubb, 2009). The non-cell autonomous function of *prkl-1* is expected considering that *prkl-1* is a part of PCP intercellular feedback signalling with the ability to affect DSH localization and function (Axelrod, 2009; Fujimura et al., 2009; Goodrich and Strutt, 2011; Jenny et al., 2005; Lin and Gubb, 2009; Tree et al., 2002; Vladar et al., 2009). Interestingly, the *prkl-1a* isoform in *C. elegans* has been shown to function solely in a cell autonomous manner (Sanchez-Alvarez et al., 2011). The results from this study indicate that both *prkl-1* isoforms display non-cell autonomous rescue capabilities of VC4 and VC5 ectopic neurite defects. The discrepancy in results may be due to the injecting concentrations of *prkl-1*. The 40 ng/µl injection concentration of *prkl-1* used in this study is extremely high when compared to the 10 ng/µl injection concentration of *prkl-1* used by Sanchez-Alvarez et al. (2011). While PRKL-1 concentration inside the VC neurons was never confirmed by reverse transcription PCR, the high concentration of *prkl-1* injected into the worm could imply that the non-cell autonomous *prkl-1* rescue of the ectopic neurite defects was due to *prkl-1* over-expression.

Interestingly, *prkl-1a* and *prkl-1b* failed to rescue the VC4 and VC5 defects as strongly as the *fntb-1* non-cell autonomous rescue. It was expected that the *prkl-1* and *fntb-1* non-cell autonomous rescues would be similar as both of these genes have been shown to interact with each other (Lin and Gubb, 2009; Mapp et al., 2011). The difference in rescue could be a result of the additional farnesylation targets of *fntb-1* including proteins that are important for cytoskeletal re-arrangements (Hara and Han, 1995; Kyathanahalli and Kowluru, 2011; Maurer-Stroh et al., 2003). Considering the many targets of FT, it is possible that *fntb-1* farnesylates another protein that is important for the intercellular signalling of the PCP pathway. The non-cell autonomous rescue of VC4 and VC5 defects by *fntb-1* may not only be a result of *prkl-1* farnesylation, but also the farnesylation of another protein important for PCP signalling. Moreover, FT has demonstrated the ability to farnesylate RAS in *C. elegans*: an important component of cell growth (Hara and Han, 1995). It is known that mutations in vulva development affect the polarity of VC4 and VC5 that may be independent of the PCP core mechanisms (Li and Chalfie, 1990). Therefore, the *fntb-1* non-cell autonomous rescue of VC4 and VC5 may be due to the restoration of proper vulva development as well as the restoration of the PCP intercellular feedback system.

4.2.2 The importance of *fntb-1* in the farnesylation of *prkl-1*

Through analysis of single and double mutants, our study indicates that farnesylation of *prkl-1* is important for its function. However, in an *fntb-1* mutant background, *prkl-1* displays a CAAX independent mild rescue of the VC4 and VC5 polarity defect indicating that *prkl-1* may also function independently of *fntb-1*. The *fntb-1*

independent function of *prkl-1* may be due to the PET domain, which has been shown to be sufficient for membrane interaction (Sweede et al., 2008). The *fntb-1* independent function of *prkl-1* may also be a result of prenyltransferease redundancy (Maurer-Stroh et al, 2003). Since FT and GGT-I share a common α-subunit, it is possible PRKL-1 is still prenylated by GGT-I. To clarify the *fntb-1* independent function of *prkl-1*, it is important to perform an *fntb-1* mutant rescue experiment in which the cysteine of the *prkl-1* CAAX motif has been deleted. The cysteine is important for the attachment of the lipid group to PRKL-1 and therefore deleting the cysteine may ensure that PRKL-1 will not be prenylated. Although *prkl-1* can function independently of *fntb-1*, it requires *fntb-1* for proper function as demonstrated by the weak rescue of a highly expressed *prkl-1 ΔCAAX* when compared to wild type rescue in a *prkl-1 (ok3182)* background. Furthermore, a changed farnesylation sequence rescues the VC4 and VC5 polarity defects as well as the wild type in a *prkl-1 (ok3182)* background.

Modifying the CTVS farnesylation sequence of *prkl-1* to CNIM should determine the importance of the prenylation of PRKL-1. Unexpectedly, the modified PRKL-1 CNIM did not restore VC polarity defects in *fntb-1; prkl-1* double mutants. The inability of the modified CAAX PRKL-1 to rescue VC4 and VC5 polarity defects may be attributed to the differences between geranylation and farnesylation. Even though the geranylation sequence PRKL-1A CNIM rescues *prkl-1 (ok3182)* single mutant VC4 and VC5 ectopic neurite defects, the rescues may be a result of farnesylation rather than geranylation; the MIG-2 CAAX domain has the ability to be farnesylated as well as geranylated

(Maurer-Stroh, S., and Eisenhaber, F., 2005). Also, GGT-I may not be expressed in the VC neurons as no experiments were performed to test for GGT-I expression.

The FNTA subunit is responsible for recognition of the CAAX motif (Maurer-Stroh et al., 2003). Since the FNTA subunit is shared by both FT and GGT-I, it is the identity of X that determines the target proteins affinity to GGT-I or FT and subsequent geranylgeranylation or farnesylation (Maurer-Stroh et al., 2003; Mulligan et al., 2010). MIG-2 is part of the Rho family GTPases, which rely upon isoprenylation for proper function (Adamson et al., 1992; Zipkin et al., 1997). In general, many GTPases containing a leucine amino acid as the X of the CAAX motif are geranylated, while those with a methionine or serine amino acid for the X of the CAAX motif are farnesylated (Adamson et al., 1992; Buss et al., 1991; Clarke, 1992; Goldstein et al., 1991; Kawata et al., 1990; Maltese and Sheridan, 1990; Tschantz et al., 1997; Yamane et al., 1991; Zhang and Casey, 1996). The MIG-2 CAAX motif is CNIM, which suggests that MIG-2 is farnesylated depending on the presence of FNTB-1 (Zipkin et al., 1997); however, there are exceptions to the rules that account for interaction with GGT-I. Methionine has a 32-fold higher affinity to FT; however, GGT-I preferentially binds with leucine and methionine (Maurer-Stroh and Eisenhaber, 2005; Roskoski and Ritchie, 1998). Although GGT-I has a greater affinity for leucine (160-fold), it still has the ability to interact with methionine (Roskoski and Ritchie, 1998). Therefore the CAAX motif of MIG-2 has the ability to interact with FT and GGT-I based on the C-terminal methionine. When considering enzyme interaction, it has recently been discovered that while the CAAX motif is a large determinant for prenyltransferase selection, the linker region before the

CAAX motif is also important (Maurer-Stroh and Eisenhaber, 2005). The PrePS prenylation predictor suite takes this linker region into consideration and determines that the modified PRKL-1A protein with the MIG-2 C-terminal results in a 1.5-fold higher preference to GGT-I than FT. Taking the prenyltransferase redundancy into account with the results, it is plausible that the farnesylation that is responsible for the PRKL-1A CNIM rescued the VC4 and VC5 defects in *prkl-1 (ok3182)* and the reason could explain why geranylation of PRKL-1A CNIM does not rescue the *prkl-1 (ok3182); fntb-1* double mutants.

Although the observed rescue of VC4 and VC5 polarity defects from all three constructs could be a result of FNTB-1 independent function, the lack of full rescue in *fntb-1* and *prkl-1* single and double mutants, as well as the rescues displayed in a *prkl-1 (ok3182)* background from all three constructs demonstrate that *fntb-1* is required for proper *prkl-1* function.

4.2.3 The *fntb-1* dependent localization of *prkl-1*

This study demonstrates the importance of PRKL-1 farnesylation from FT for proper localization. The qualitative results confirm that either the absence of the CAAX motif from PRKL-1 or the absence of FNTB-1 from VC4 and VC5 results in a change of PRKL-1 localization. The change of localization coincides with the ectopic neurite defects observed in VC4 and VC5 suggesting that FNTB-1 is responsible for the correct localization and function of PRKL-1 in the regulation of neuronal polarity. Also, we show that PRKL-1 maintains a symmetrical localization in the VC neurons. The lack of asymmetrical localization corresponds to a recent study performed in *Drosophila*

mushroom body neurons where PRKL does not adopt an asymmetric localization but rather localizes at the axonal branches (Ng, 2012). Therefore proximal localization of PRKL-1 may not be necessary for proper planar cell polarity function in neurons.

There are problems with qualitative methods used for PRKL-1 localization that could account for the results in this study. The change in PRKL-1 localization may be a result of endoplasmic reticulum quality control (Hurtley and Helenius, 1989). Deleting the CAAX domain and attaching GFP to PRKL-1 may cause the endoplasmic reticulum to retain the protein, which occurs with many misfolded and abnormal proteins (Hurtley and Helenius, 1989). The GFP punctae that were seen with the wild type and the deleted *prkl-1* constructs may by located in the endoplasmic reticulum and not a true representation of PRKL-1 localization. It is difficult to determine the cellular location of PRKL-1 in the VC neurons. In the classical example of the PCP pathway, PRKL is localized to the proximal plasma membrane where it interacts with VANG (Axelrod, 2009; Goodrich and Strutt, 2011; Ma et al., 2003; Tree et al., 2002; Vladar et al., 2009). In mice, PRKL has been shown localizing to the nucleus and cytoplasmic membranes in a farnesyltransferase dependent manner (Tao et al., 2012). Experiments using nuclear and cytoplasmic membrane makers, as well as antibodies could clarify the localization of PRKL-1 in the VC neurons.

4.2.4 Vulva defects in *fntb-1* mutants

Ablation of the vulva results in VC4 and VC5 adopting an AP polarity similar to the rest of the VC neurons, thereby making it difficult to determine VC4 and VC5 PCP defects in mutants with vulva defects (Li and Chalfie, 1990). We noticed that *fntb-1* mutants display vulva morphogenic defects (data not shown). Since the penetrance of the vulva defects was never quantified, it is difficult to analyze some of the rescue experiments performed. In particular, we showed that *fntb-1* has the ability to function non-cell autonomously; however, *fntb-1* expressed in the vulva may be restoring vulva defects resulting in the rescue of some, but not all of the VC ectopic neurites. The hypodermal-specific *fntb-1* rescues may not be a result of planar cell polarity. This model seems even more convincing since we showed that *fntb-1* may rescue VC polarity defects through another pathway independent of *prkl-1*. However, since vulva defects still exist in the rescued lines (data not shown), it suggests that *fntb-1* functions non-cell autonomously and rescues VC planar cell polarity defects independent of vulva morphogenesis. Further quantification of the vulva defects in *fntb-1* mutants and rescue lines will provide a better insight into the mechanisms, pathways and results of the rescue experiments.

4.3 Future directions

In order to better understand the mechanism responsible for the polarization of VC4 and VC5 it is important to discover the components involved in neuronal polarization. The *prkl-1* suppressor screen discovered at least five mutants that may be involved with the PCP like pathway in the polarization of VC4 and VC5. Future studies should focus on completing the genetic screen, including the genetic mapping and cloning of mutants in an attempt to discover novel genes that will help clarify the concept of VC4 and VC5 polarization.

The extrinsic guidance cue that emanates from the vulva and orients VC4 and VC5 remains elusive. This study performed a genetic screen that was independent of the vulva and discovered a gene that affects VC4 and VC5 polarity: *fntb-1*. During the characterization of *fntb-1*, the non-cell autonomous rescue data suggest that there may be another polarity protein in the vulva that is farnesylated to restore proper VC4 and VC5 orientation. Since the targets of *fntb-1* require a CAAX motif, a future RNAi screen looking for VC4 and VC5 ectopic neurites by targeting proteins that have a farnesylation CAAX motif may result in the discovery of unknown polarity genes that interact with *fntb-1* in the vulva to regulate neuronal polarization of VC4 and VC5. Also, a future genetic screen with *pcol-10::fntb-1; fntb-1(e6.1)* looking for VC4 and VC5 polarity defects would provide another excellent opportunity to discover the unknown polarity genes that interact with *fntb-1* in the vulva to regulate neuronal polarization.

Studies investigating neuronal polarity have yet to determine the involvement and importance of the PCP pathway. Polarity genes have been found to be important in

neuronal polarity; however, it is difficult to distinguish whether their importance is through the PCP pathway or the PAR complex. A previous study in *C. elegans* has implicated the involvement of polarity genes *prkl-1*, *vang-1*, *fmi-1*, and *dsh-1* in the neuronal polarization of VC4 and VC5; however, it is unclear whether *dsh-1* functions in similar or parallel pathways (Sanchez-Alvarez et al., 2011). Since both the PCP pathway and the PAR complex interact with similar downstream effectors it is difficult to separate the PCP pathway from the PAR complex; however, future cell specific genetic studies with the members of the PAR complex and polarity genes may be able to distinguish which pathway the polarity genes are involved with for the polarization of VC4 and VC5.

4.4 Conclusion and significance

In conclusion, this study encompassed a *C. elegans* genetic screen that has potentially led to the discovery of six novel genes involved with VC4 and VC5 neuronal polarization. We show that one of the discovered genes, *fntb-1*, interacts with *prkl-1* to polarize VC4 and VC5. While *fntb-1* has previously been linked to neuronal migration defects, this is the first time that *fntb-1* has been demonstrated to be involved in neuronal polarization. Through cell rescue experiments and localization analysis we demonstrate that *fntb-1* is required for the localization and function of *prkl-1* as a part of a PCP-like pathway.

While the polarization of VC4 and VC5 appears to have no obvious physiological effects on the egg laying ability of *C. elegans*, the discovery that *fntb-1* interacts with *prkl-1* provides further insight into the molecular mechanisms of the PCP pathway. The discovery of *fntb-1* involvement in neuronal polarization further defines the PCP pathway as well as neuronal polarization, which is important in our understanding of neuron development and differentiation. A better comprehension of neuron differentiation becomes increasingly important when attempting to regenerate neurons after injuries such as acute ischemic stroke and spinal cord injuries (Ben-Hur, 2010; Haas et al., 2005). Because FTIs are being studied as a therapeutic method to control cancers, the discovery of FT involvement in neuronal polarity highlights other possible side-effects of this treatment. Finally, due to the broad and various functions of the PCP pathway, further investigation of PCP pathway interactions provides an opportunity to develop novel therapeutic treatments for a variety of diseases including cancer migration and neural tube closure defects.

References

Adamson, P., et al. (1992). Post-translational modifications of $p21^{rho}$ proteins. J Biol Chem. 267: 20033-20038.

Adler, P. N., Taylor, J., and Charlton, J. (2000). The domineering non-autonomy of *frizzled* and *Van Gogh* clones in the *Drosophila* wing is a consequence of a disruption in local signaling. Mech Dev. 96: 197-207.

Andersson, E. R., et al. (2008). *Wnt5a* regulates ventral midbrain morphogenesis and the development of A9-A10 dopaminergic cells *in vivo.* PLoS One. 3:e3517.

Arimura, N., et al. (2004). Role of CRMP-2 in neuronal polarity. J Neurobiol. 58: 34-47.

Arimura, N., and Kaibuchi, K. (2005). Key regulators in neuronal polarity. Neuron 48: 881-884.

Axelrod, J. D. (2009). Progress and challenges in understanding planar cell polarity signaling. Semin Cell Dev Biol. 20: 964-971.

Bastock, R., Strutt, H., and Strutt, D. (2003). Strabismus is asymmetrically localised and binds to Prickle and Dishevelled during *Drosophila* planar polarity patterning. Development 130: 3007-3014.

Bayly, R., and Axelrod, J. D. (2011). Pointing in the right direction: new developments in the field of planar cell polarity. Nat Rev Genet. 12: 385-391.

Bei, Y., et al. (2002). SRC-1 and Wnt signaling act together to specify endoderm and to control cleavage orientation in early *C. elegans* embryos. Dev Cell. 3: 113-125.

Ben-Hur, T. (2010). Reconstructing neural circuits using transplanted neural stem cells in the injured spinal cord. J Clin Invest. 120: 3096-3098.

Benzing, T., Simons, M., and Walz, G. (2007). Wnt signaling in Polysistic Kidney Disease. J Am Soc Nephrol. 18: 1389-1398.

Bhanot, P., et al. (1996). A new member of the *frizzled* family from *Drosophila* functions as a Wingless receptor. Nature 382: 225-230.

Bingham, S. M., et al. (2009). Multiple mechanisms mediate motor neuron migration in the zebrafish hindbrain. Dev Neurobiol. 70: 87-99.

Blakely, B. D., et al. (2011). Wnt5a regulates midbrain dopaminergic axon growth and guidance. PLoS One. 6: e18373.

Bosoi, C. M., et al. (2011). Identification and characterization of novel rare mutations in the planar cell polarity gene *prickle1* in human neural tube defects. Hum Mutat. 32: 1371-1375.

Bradke, F., and Dotti, C. G. (1999). The role of local actin instability in axon formation. Science 283: 1931-1934.

Bradke, F., and Dotti, C. G. (2000). Establishment of neuronal polarity: lessons from cultured hippocampal neurons. Curr Opin Neurobiol. 10: 574-581.

Brenner, S. (1974). The genetics of *Caenorhabditis elegans*. Genetics 77: 71-94.

Buss, J. E., et al. (1991). The COOH-terminal domain of the Rap1A (Krev-1) protein is isoprenylated and supports transformation by an H-Ras:Rap1A chimeric protein. Mol Cell Biol. 11: 1523-1530.

Caceres, A., Banker, G., and Binder, L. (1986). Immunocytochemical localization of tubulin and microtubule-associated protein 2 during the development of hippocampal neurons in culture. J Neurosci. 6: 714-722.

Carreira-Barbosa, F., et al. (2003). Prickle 1 regulates cell movements during gastrulation and neuronal migration in zebrafish. Development 130: 4037-4046.

Carthew, R. W. (2007). Pattern formation in the *Drosophila* eye. Curr Opin Genet Dev. 17: 309-313.

Casal, J., Lawrence, P. A., and Struhl, G. (2006). Two separate molecular systems, Dachsous/Fat and Starry night/Frizzled, act independently to confer planar cell polarity. Development 133: 4561-4572.

Chan, D. W., et al. (2006). Prickle-1 negatively regulates Wnt/β-Catenin pathway by promoting Dishevelled ubiquitination/degradation in liver cancer. Gastroenterology 131: 1218-1227.

Chen, W., et al. (2003). Dishevelled 2 recruits β-Arrestin to mediate Wnt5A-stimulated endocytosis of Frizzled 4. Science 301: 1391-1394.

Chen, W. S., et al. (2008). Asymmetric homotypic interactions of the atypical cadherin Flamingo mediate intercellular polarity signaling. Cell 133: 1093-1105.

Ciruna, B., et al. (2006). Planar cell polarity signalling couples cell division and morphogenesis during neurulation. Nature 439: 220-224.

Clarke, S. (1992). Protein isoprenylation and methylation at carboxyl-terminal cysteine residues. Annu Rev Biochem. 61: 355-386.

Colavita, A., et al. (1998). Pioneer axon guidance by UNC-129, a *C. elegans* TGF-beta. Science 281: 706-709.

Cold Spring Harbor Laboratory Press (1997). *C. elegans* II. 2nd edition. Riddle, D. L., et al., editors. Cold Spring Harbor (NY).

Cooper, M. T. D., and Bray, S. J. (1999). Frizzled regulation of Notch signalling polarizes cell fate in the *Drosophila* eye. Nature 397: 526-530.

Craig, A., M., and Banker, G. (1994). Neuronal polarity. Annu Rev Neurosci. 17 : 267-310.

Curtin, J. A., et al. (2003). Mutation of Celsr1 disrupts planar polarity of inner ear hair cells and causes severe neural tube defects in the mouse. Curr Biol. 13: 1129-1133.

Dotti, C. G., Banker, G. A., and Binder, L. I. (1987). The expression and distribution of the microtubule-associated proteins tau and microtubule-associated protein 2 in hippocampal neurons in the rat in situ and in cell culture. Neuroscience 23: 121-130.

Dotti, C. G., Sullivan, C. A., and Banker, G. A. (1988). The establishment of polarity by hippocampal neurons in culture. J Neurosci. 8: 1454-1468.

Eckert, G. P., et al. (2009). Regulation of the brain isoprenoids farnesyl- and geranylgeranylpyrophosphate is altered in male Alzheimer patients. Neurobiol Dis. 35: 251-257.

Etienne-Manneville, S., and Hall, A. (2003). Cdc42 regulates GSK-3β and adenomatous polyposis coli to control cell polarity. Nature 421: 753-756.

Fire, A., Harrison, S. W., and Dixon, D. (1990). A modular set of *lacZ* fusion vectors for studying gene expression in *Caenorhabditis elegans*. Gene 93: 189-198.

Fujimura, L., et al. (2009). Prickle promotes neurite outgrowth via the Dishevelled dependent pathway in C1300 cells. Neurosci Lett. 467: 6-10.

Gao, B., et al. (2011). Wnt signaling gradients establish planar cell polarity by inducing Vangl2 phosphorylation through Ror2. Dev Cell. 20: 163-176.

Gao, C., and Chen, Y. G. (2010). Dishevelled: The hub of Wnt signaling. Cell Signal. 22: 717-727.

Goldstein, B. (1993). Establishment of gut fate in the E lineage of *C. elegans*: the roles of lineage-dependent mechanisms and cell interactions. Development 118: 1267-1277.

Goldstein, B. (1995) (1). An analysis of the response to gut induction in the *C. elegans* embryo. Development 121: 1227-1236.

Goldstein, B. (1995) (2). Cell contacts orient some cell division axes in the *Caenorhabditis elegans* embryo. J Cell Biol. 129: 1071-1080.

Goldstein, J. L., et al. (1991). Nonfarnesylated tetrapeptide inhibitors of protein Farnesyltransferase. J Biol Chem. 266: 15575-15578.

Goodrich, L. V., and Strutt, D. (2011). Principles of planar polarity in animal development. Development 138: 1877-1892.

Goold, R. G., Owen, R., and Gordon-Weeks, P. R. (1999). Glycogen synthase kinase 3β phosphorylation of microtubule-associated protein 1B regulates the stability of microtubules in growth cones. J Cell Sci. 112: 3373-3384.

Gordon-Weeks, P. R., et al. (1993). A phosphorylation epitope on MAP 1B that is transiently expressed in growing axons in the developing rat nervous system. Eur J Neurosci. 5: 1302-1311.

Govek, E. E., Newey, S. E., and Aelst, L. V. (2005). The role of Rho GTPases in neuronal development. Genes Dev. 19: 1-49.

Gray, R. S., Roszko, I., and Solnica-Krezel, L. (2011). Planar cell polarity: Coordinating morphogenetic cell behaviors with embryonic polarity. Dev Cell. 21: 120-133.

Green, J. L., Inoue, T., and Sternberg, P. W. (2008). Opposing Wnt pathways orient cell polarity during organogenesis. Cell 134: 646-656.

Gubb, D., and Garcia-Bellido, A. (1982). A genetic analysis of the determination of cuticular polarity during development in *Drosophila melanogaster.* J Embryol Exp Morph. 68: 37-57.

Gubb, D., et al. (1999). The balance between isoforms of the Prickle LIM domain protein is critical for planar polarity in *Drosophila* imaginal discs. Genes Dev. 13: 2315-2327.

Haas, S., Weidner, N., and Winkler, J. (2005). Adult stem cell therapy in stroke. Curr Opin Neurol. 18: 59-64.

Habas, R., Kato, Y., and He, X. (2001). Wnt/Frizzled activation of Rho regulates vertebrate gastrulation and requires a novel formin homology protein Daam1. Cell 107: 843-854.

Halpin, S., and Dehmelt, L. (2006). The MAP1 family of microtubule-associated proteins. Genome Biol. 7: 224.

Hara, M., and Han, M. (1995). Ras Farnesyltransferase inhibitors suppress the phenotype resulting from an activated mutation in *Caenorhabditis elegans*. Proc Natl Acad Sci USA. 92: 3333-3337.

Hashimoto, M., and Hamada, H. (2010). Translation of anterior-posterior polarity into left-right polarity in the mouse embryo. Curr Opin Genet Dev. 20: 433-437.

Hawkins, N. C., et al. (2005). MOM-5 Frizzled regulates the distribution of DSH-2 to control *C. elegans* asymmetric neuroblast divisions. Dev Biol. 284: 246-259.

Hilliard, M. A., and Bargmann, C. I. (2006). Wnt signals and Frizzled activity orient anterior-posterior axon outgrowth in *C. elegans*. Dev Cell. 10: 379-390.

Hoffmann, M., et al. (2010). Intestinal tube formation in *Caenorhabditis elegans* requires *vang-1* and *egl-15* signaling. Dev Biol. 339: 268-279.

Hurtley, S. M. and Helenius, A. (1989). Protein oligomerization in the endoplasmic reticulum. Annu Rev Cell Biol. 5: 277-307.

Jenny, A., et al. (2005). Diego and Prickle regulate Frizzled planar cell polarity signalling by competing for Dishevelled binding. Nat Cell Biol. 7: 691-697.

Jorgensen, E. M., and Mango, S. E. (2002). The art and design of genetic screens: *Caenorhabditis elegans*. Nat Rev Genet. 3: 356-369.

Kawata, M., et al. (1990). Posttranslationally processed structure of the human platelet protein smg p21B: Evidence for geranylgeranylation and carboxyl methylation of the C-terminal cysteine. Proc Natl Acad Sci USA 87: 8960-8964.

Keller, R. (2002). Shaping the vertebrate body plan by polarized embryonic cell movements. Science 298: 1950-1954.

Kyathanahalli, C. H., and Kowluru, A. (2011). A farnesylated G-protein suppresses Akt phosphorylation in INS 832/13 cells and normal rat islets: Regulation by pertussis toxin and PGE_2. Biochem Pharmacol. 81: 1237-1247.

Lapebie, P., Borchiellini, C., and Houliston, E. (2011). Dissecting the PCP pathway: One or more pathways?: Does a separate Wnt-Fz-Rho pathway drive morphogenesis? Bioessays 33: 759-768.

Lawrence, P. A., Casal, J., and Struhl, G. (2002). Towards a model of the organisation of planar polarity and pattern in the *Drosophila* abdomen. Development 129: 2749-2760.

Le Grand, F., et al. (2009). Wnt7a activates the planar cell polarity pathway to drive the symmetric expansion of satellite stem cells. Cell Stem Cell. 4: 535-547.

Li, C., and Chalfie, M. (1990). Organogenesis in *C. elegans*: positioning of neurons and muscles in the egg-laying system. Neuron 4: 681-695.

Lin, Y. Y., and Gubb, D. (2009). Molecular dissection of *Drosophila* Prickle isoforms distinguishes their essential and overlapping roles in planar cell polarity. Dev Biol. 325: 386-399.

Logan, C. Y., and Nusse, R. (2004). The Wnt signaling pathway in development and disease. Annu Rev Cell Dev Biol. 20: 781-810.

Long, S. B., Casey, P. J., and Beese, L. S. (2002). Reaction path of protein Farnesyltransferase at atomic resolution. Nature 419: 645-650.

Ma, D., et al. (2003). Fidelity in planar cell polarity signalling. Nature 421: 543-547.

Maltese, W. A., and Sheridan, K. M. (1990). Isoprenoid modification of G25K (G_p), a low molecular mass GTP-binding protein distinct from $p21^{ras}$. J Biol Chem. 265: 17883-17890.

Mandell, J. W., and Banker, G. A. (1996). A spatial gradient of tau protein phosphorylation in nascent axons. J Neurosci. 16: 5727-5740.

Mapp, O. M., et al. (2011). Zebrafish Prickle1b mediates facial branchiomotor neuron migration via a farnesylation-dependent nuclear activity. Development 138: 2121-2132.

Matakatsu, H., and Blair, S. S. (2004). Interactions between Fat and Dachsous and the regulation of planar cell polarity in the *Drosophila* wing. Development 131: 3785-3794.

Maurer-Stroh, S., and Eisenhaber, F. (2005). Refinement and prediction of protein prenylation motifs. Genome Biol. 6: R55.

Maurer-Stroh, S., Washietl, S., and Eisenhaber, F. (2003). Protein prenyltransferases. Genome Biol. 4: 212.

Mello, C. and Fire, A. (1995). DNA transformation. Methods Cell Biol. 48: 451-482.

Mello, C. C., et al. (1991). Efficient gene transfer in *C. elegans*: extrachromosomal maintenance and integration of transforming sequences. EMBO J. 10: 3959-3970.

Menager, C., et al. (2004). PIP_3 is involved in neuronal polarization and axon formation. J Neurochem. 89: 109-118.

Miller III, D. M. and Niemeyer, C. J. (1995). Expression of the *unc-4* homeoprotein in *Caenorhabditis elegans* motor neurons specifies presynaptic input. Development 121: 2877-2886.

Miller, D. M. et al. (1992). *C. elegans unc-4* gene econdes a homeodomain protein that determines the pattern of synaptic input to specific motor neurons. Nature 355: 841-845.

Montcouquiol, M., Crenshaw III, E. B., and Kelley, M. W. (2006). Noncanonical Wnt signaling and neural polarity. Annu Rev Neurosci. 29: 363-386.

Moon, R. T., et al. (1993). *Xwnt-5*A: a maternal *wnt* that affects morphogenetic movements after overexpression in embryos of *Xenopus laevis*. Development 119: 97-111.

Mulligan, T., et al. (2010). Prenylation-deficient G protein gamma subunits disrupt GPCR signaling in the zebrafish. Cell Signal. 22: 221-233.

Ng, J. (2012). Wnt/PCP proteins regulate stereotyped axon branching extension in *Drosophila*. Development 139: 165-177.

Nishimura, T., et al. (2003). CRMP-2 regulates polarized Numb-mediated endocytosis for axon growth. Nat Cell Biol. 5: 819-826.

Nishimura, T., et al. (2005). PAR-6-PAR-3 mediates Cdc42-induced Rac activation through the Rac GEFs STEF/Tiam1. Nat Cell Biol. 7: 270-277.

Okuda, H., et al. (2007). Mouse *prickle1* and *prickle2* are expressed in postmitotic neurons and promote neurite outgrowth. FEBS Lett. 581: 4754-4760.

Ou, C. Y., and Shen, K. (2011). Neuronal polarity in *C. elegans.* Dev Neurobiol. 71: 554-566.

Panakova, D., et al. (2005). Lipoprotein particles are required for Hedgehog and Wingless signalling. Nature 435: 58-65.

Park, M., and Moon, R. T. (2002). The planar cell-polarity gene *stbm* regulates cell behaviour and cell fate in vertebrate embryos. Nat Cell Biol. 4: 20-25.

Pinson, K. I., et al. (2000). An LDL-receptor-related protein mediates Wnt signalling in mice. Nature 407: 535-538.

Prasad, B. C., and Clark, S. G. (2006). Wnt signaling establishes anteroposterior neuronal polarity and requires retromer in *C. elegans*. Development 133: 1757-1766.

Qian, D., et al. (2007). Wnt5a functions in planar cell polarity regulation in mice. Dev Biol. 206: 121-133.

Robinson, A., et al. (2012). Mutations in the planar cell polarity genes *celsr1* and *scrib* are associated with the severe neural tube defect craniorachischisis. Hum Mutat. 33: 440-447.

Rocheleau, C. E., et al. (1997). Wnt signaling and an APC-related gene specify endoderm in early *C. elegans* embryos. Cell 90: 707-716.

Roskoski Jr., R., and Ritchie, P. (1998). Role of the carboxyterminal residue in peptide binding to protein Farnesyltransferase and protein Geranylgeranyltransferase. Arch Biochem Biophys. 356: 167-176.

Rothbacher, U., et al. (2000). Dishevelled phosphorylation, subcellular localization and multimerization regulate its role in early embryogenesis. EMBO J. 19: 1010-1022.

Sanchez-Alvarez, L., et al. (2011). VANG-1 and PRKL-1 cooperate to negatively regulate neurite formation in *Caenorhabditis elegans*. PLoS Genet. 7: e1002257.

Schlesinger, A., et al. (1999). Wnt pathway components orient a mitotic spindle in the early *Caenorhabditis elegans* embryo without requiring gene transcription in the responding cell. Genes Dev. 13: 2028-2038.

Sebti, S. M. (2005). Protein farnesylation: implications for normal physiology, malignant transformation, and cancer therapy. Cancer Cell 7: 297-300.

Shafer, B., et al. (2011). Vangl2 promotes Wnt/Planar Cell Polarity-like signaling by antagonizing Dvl1-mediated feeback inhibition in growth cone guidance. Dev Cell. 20: 177-191.

Shi, S. H., Jan, L. Y., and Jan, Y. N. (2003). Hippocampal neuronal polarity specificed by spatially localized mPar3/mPar6 and PI 3-Kinase activity. Cell 112: 63-75.

Shimizu, K., Sato, M., and Tabata, T. (2011). The Wnt5/Planar Cell Polarity pathway regulates axonal development of the *Drosophila* mushroom body neuron. J Neurosci. 31: 4944-4954.

Simon, M. A. (2004). Planar cell polarity in the *Drosophila* eye is directed by graded Four-jointed and Dachsous expression. Development 131: 6175-6184.

Singh, J., et al. (2010). Abelson family kinases regulate Frizzled planar cell polarity signaling via Dsh phosphorylation. Genes Dev. 24: 2157-2168.

Spencer, A. G., et al. (2001). A RHO GTPase-mediated pathway is required during P cell migration in *Caenorhabditis elegans*. PNAS 98: 13132-13137.

Strutt, D. I., and Mlodzik, M. (1995). Ommatidial polarity in the *Drosophila* eye is determined by the direction of furrow progression and local interactions. Development 121: 4247-4256.

Strutt, H., and Strutt, D. (2002). Nonautonomous planar polarity patterning in *Drosophila*: Dishevelled-independent functions of Frizzled. Dev Cell. 3: 851-863.

Stuebner, S., et al. (2010). *Fzd3* and *fzd6* deficiency results in a severe midbrain morphogenesis defect. Dev Dyn. 239: 246-260.

Sweede, M., et al. (2008). Structural and membrane binding properties of the prickle PET domain. Biochemistry 47: 13524-13536.

Tada, M., and Smith, J. C. (2000). *Xwnt11* is a target of *Xenopus* Brachyury: regulation of gastrulation movements via Dishevelled, but not through the canonical Wnt pathway. Development 127: 2227-2238.

Tamai, K., et al. (2000). LDL-receptor-related proteins in Wnt signal transduction. Nature 407: 530-535.

Tao, H., et al. (2011). Mutations in Prickle orthologs cause seizures in flies, mice and humans. Am J Hum Genet. 88: 138-149.

Tavernarakis, N., et al. (1997). *unc-8*, a DEG/ENaC family member, encodes a subunit of a candidate mechanically gated channel that modulates *C. elegans* locomotion. Neuron 18: 107-119.

Taylor, J., et al. (1998). *Van Gogh:* A new *Drosophila* tissue polarity gene. Genetics 150: 199-210.

Tepass, U., et al. (2000). Cadherins in embryonic and neural morphogenesis. Nat Rev Mol Cell Biol. 1: 91-100.

Thorpe, C. J., et al. (1997). Wnt signaling polarizes an early *C. elegans* blastomere to distinguish endoderm from mesoderm. Cell 90: 695-705.

Tissir, F., and Goffinet, A. M. (2010). Planar cell polarity signaling in neural development. Curr Opin Neurobiol. 20: 572-577.

Torban, E., et al. (2004). Independent mutations in mouse *vangl2* that cause neural tube defects in *Looptail* mice impair interaction with members of the *dishevelled* family. J Biol Chem. 279: 52703-52713.

Tree, D. R. P., et al. (2002). Prickle mediates feedback amplification to generate asymmetric planar cell polarity signaling. Cell 109: 371-381.

Tschantz, W. R., Furfine, E. S., and Casey, P. J. (1997). Substrate binding is required for release of product from mammalian protein Farnesyltransferase. J Biol Chem. 272: 9989-9993.

Umbhauer, M., et al. (2000). The C-terminal cytoplasmic lys-thr-X-X-X-trp motif in frizzled receptors mediates Wnt/β-catenin signalling. EMBO J. 19: 4944-4954.

Usui, T., et al. (1999). Flamingo, a seven-pass transmembrane cadherin, regulates planar cell polarity under the control of Frizzled. Cell 98: 585-595.

Vinson, C. R., Conover, S., and Adler, P. N. (1989). A *Drosophila* tissue polarity locus encodes a protein containing seven potential transmembrane domains. Nature 338: 263-264.

Vivancos, V., et al. (2009). Wnt activity guides facial branchiomotor neuron migration, and involves the PCP pathway and JNK and ROCK kinases. Neural Dev. 4: 7.

Vladar, E. K., Antic, D., and Axelrod, J. D. (2009). Planar cell polarity signaling: The developing cell's compass. Cold Spring Harb Perspect Biol. 1:a002964.

Walston, T., et al. (2004). Multiple Wnt signaling pathways converge to orient the mitotic spindle in early *C. elegans* embryos. Dev Cell. 7: 831-841.

Walston, T., et al. (2006). *mig-5/Dsh* controls cell fate determination and cell migration in *C. elegans*. Dev Biol. 298: 485-497.

Walston, T. D., and Hardin, J. (2006). Wnt-dependent spindle polarization in the early *C. elegans* embryo. Semin Cell Dev Biol. 17: 204-213.

Wang, Y. (2009). Wnt/Planar cell polarity signaling: A new paradigm for cancer therapy. Mol Cancer Ther. 8: 2103-2109.

Wang, Y., and Nathans, J. (2007). Tissue/planar cell polarity in vertebrates: new insights and new questions. Development 134: 647-658.

White , J. G., et al. (1976). The structure of the ventral nerve cord of *Caenorhabditis elegans.* Philos Trans R Soc Lond B Biol Sci. 275: 327-348.

White, J. G., et al. (1986). The structure of the nervous system of the nematode *Caenorhabditis elegans.* Philos Trans R Soc Lond B Biol Sci. 314: 1-340.

White, J. G., Southgate, E., and Thomson, J. N. (1992). Mutations in the *Caenorhabditis elegans unc-4* gene alter the synaptic input to ventral cord motor neurons. Nature 355: 838-841.

Wong, H. C., et al. (2003). Direct binding of the PDZ domain of Dishevelled to a conserved internal sequence in the C-terminal region of Frizzled. Mol Cell. 12: 1251-1260.

Wu, M., and Herman, M. A. (2006). A novel noncanonical Wnt pathway is involved in the regulation of the asymmetric B cell division in *C. elegans.* Dev Biol. 293: 316-329.

Wu, M., and Herman, M. A. (2007). Asymmetric localizations of LIN-17/Fz and MIG-5/Dsh are involved in the asymmetric B cell division in *C. elegans.* Dev Biol. 303: 650-662.

Yamane, H. K., et al. (1991). Membrane-binding domain of the small G protein G25K contains an S-(all-*trans*-geranylgeranyl) cysteine methyl ester at its carboxyl terminus. Proc Natl Acad Sci USA. 88: 286-290.

Yang, C. H., Axelrod, J. D., and Simon, M. A. (2002). Regulation of Frizzled by Fat-like cadherins during planar polarity signaling in the *Drosophila* compound eye. Cell 108: 675-688.

Yang, S. H., et al. (2012). Severe hepatocellular disease in mice lacking one or both CaaX prenyltransferases. J Lipid Res. 53: 77-86.

Yin, C., et al. (2008). Cooperation of polarized cell intercalations drives convergence and extension of presomitic mesoderm during zebrafish gastrulation. J Cell Biol. 180: 221-232.

Zhai, L., Chaturvedi, D., and Cumberledge, S. (2004). *Drosophila* Wnt-1 undergoes a hydrophobic modification and is targeted to lipid rafts, a process that requires Porcupine. J Biol Chem. 279: 33220-33227.

Zhang, F. L., and Casey, P. J. (1996). Protein prenylation: molecular mechanisms and functional consequences. Annu Rev Biochem. 65: 241-269.

Zhang, X., et al. (2007). Dishevelled promotes axon differentiation by regulating atypical protein kinase C. Nat Cell Biol. 9: 743-754.

Zheng, L., Zhang, J., and Carthew, R. W. (1995). *frizzled* regulates mirror-symmetric pattern formation in the *Drosophila* eye. Development 121: 3045-3055.

Zipkin, I. D., Kindt, R. M., and Kenyon, C. J. (1997). Role of a new Rho family member in cell migration and axon guidance in *C. elegans*. Cell 90: 883-894.

APPENDIX A – LIST OF PRIMERS

STRAIN/PLASMID	PRIMER SEQUENCE (5'-3')	MELTING TEMP (°C)	BAND SIZES
vang-1 (tm1422)	AAAATGTCATAAACGCCGAGTC	58.9	N2: 800bp, *vang-1*: 200bp
	TTTTAGGGTACCTAGCTTGTGC	60.8	
prkl-1 (ok3182)	CACGTTCACAATTGTAATTC	54.3	N2: 400bp, *prkl-1*: 600bp
	AATAGTCTCCCAGGGCCAAG	62.5	
	CGATAAGAAGTACTCTCATG	56.3	
pfntb-1::fntb-1	TCGTTCTCAACGGCACCGGGAA	66.4	*pfntb-1:*2.5KB
	TCCGTTGGCTGCTTCGGCTTTG	66.4	
punc-4::fntb-1	TCACTCACAACGATGGATACG	60.6	*punc-4*: 2.7KB
	ACGGAATGGGATCGAAGATGTCATTTTC ACTTTTTGGAAGAAGAAGATCC	71.3	
	ATGACATCTTCGATCCCATTCCGT	62.9	*fntb-1*: 3.1KB
	CGTACGGCCGACTAGTAGGAAACAGTTA TG	68.7	
	CCACCTCTGTCTTCAAGGCG	64.5	*punc-4::fntb-1*: 5.8KB
	GGTATATTGGGAATGTATTCTGTC	59.4	
pcol-10::fntb-1	TCACTCACAACGATGGATACG	60.6	*pcol-10*: 1.2KB
	ACGGAATGGGATCGAAGATGTCATGGT ACCTTATTCAGTGTTACCC	72.7	
	ATGACATCTTCGATCCCATTCCGT	62.9	*fntb-1*: 3.1KB
	CGTACGGCCGACTAGTAGGAAACAGTTA TG	68.7	
	TCTTCATCCCTTCAACATTTGG	58.9	*pcol-10::fntb-1*: 4.3KB
	GGTATATTGGGAATGTATTCTGTC	59.4	
punc-4::gfp::prkl-1 CNIM	TCTTGTTGAATTAGATGGTGATG	57.4	*punc-4::gfp::prkl-1a*: 2.4KB
	AGACTTCTTCTTTTTCTGTGGTTTCGGAT GAAGACCGCCTCCCGACATCATC	75	
	AAACCACAGAAAAAGAAGAAGTCTTGC AATATTATGTGAGGATCCCCGGGATTG	72.3	*prkl-1a CNIM:* 980bp
	CGTACGGCCGACTAGTAGGAAACAGTTA TG	68.7	
	TGAAGGTGATGCAACATACG	58.4	*punc-4::gfp::prkl-1a CNIM*: 2.5KB
	TTTGACACCAGACAAGTTGGT	58.7	